Optimization of Aperiodically Spaced Phased Arrays for Wideband Applications

Benjamin M.W. Baggett

Thesis submitted to the Faculty of the
Virginia Polytechnic Institute and State University
in partial fulfillment of the requirements for the degree of

Master of Science
in
Electrical Engineering

Timothy Pratt, Chair
William A. Davis
J. Michael Ruohoniemi

May 3, 2011
Blacksburg, Virginia

Keywords: Phased Array, Antennas, Aperiodic, Optimization, Wideband, Particle Swarm

Optimization of Aperiodically Spaced Phased Arrays for Wideband Applications

Benjamin M.W. Baggett

(ABSTRACT)

Over the years, phased array antennas have provided electronic scanning with high gain and low sidelobe levels for many radar and satellite applications. The need for higher bandwidth as well as greater scanning ability has led to research in the area of aperiodically spaced antenna arrays. Aperiodic arrays use variable spacing between antenna elements and generally require fewer elements than periodically spaced arrays to achieve similar far field pattern performance. This reduction in elements allows the array to be built at much lower cost than traditional phased arrays.

This thesis introduces the concept of aperiodic phased arrays and their design via optimization algorithms, specifically Particle Swarm Optimization. An axial mode helix is designed as the antenna array element to obtain the required half power beamwidth and bandwidth. The final optimized aperiodic array is compared to a traditional periodic array and conclusions are made.

Acknowledgments

I would first like to thank Dr. Timothy Pratt for serving as my committee chairman and my advisor during my M.S. degree. His knowledge, advice, and support have been truly invaluable throughout my undergraduate as well as graduate career. I would like to thank Dr. William Davis and Dr. Mike Ruohoniemi for serving on my graduate committee. I would like to thank Dr. Davis for all of the helpful advice and direction he gave me during my time working in the Virginia Tech Antenna Group. I would like to thank Dr. Ruohoniemi for all the work opportunities he gave me as part of the SuperDARN Radar Group at Virginia Tech.

I would like to thank Dr. Jaime De La Ree for funding my graduate research through a graduate teaching assistantship. I truly enjoyed teaching the undergraduate electronics labs and sharing my knowledge, advice, and experiences with undergraduate students.

I would also like to thank all the members of VTAG that I have worked with during my time spent in the lab. The group consists of a large, diverse group of bright individuals that I am happy to call my friends. The interactions both in and outside of the lab were very helpful and something I will never forget. I would especially like to thank Tae Young Yang for all of his advice, technical assistance, and encouragement throughout my entire graduate career.

Finally, I would like to thank my parents, Anthony and Mary Baggett, along with my sister Jaime and girlfriend Kelsea, for their love and continued support. The patience and support they gave me during my stay at Virginia Tech was truly invaluable and will never be forgotten.

Contents

List of Figures

List of Tables

Chapter 1

Introduction

1.1 Phased Array Antennas

In today's technological society, there is a high demand to create products that are more efficient and economical than their predecessors. The development of microwave radar in the early 1940s led to a search for narrow beam antennas with beams that could scan the horizon and track aircraft, and created a large demand for innovation in the area of antenna design. Over the years, many different antennas have been designed to accommodate the industry's growing needs in the area of radar surveillance and tracking. One major requirement for radar antennas has been the ability to scan the antenna to provide surveillance of a large volume of space. Traditionally this was done by mechanically rotating the antenna on a pedestal. As the demands and applications became more complicated, electronically scanned phased array antennas were developed.

Phased array antennas were designed to allow the antenna to electronically scan its main beam rather than mechanically scan. These arrays are groups of small antennas known as elements in which the relative phase between elements is varied such that the radiation pattern is reinforced in a desired direction and suppressed in undesired directions. Electronic phase shifters are commonly used. However, for wide bandwidth applications, a true time delay

between elements must be incorporated. In order to control sidelobe level, an amplitude distribution is placed across the array aperture. Figure 1.1 below shows a typical 1-D phased array and some of the beams it can produce [1].

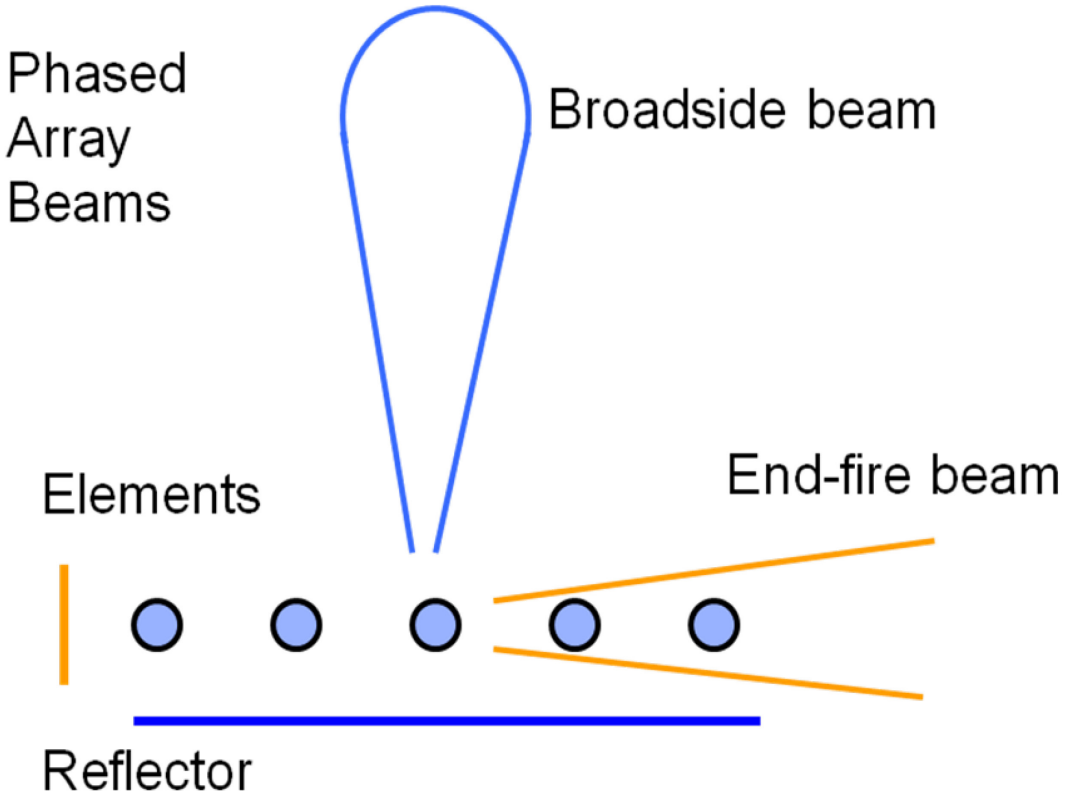

Figure 1.1 One-dimensional phased array

In addition to faster scan rates, phased arrays also allow greater frequency agility. However, one drawback is that these arrays are much more costly to build than the traditional reflector antennas for surveillance and tracking radar systems. Phased arrays can generate multiple beams, and can switch rapidly from surveillance of the distant horizon to tracking multiple targets, thus replacing several separate radar systems with a single, albeit expensive and complex, antenna system.

Phased arrays typically have elements spaced periodically with spacings between a half wavelength and 0.7 wavelengths apart. If the spacing becomes larger than this, the maximum scan angle of the array is greatly reduced due to the introduction of grating lobes while scanning. The antenna patterns for these arrays are easy to compute and the results are highly predictable. These conveniences, along with many others, show why these arrays are widely used today for most radar applications. Other applications such as multiple beam satellite antennas and fixed beam antennas also find phased arrays to be very useful.

More recent applications for radar antennas require greater frequency agility. This agility allows the array to perform multiple functions simultaneously, including tracking multiple targets at the same time. However, since all radars must operate in allocated bands, frequency agility beyond 1 GHz or so is not possible. Phased arrays with periodic element spacings are often unable to meet these new requirements. Therefore, there has been an increased interest in the area of aperiodic phased arrays. These arrays contain elements that are placed at irregular distances from one another. If designed properly, aperiodic phased arrays have the ability to achieve performance equal to that of periodic arrays while requiring fewer elements and allowing for a wider range of operating frequencies. The ability to loosen the antenna grid is also of prime importance in high frequency applications. At very high frequencies, the wavelength becomes so small that building a half-wavelength periodic array can be mechanically

difficult because of the low tolerance for error. Aperiodic antenna arrays allow the construction of these antennas to be mechanically feasible.

The design of aperiodic phased arrays is a highly complex problem. Unlike periodic arrays, aperiodic arrays have 2N degrees of freedom because of their variable locations, where N represents the number of elements in the array. This additional degree of freedom causes the mathematics involved in the synthesis of aperiodic arrays to be less straightforward than for its periodic counterpart. Research interest in this area started in the early 1960s. The conclusion of this research was that the aperiodic array design problem is highly complex, and that designing these arrays analytically is next to impossible. Many researchers suggested using computers to help solve the problem, however computing power was very limited during this time [2]. In this thesis, the aperiodic array design will be treated as an optimization problem using Particle Swarm Optimization (PSO). This optimization technique allows us to search the solution space for an optimal solution. In this study, the optimizer was designed to search for array patterns with the lowest sidelobe level and a half-power beamwidth closest to the periodic reference array.

The goal of this thesis is to design a uniformly illuminated aperiodic phased array that has comparable far-field pattern performance to the periodic counterpart in terms of sidelobe level and beamwidth. If this can be done, the aperiodic array will be more desirable because it will require fewer elements and will be able to operate over a wider bandwidth than the periodic array. The initial objective in this thesis was to design an array that could scan to ±30 degrees in azimuth, while maintaining a 2-to-1 operational bandwidth. An axial-mode helix antenna was selected as the array element to meet this bandwidth requirement. This element was also chosen for its polarization properties. Circular polarization is useful in radar surveillance because reflections from rain will be rejected while reflections from corner reflectors will be reinforced.

The results of this aperiodic array will be compared to a periodic array and conclusions will be drawn as to how they compare.

1.2 Thesis Overview

Chapter 2 provides a literature review and describes previous research conducted in the area of aperiodic antenna arrays. Chapter 3 discusses the theory of aperiodic arrays and the use of optimization techniques such as Particle Swarm Optimization to aid in designing an optimal array. Applications for these arrays will also be discussed in this chapter. Chapter 4 reports the design process used in this research. The helix antenna element design and the optimization design are discussed in depth in this chapter. Also, FEKO analysis of the array was simulated to show that mutual coupling is not a factor and can be ignored. Chapter 5 contains the simulated far-field pattern results for the optimized aperiodic array design. This design is compared to the equivalent periodic array. A full-wave FEKO analysis of the final optimized array was performed and compared to the MATLAB results. Finally, Chapter 6 concludes the research and provides suggestions for future work to be completed in this area.

Chapter 2

Background

2.1 Radar History

The development of radar was due largely in part to the threat of German bomber attack in World War II. The United States and Britain independently researched radar and both developed functional radars by the early 1940s. In the United States, the US Navy produced a set of 200 MHz radars capable of detecting targets up to 50 miles. These systems were designated as the XAF Radar. The XAF system was fitted to the USS New York battleship, and successful tests were conducted in the Potomac and Atlantic. In May of 1939, the Navy ordered 30 XAF radars for integration on their battleships. The radars were successful at detecting surface ships, aircraft, and submarines; all 30 XAF ships were operational by December of 1941. Because of the radar's ability to detect ships in night or in heavy smoke, the US Navy recommended that no more battleships be built. Submarines were built instead with the capability of underwater launched ICBMS [1].

During the same time, the US Army was developing its own radar system. It was the responsibility of the army to provide an air defense system. The original system designed in the early 1930s had very short range. This proved to be useless if the planes were flying well above the clouds. Also, faster planes gave very little audible warning of approach. All of these

problems required additional funding in order to fix the problems. In May of 1937, Congress allotted $250,000 for radar development by the US Army. By June 1937, the SCR radar was developed in 100 MHz and 200 MHz versions. The system required three antennas; one for target detection, one for horizontal location, and one for vertical location. This system became the first 3-D radar and the first test unit was built in September of 1938. Unfortunately, this radar was destroyed by a hurricane and had to be rebuilt in October of that year. In December of 1941, SCR 268 and SCR 270 radars were placed in Panama and Hawaii. These systems demonstrated tracking ability above the clouds. Six systems were placed in Oahu, Hawaii and proved to be very pivotal during the Pearl Harbor attacks by the Japanese [1].

In addition to the United States development of radar, the United Kingdom also pursued research in this area. The threat of a German air attack on Britain was looming, and the need to detect aircraft at a far distance was very great. Robert Watson-Watt, of the National Physical Lab, set up a radar development group at Orfordness marshes on the east coast of England. The goal was to design a 27 MHz early warning radar; however, the first demonstration in 1935 was a complete failure. In September of 1935, five radar stations were linked together and called the Chain Home System. Watson-Watt recruited the best minds in the country, and by 1937 five stations were operating with a target detection range of 90 miles. After Britain and France declared war on Germany in 1939, the Chain Home System was on a 24 hour watch. All stations were linked via telephone to a central command location in Hendon, England. No similar system was used to link the radar systems in Oahu, Hawaii to a central command post [1].

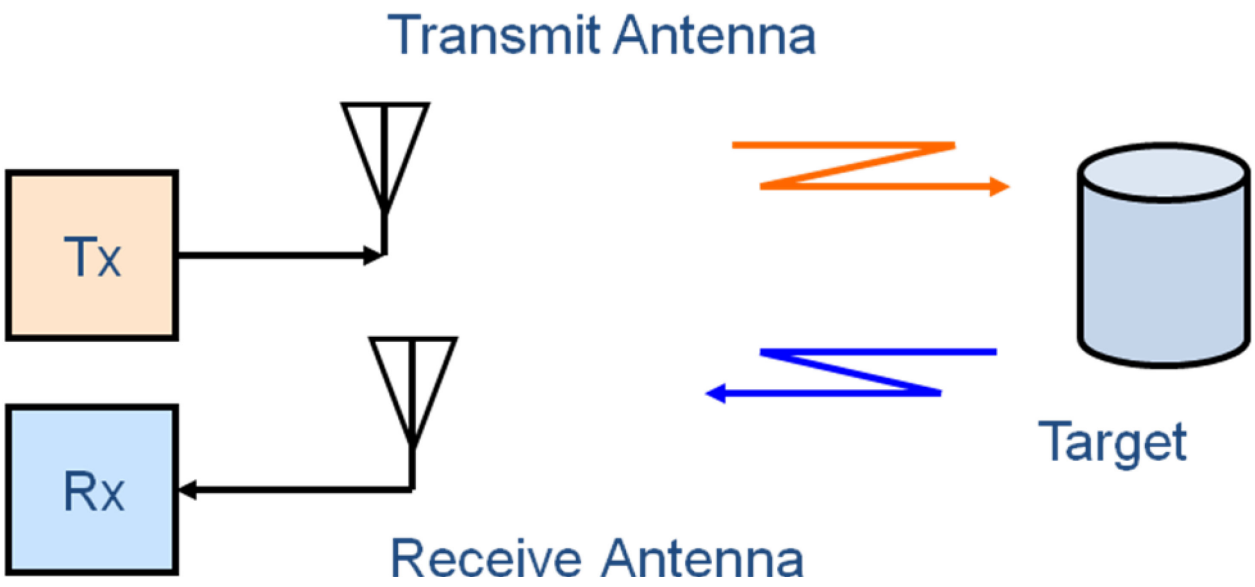

Figure 2.1 Basic pulse radar in 1936

Until 1939, no RF source existed that could produce more than 2 kW. In order to achieve narrow beams for fire control, microwave frequencies were needed. A new source had to be designed to accommodate higher frequencies and higher power. In February of 1939, Randall and Boot developed the magnetron at Birmingham University. The magnetron was capable of providing 8 kW at 9.8 cm wavelength. Rapid developments were made for 5.0 cm and 1.9 cm wavelengths. By 1941, a 3.0 MW pulse was achieved. In August of 1940, in what became known as the Tizzard Mission, Great Britain took the magnetron to the United States and returned with the US developed T/R cell. Bell Labs in the United States had fire control radar at 600 MHz but could not exceed 2 kW pulse. The introduction of the magnetron from the Tizzard

Mission would prove to be one of the most important moments for future US radar development [1].

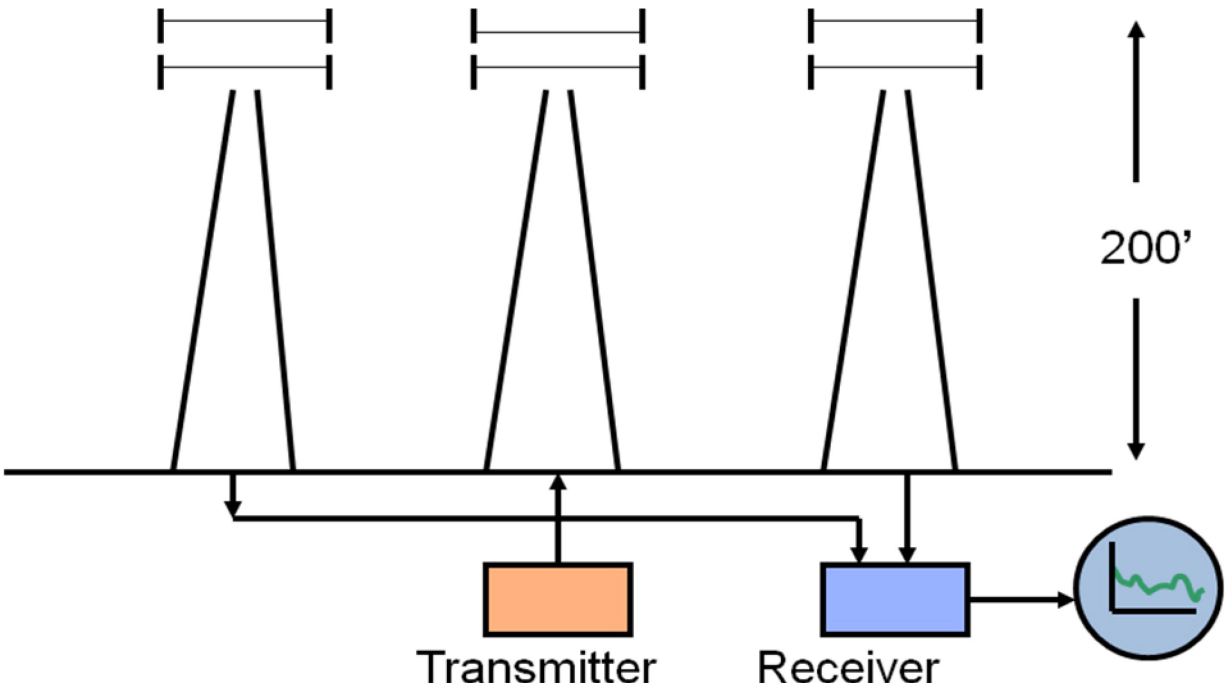

Figure 2.2 Chain Home Radar System

2.2 Phased Array Background

The original radars designed during WWII used rotating reflector antennas in order to transmit and receive RF energy. For simple applications, these antennas worked fine. However, as the applications became more complicated, these reflector antennas were no longer sufficient. Reflector antennas have many disadvantages in radar applications. The regular scanning rate requires a constant dwell time, forcing the radar to dwell on each target the same length of time. Also, targets are only seen once per revolution. These antennas also restrict the radar to only one beam type, such as surveillance, tracking, etc. Finally, mechanical issues are associated with physically rotating a large reflector dish. All of these disadvantages created interest in searching for a better antenna solution.

The ideal radar antenna has many different properties. These include high gain, low beamwidth, option for low gain, multiple beams, different beam types, variable scan rate, variable dwell time, random pointing, and many others. All of these properties can be achieved with a phased array. A phased array is a group of antenna elements arranged in such a way that the effective radiation pattern is reinforced in a desired direction and suppressed in other undesired directions. Phased arrays have greater flexibility and more functions than a traditional reflector antenna, however high cost and complexity of the array are the two main limiting factors. The high cost of building a phased array can be justified when any of the above properties of phased arrays are required.

Phased arrays can be made one-dimensional or two-dimensional, however 1-D arrays are the simplest to design. These arrays have elements arranged in a straight line with a distance, d, between each element. The distance, d, is usually on the order of 0.5 to 1 wavelength in order to avoid introducing copies of the main beam into the visible region, called grating lobes. The main

beam is steered by changing the relative phase between individual elements in the array. Electronic phase shifters are commonly used, however for wide bandwidth applications, a true time delay between elements must be incorporated. In order to control sidelobe level, an amplitude distribution is placed across the array aperture. Figure 2.3 below shows a typical 1-D phased array and some of the beams it can produce. Figure 2.4 shows how these arrays are phased in order to steer the main beam. All analysis for one-dimensional arrays can be extended to two and three-dimensional arrays [1].

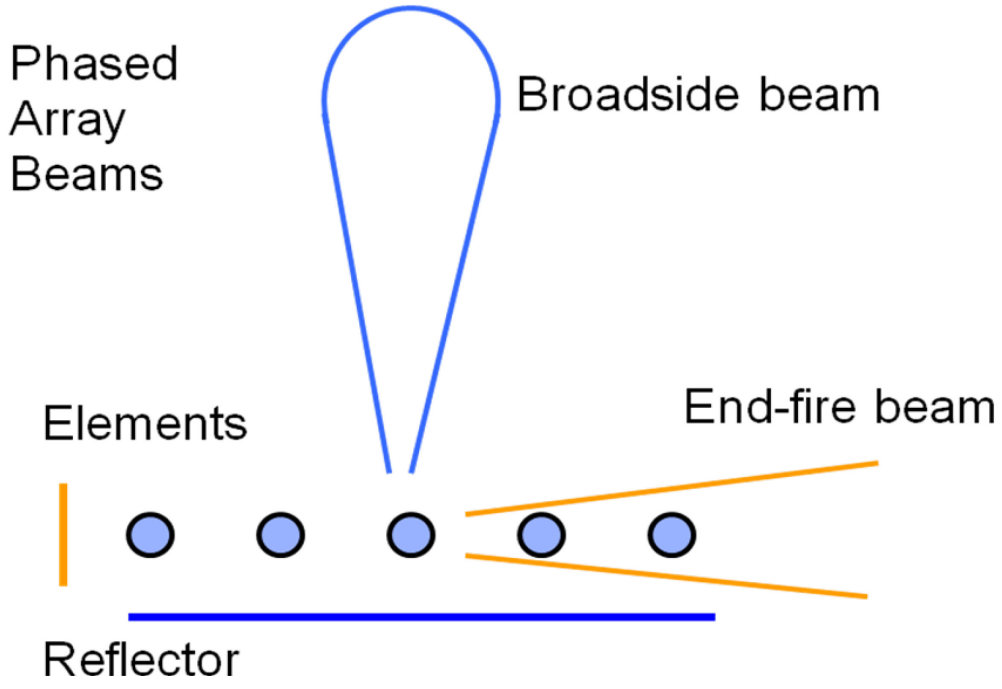

Figure 2.3 One-dimensional phased array

Although phased arrays claim many advantages, they also have many disadvantages in certain applications. Most phased arrays are periodic, which require equal spacing between elements. This causes problems for many different applications. The most important application where periodic arrays are inferior is in wideband array applications. In wideband applications, the spacing between elements must be large, usually greater than half-wavelength. Depending on the desired bandwidth of the array, the spacing between elements can exceed one wavelength. If this occurs, grating lobes appear in the visible region, making the tracking of targets virtually impossible.

Another disadvantage to periodic arrays is cost. In order to secure high gain and low beamwidth, a very large array of elements must be produced. Depending on the frequency of operation, this could require thousands of individual antenna elements, making the array very expensive to produce. Because of this, research has been conducted into alternative arrays which would require fewer elements, thus reducing the cost of the phased array [1].

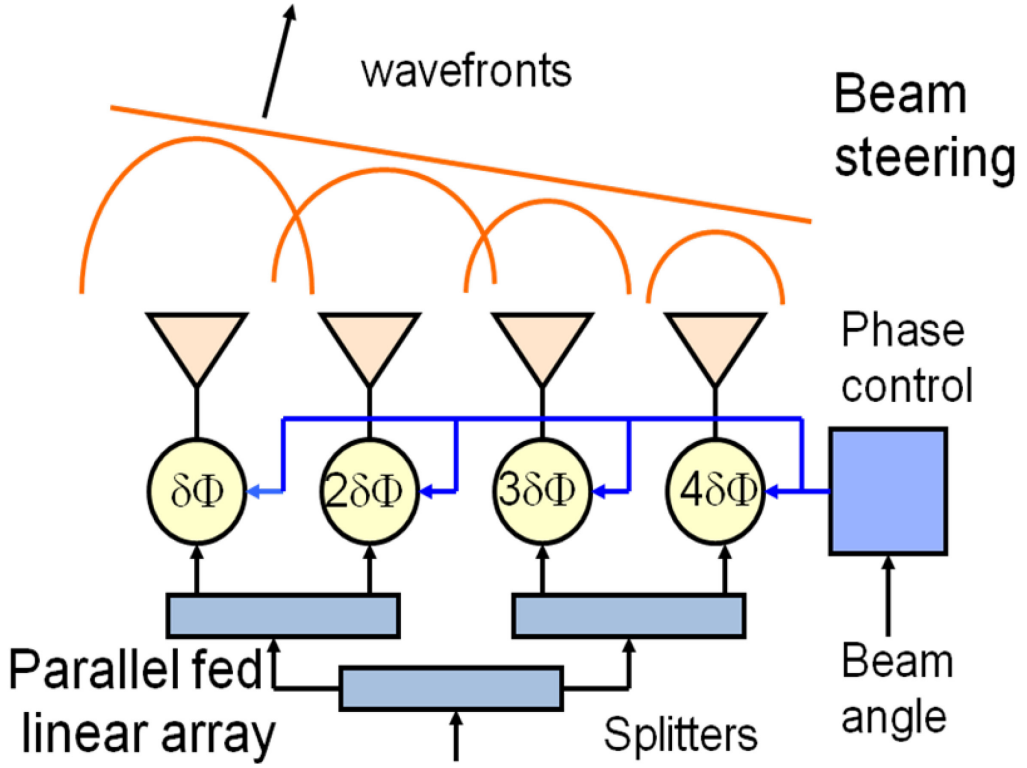

Figure 2.4 Beam steering of phased array

2.3 Previous Aperiodic Array Research (1960s)

Because of the limitations and high cost of periodic phased arrays, engineers and physicists have been studying other forms of arrays as far back as the 1960s. In the 1960s, there was a large interest in the area of aperiodic antenna arrays. Aperiodic arrays are ones in which the spacing between elements is not fixed, but irregular across the array aperture. Researchers claimed that this irregular spacing helped eliminate grating lobes, making aperiodic arrays a prime candidate for high bandwidth applications where scanning is required. Also, the aperiodicity of the array requires fewer elements than the periodic array, drastically reducing the cost of the array. In addition, amplitude tapering could be eliminated, further decreasing the cost of the array by reducing the number of power amplifiers needed in the array backbone. The aperiodic array problem is a very complex non-linear problem. With limited computing resources, researchers in the 1960s approached the problem in many different ways, lending their insight into the aperiodic array problem.

2.3.1 Unz

Unz [3] was one of the first researchers to investigate aperiodic antenna arrays, or space-tapered arrays. In the paper, "Linear Arrays with Arbitrarily Distributed Elements", the author derives a matrix relationship between the elements of an arbitrarily spaced linear array and its far zone pattern. The total radiated power, gain, Q-factor, and figure of merit are defined. The author claims that in an arbitrarily spaced linear array with L elements there are 2L degrees of freedom, compared to L degrees of freedom for an equally spaced linear array. The two degrees of freedom for each element are the complex amplitude of the element and its position along the array axis. More degrees of freedom allow fewer elements to be required in the array in order to

get performance comparable to an equally spaced array. If the same number of elements are used, performance can be improved. Unz claimed the approach may be extended to both two and three dimensional arrays [3].

2.3.2 King et al.

King et al. [4] were also pivotal in the early design and development of aperiodic array theory. The authors' goal of their paper, "Unequally-spaced, Broad-band antenna arrays", is to create an array element distribution that requires fewer elements than a uniformly spaced array while simultaneously replacing grating lobes with sidelobes lower in magnitude than the main beam. Multiple spacing schemes are presented including logarithmic spacing, prime number spacing, arithmetic progression, elimination of multiples, and controlled cosines spacing. It is shown that in order to maintain a 2-to-1 bandwidth and scan to ±90° while eliminating grating lobes, the controlled cosine method is preferred. Several assumptions about the array are made within the paper. All array elements have a minimum spacing of one-half wavelength at the lowest frequency, all elements are assumed to be isotropic radiators, each element has equal amplitude illumination, each element has an equal time phase to exist with beam broadside, and the array is symmetrical about its center. It is determined that the elimination of multiples scheme could be used at one frequency and without beam steering and maintain sidelobes that are 4.5 dB below those of an equally-spaced array. In applications where beam steering is not required, this method offers an alternative to that of tapering the amplitude illumination of an equally-spaced array [4].

The controlled cosine method presented by the author provides an array with 2-to-1 bandwidth, steerable to ±90° and no sidelobe above -5 dB. This method successfully eliminates the grating lobes that would appear in an equally-spaced array of 2-to-1 bandwidth with no beam steering. The beamwidth of the non-uniformly spaced array is nearly the same as for the uniform

case. The non-uniformly spaced array requires fewer elements than the uniformly spaced case, therefore gain will be reduced. Reduced gain must be considered against the advantage of achieving a narrow beam over a broad band with a reduced number of elements. Derivation of other sets of distances by the controlled cosine method promises pattern improvement [4].

2.3.3 Swenson and Y.T. Lo

Written by Swenson and Y.T. Lo, "The University of Illinois Radio Telescope" proposes the use of a non-uniformly spaced antenna array for use in radio astronomy. The author describes the overall design of the parabolic reflector antenna, including the use of the earth as a natural support structure for the reflector. The authors discuss beamwidth and sidelobe requirements and assert that the use of a non-uniformly spaced array as the feed structure is the optimal solution in terms of cost and performance. It is required that this antenna must be able to scan ±30° from zenith and maintain low sidelobe levels over the usable scanning range [5].

The authors realize that uniformly spaced arrays are superior in the sense of mathematical convenience, but are greatly inferior in terms of economy. The desired radiation pattern for this antenna can be conceived from a cosine-squared aperture distribution of current. The uniform spacing array was calculated and it was shown that only 18 percent of the total field is contributed by the outer 194 elements. The author suggests using a space-taper on the outer 194 elements to achieve the same performance while drastically reducing the number of elements used. The spacing function for the outer 194 elements is derived and it is shown that similar performance to the uniform array can be achieved by using a sine based spacing function with each element having equal weighting. The interior elements (194 total) are maintained at uniform spacing with a cosine-square amplitude taper. Results show that this design maintains low sidelobe levels while reducing the number of elements to 68.5% of the original uniformly spaced array. In summary, the authors list many reasons why non-uniform spacing is preferred

over uniform spacing, especially in the case of large arrays. Some of these benefits include elimination of grating lobes, fewer required elements, and lower side lobe level. Shown below in Figure 2.5 is a picture of the actual antenna array that was built at the University of Illinois [5].

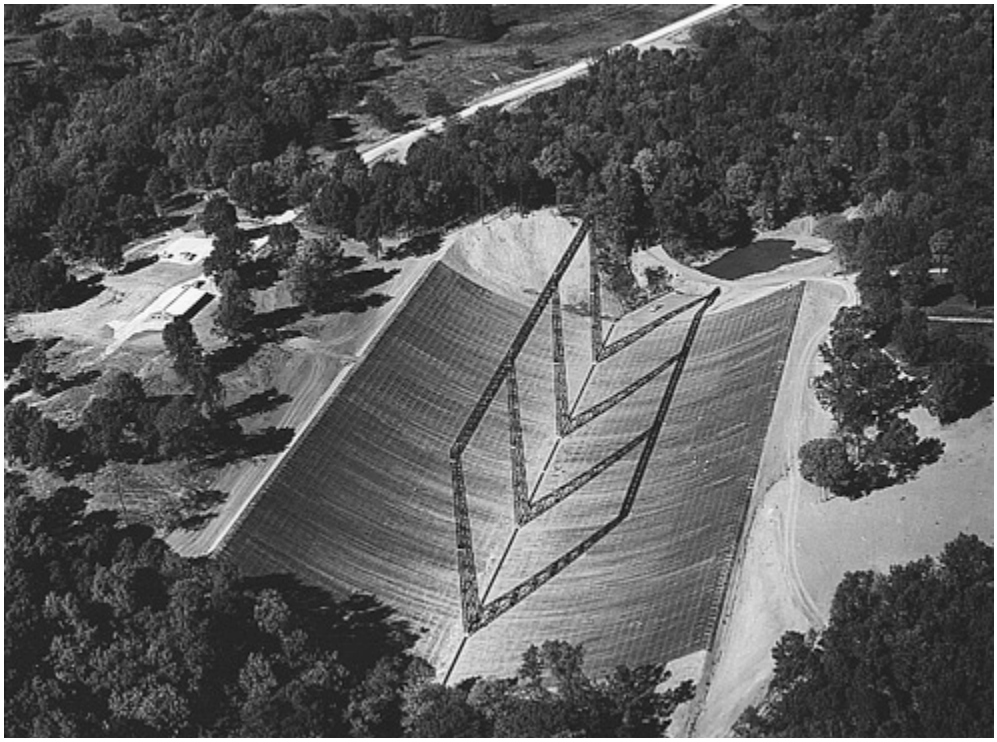

Figure 2.5 Aerial view of the radio telescope at the University of Illinois

2.3.4 Harrington

In the paper "Sidelobe Reduction by Nonuniform Element Spacing", Harrington suggests a graphical technique in order to decrease sidelobe levels of a uniformly spaced array by nonuniformly spacing the elements. A relationship between the desired pattern and the element spacing is described mathematically. The equation gives the fractional changes in element spacing from uniform spacing needed in order to obtain certain sidelobe characteristics. Sidelobes around the main beam can be reduced drastically, up to 2/N times the main lobe amplitude. The grating lobe that would exist in the uniform case is also eliminated, validating King's results. Harrington concluded that sidelobes in the vicinity of the main beam can be reduced drastically but at the cost of increasing the outer sidelobes. An example of a 24-element uniform array that implements nonuniform spacing is given. All conclusions are validated by this example. An end-fire array under the "increased directivity" condition is also shown. The results show that the nonuniform array can achieve higher directivity than the uniform array by additional increases in the progressive phase shift between elements [6].

Overall, the amount of reduction of sidelobe level using this method is significant, especially for large arrays. In practice, nonuniform implementation is often simpler than the uniform amplitude taper. Also, the high-power capabilities of having each element fed equal amplitudes is considered an advantage over amplitude tapered uniform arrays. The author suggests more consideration of nonuniformly spaced arrays over uniformly spaced arrays whenever large arrays are designed for all of these reasons mentioned. He suggests more work can be done in the optimization of these arrays [6].

2.3.5 Willey

In the paper "Space tapering of linear and planar arrays", Willey presents a graphical technique for obtaining a space-tapered array from a uniformly spaced reference array in both linear and planar arrays. Examples of linear arrays and circular planar arrays are given which show that the graphical techniques suggested give results that are close approximates to the Taylor distribution reference pattern. Mathematical formulas are derived for the maximum number of elements to be used in a space-tapered array given a minimum spacing. The minimum spacing is determined based on the physical size of the element and the effects of mutual coupling between adjacent elements. The maximum number of elements is derived by relating the k^{th} moment of the reference pattern to that of the space-tapered pattern. It is shown that this maximum number of elements provides the best approximation to the desired illumination function. Mathematical formulas are given for the maximum sidelobe level of non-uniformly spaced arrays in general. It is shown that the techniques provided in the paper match very closely to these estimated values. It is shown that space-tapered arrays, in general, can be used to reduce side-lobe levels beyond the uniformly spaced array. The gain of the array is also considered for the space-tapered case. It can be shown that the gain of the array will be the gain of the individual element (after mutual coupling effects) times the number of elements. In practice, this will not be true because the power incident upon the array will depend on the cosine of the incident angle. Therefore, the gain will be maximum (the gain of the ideal element) at some "matched" angle and will taper off as the beam is scanned from that angle. The reason for this is because in practice the element will be mismatched across most scan angles. When the element is "matched" at boresight, the gain will be maximum at boresight and fall off during scanning at a more rapid rate than the cosine of the scan angle [7].

Experimental results are given for an actual space-tapered circular array that was built. The results show a close correspondence between the computed and measured patterns of the

array. Differences in theoretical and measured patterns are explained by mutual coupling and effects of the feed system. Dummy elements were used to fill out the array in order that all active element patterns would be nearly identical. The gain and sidelobe structure were shown to be increasingly better when dummy elements were used.

The author concludes that space-tapering is an effective method to reduce the number of elements, reduce sidelobes, and eliminate grating lobes while maintaining pattern characteristics that are close to the uniform reference array. The experimental data shows that beams from a space tapered array can be scanned through a large angle without serious deterioration of the pattern. The beamwidth varied as array theory would predict, and the increase in sidelobe level is predicted by array theory. The author suggests that combined amplitude and density tapering should provided an even better correlation between space tapered and reference array patterns. One final note the author makes is the use of spacing tapered arrays in allowing separate transmitting and receiving elements to be placed in a single aperture. This technique can be used where space considerations do not permit separate antennas or where high power requirements would make duplexing undesirable. Finally, the author claims that space-tapering can be extended to other planar shapes as well as three dimensional arrays. Further research into these areas is suggested [7].

2.3.6 Andreasen

In this paper, "Linear arrays with variable interelement spacing", Andreasen describes the advantages of using aperiodic arrays over periodic arrays. The author concludes that arrays with constant excitations and irregular spacing between elements can be designed to have significantly fewer elements than the periodic counterpart. He claims the sidelobe level depends more on the number of elements in the array and less on the spacing between elements, especially when the average interelement spacing exceeds two wavelengths. Through his

computations, he concluded that the 3-dB beamwidth depends mostly on the length of the array aperture. Also, the product of bandwidth and steerability can be made much larger than for periodic arrays. Andreasen approached this problem as an optimization problem, being the first to do so. He claimed that the ideal approach to this problem would be an analytical theory approach; however, the theory of aperiodic arrays had not been developed so a computer simulation approach was used instead. He noted that this problem does not have a unique solution, rather there are multiple solutions, so that no one solution is ever truly optimal [2].

2.3.7 Y.T. Lo

In the paper, "A Study of Space-Tapered Arrays", Y.T. Lo provides a literature review of many previous research attempts in the area of aperiodic arrays. After further investigating the methods offered by Unz, Swenson, Willey, Andreasen, Skolnik, etc., the author suggests that most arrangements have a moderate sidelobe level, and only very few have low sidelobe level. He claims that space-tapered arrays yield a better chance to have low sidelobes over periodic arrays; but many with low levels are actually not space-tapered. It is worth noting that the arrays in which the author investigated were very small arrays, which in general do not yield low sidelobe level and do not benefit from aperiodic spacings. The overall goal of the paper is to show that the "optimal" solutions found by many of the authors above are not optimal in any sense. The author investigated his own arrays and found significantly lower sidelobe levels than any of the previous authors. The results in this investigation show that some of the conclusions reached by previous authors could be somewhat optimistic and should be reexamined. The author also concludes that there is little possibility in obtaining an array with the lowest sidelobe level, unless a true optimization procedure is found. Therefore, Lo states that one should not be surprised to find that there may be little difference between the pseudo-optimum procedures previously presented and many guess-and-check methods [8].

2.4 Current Aperiodic Array Research

Researchers are still attempting to advance research in the area of the aperiodic antenna arrays. Radar, satellite, and many other applications are driving research in the area of aperiodic arrays. Computing resources are more readily available today so tackling the problem is becoming much more realistic. The problem has been approached both as an analytical problem and as an optimization problem.

2.4.1 Toso

In multiple papers, Toso describes aperiodic phased arrays for satellite multi-beam applications. He claims aperiodic arrays are advantageous because they can be used to eliminate grating lobes and reduce the number of elements in the array, thus reducing cost and complexity. He notes that allowing the elements to have equal fed amplitudes maximizes the antenna power efficiency since all of the amplifiers work at their most efficient working point. He does describe some of the disadvantages as well. He claims with a reduced number of elements comes a reduced maximum EIRP achievable if not compensated by an increase in power in each active chain. Also, the aperiodicity associated with non regular lattices may jeopardize the use of generic building blocks, especially for feeding networks. This could have negative effects on costs of the system; however, this problem could be mitigated by using a set of different types of subarrays to fill the whole aperture [9].

Toso uses a deterministic approach to design an aperiodic array that is equivalent to a periodic array with a cosine amplitude taper. He divides the area subtended by the reference taper function into slices of area proportional to the array amplitude excitation. An element is then placed at the center of each of these slices, forming the aperiodic array. In addition, Toso also adds an amplitude taper to the array to create an amplitude/density approach, which more

accurately recreates the far-field pattern from the periodic array. He concludes that aperiodic arrays can be used to eliminate grating lobes and reduce sidelobes further than the periodic counterpart. Fewer elements can be used in order to decrease costs. Pattern performance can be increased further by applying an amplitude taper in addition to the element space taper [9].

2.4.2 Haupt

Many researchers have attempted to solve the aperiodic array problem analytically. However, it has been shown that it is very difficult to apply arbitrary requirements to arrays generated using these deterministic methods. As a result, aperiodic array antenna positions are often generated with iterative search algorithms. In his paper, "Thinning Arrays Using Genetic Algorithms", Haupt presents multiple ways to optimally thin antenna arrays. The goal is to eliminate as many elements as possible while maintaining a low sidelobe and wide scanning ability. Simulation results for 200 element linear arrays as well as 200 element planar arrays are presented. It is shown that the arrays can be thinned to obtain sidelobes of less than 20 dB as well as maintain scanning ability and high bandwidth. Haupt admits that the Genetic Algorithm is slow and not very useful for real-time pattern control; however, the algorithm is quite useful for optimizing array designs. The goal of his paper is to show that Genetic Algorithm can be used for not only array thinning, but many other applications in scattering and antenna theory. Other researchers such as Barott, Abdolee, Vakilian, and Rahman confirmed Haupt's claims in their own independent research [10].

2.4.3 Bray and Werner

In this paper, "Optimization of Thinned Aperiodic Linear Phased Arrays Using Genetic Algorithms to Reduce Grating Lobes During Scanning", the authors gave the first complete analysis of an aperiodic array. The array locations were optimized using the Genetic Algorithm from Haupt. The antenna element was chosen as a dipole, one of the few papers to include an

actual antenna element instead of just assuming point sources. The aperiodic array was optimized at a given scan angle with resulting sidelobes that were constant up to and including that scan angle. This paper was one of the few to include practical considerations in the design of the array, including mutual coupling and input impedance restrictions. A full-wave analysis was performed in order to show that mutual coupling was not a major issue in the design. Also, the Genetic Algorithm placed input impedance restrictions on the dipole element. This occurred without adversely affecting the performance of the array. Also, the Genetic Algorithm was used to show that matching networks could be made for each individual element in the array. Overall, this paper showed that aperiodic arrays could be used with realistic antenna elements and still maintain low sidelobes and wide scanning ability. It was one of the few papers to take into account practical considerations when designing the array [11].

2.5 Conclusions of Previous Research

Researchers from the 1960s attempted many different methods of solving the aperiodic array design problem. Most attempted to solve the problem using analytical techniques. Several authors were successful, but the technique could only be applied to very small arrays because of the computational complexity. Other researchers suggested the use of computers in order to solve the problem [2]; however, computing resources at this time were not readily available and not powerful enough to solve the problem. The overall consensus from the 1960s research was that the problem is highly complex and that solving it analytically is next to impossible. Once computing resources became available, the methods of solving this problem changed.

Current research in the area of aperiodic arrays almost exclusively takes advantage of today's computing power to help solve the problem. Many researchers have tried to solve the problem analytically with the aid of computers [9]. Many have had limited success with small to moderately sized arrays. However, another group of researchers approached the problem as an optimization problem [10, 11]. Researchers have taken advantage of the newly invented Genetic Algorithm to help them search the solution space for an optimal design, in whichever way they decide to define it [11]. The consensus of research today is that solving the problem analytically for large arrays is still very complicated, even with the help of computers. The problem is a highly non-linear problem, and the solution is not as mathematically convenient as for periodic antenna arrays. Most researchers have concluded that the best way to design these arrays is to approach the design as an optimization problem [2, 10, 11]. Many optimization algorithms have proven to be successful tools for solving these electromagnetic problems, providing good results in a reasonable amount of time.

Chapter 3

Theory of Aperiodic Arrays

3.1 Introduction

This chapter describes the theory and analysis of both periodic and aperiodic antenna arrays. Section 3.2 describes periodic array theory and provides the mathematical tools needed to analyze these arrays. Section 3.3 describes aperiodic arrays and the advantages and disadvantages they claim over the periodic counterpart. This section also describes the mathematical complexity in evaluating these arrays, and provides alternative methods for analyzing them. Section 3.4 presents the approach used in this thesis to investigate aperiodic arrays. Finally, Section 3.5 looks at several real world applications for aperiodic antenna arrays.

3.2 Periodic Array Theory

The majority of antenna arrays designed today are periodic arrays. Periodic arrays are antenna arrays in which the individual spacing between elements is kept constant, usually between half a wavelength and 0.7 wavelengths. Element spacing greater than half-wavelength causes grating

lobes to enter the visible region when the main beam is scanned beyond a specific angle from broadside. If the spacing between elements is designed to be smaller than a half-wavelength, mutual coupling effects become substantial and need to be taken into account in the array analysis.

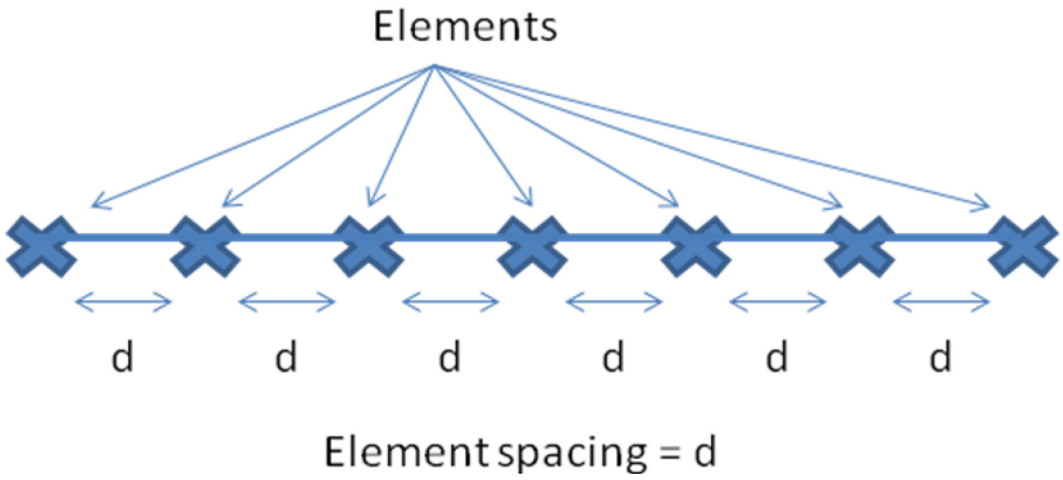

Figure 3.1 Typical one-dimensional periodic array with element spacing, d

The far-field pattern for a periodic array is relatively simple to calculate. The amplitude and phase contribution of each individual element in a transmitting array is summed across the visible region. Equation 3.1 below describes the general form for calculating the array factor [12]. This equation assumes point sources as the antenna element and no mutual coupling effects between elements.

$$AF = I_0 e^{j\xi_0} + I_1 e^{j\xi_1} + I_2 e^{j\xi_2} + \ldots$$ **Equation 3.1**

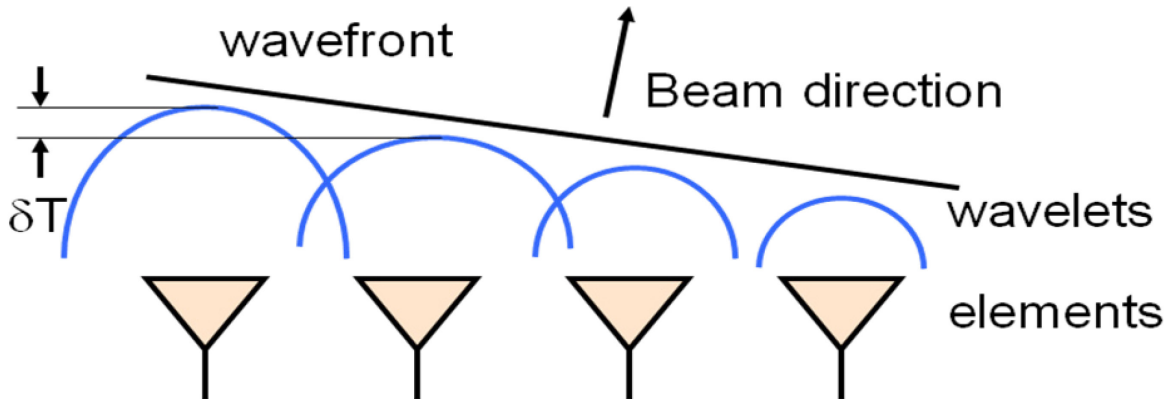

Figure 3.2 Array showing phase difference due to transmitting wave [1]

The terms ξ_0, ξ_1, etc. represent the phase shifts from the elements to a point in space due to propagation (usually in the far field). I_0, I_1, etc. represent the complex phase shift introduced to each element in the transmission line path. For arrays containing a copious number of individual elements, this summation can be very lengthy and inconvenient. Because the array has periodic distances between elements, the equation can be simplified to [12]

$$AF = \sum_{n=0}^{N-1} I_n e^{j\beta nd\cos\theta}$$ **Equation 3.2**

where I_n represents the complex amplitude of the excitation applied to the n^{th} element, β represents the free-space wave number, d represents the distance between elements, and θ is the far-field observation angle measured from boresight.

As mentioned earlier, this formula assumes isotropic radiators as the antenna element. In order to accurately compute the far-field pattern, the actual antenna element pattern must be multiplied by the array factor to get the far-field power pattern.

$$Total\ Pattern = AF * EP \qquad \textbf{Equation 3.3}$$

AF represents the array factor calculated from Equation 3.2, and EP represents the individual antenna element pattern. Because this array has a fixed element spacing, there are N degrees of freedom associated with the N element complex amplitudes that can be placed across the aperture. If we assume that the amplitudes of the individual antenna elements are equal (uniformly excited array), we can re-write the array factor as [12]

$$AF = A_0 \sum_{n=0}^{N-1} e^{jn\psi} \qquad \textbf{Equation 3.4}$$

where A_0 is the uniform amplitude applied across the array and

$$\psi = \beta d \cos\theta + \alpha \qquad \textbf{Equation 3.5}$$

where α represents the progressive phase shift applied across the array. Using geometric series expansion, this array factor can be expanded to

$$AF e^{j\psi} = A_0(e^{j\psi} + e^{j2\psi} + \cdots + e^{jN\psi}) \qquad \textbf{Equation 3.6}$$

After a few short mathematical steps, Equation 3.4 can be re-written as [12]

$$AF = A_0 \frac{\sin \frac{N\psi}{2}}{\sin \frac{\psi}{2}} \qquad \textbf{Equation 3.7}$$

Dividing this by the maximum value from Equation 3.6 gives the normalized array factor for a uniformly excited, periodically spaced antenna array. The array factor therefore has the familiar sin X / X or sinc X shape well known from Fourier transform theory. First sidelobe level is -13.2 dB and beamwidth is 51 λ/D [12].

$$AF_{norm} = \frac{\sin \frac{N\psi}{2}}{N \sin \frac{\psi}{2}} \qquad \textbf{Equation 3.8}$$

Equation 3.8 can readily be used to determine sidelobe level, beamwidth, and directivity for such arrays. Maximum side lobe level is defined as the ratio of the maximum side lobe peak to the amplitude of the main lobe. This represents how well the power is concentrated into the main lobe [12]. In a periodic array the maximum sidelobe will always be the one closest to the main beam, called the first sidelobe. If the elements are driven in phase to produce a broadside beam, the array factor always produces a symmetrical pattern, independent of the amplitude distribution on the array. Scanning the beam away from broadside maintains a symmetrical beam shape so long as the phase shift between elements has a linear progression.

The beamwidth is usually defined as the half-power beamwidth (3 dB beamwidth) or HPBW. This is a measure of the angular separation of points where the main beam is equal to one-half of its maximum value, or -3 dB relative to the normalized maximum gain of the beam, 0 dB. Finally, directivity represents the ratio of the radiation intensity in a certain direction to the average radiation intensity throughout all space [12].

Figures 3.3, 3.4, 3.5, and 3.6 below show a few well known examples of periodic array far field power patterns. Figure 3.3 shows the pattern of a half-wavelength spaced array of 21 isotropic elements at broadside. First side lobe level is -13.2 dB and HPBW is 4.9°, which agrees with published results [12]. Figure 3.4 shows the same periodic array but with a cos(x) amplitude taper applied across the aperture. This taper causes the magnitude of the sidelobes to decrease while simultaneously increasing the HPBW.

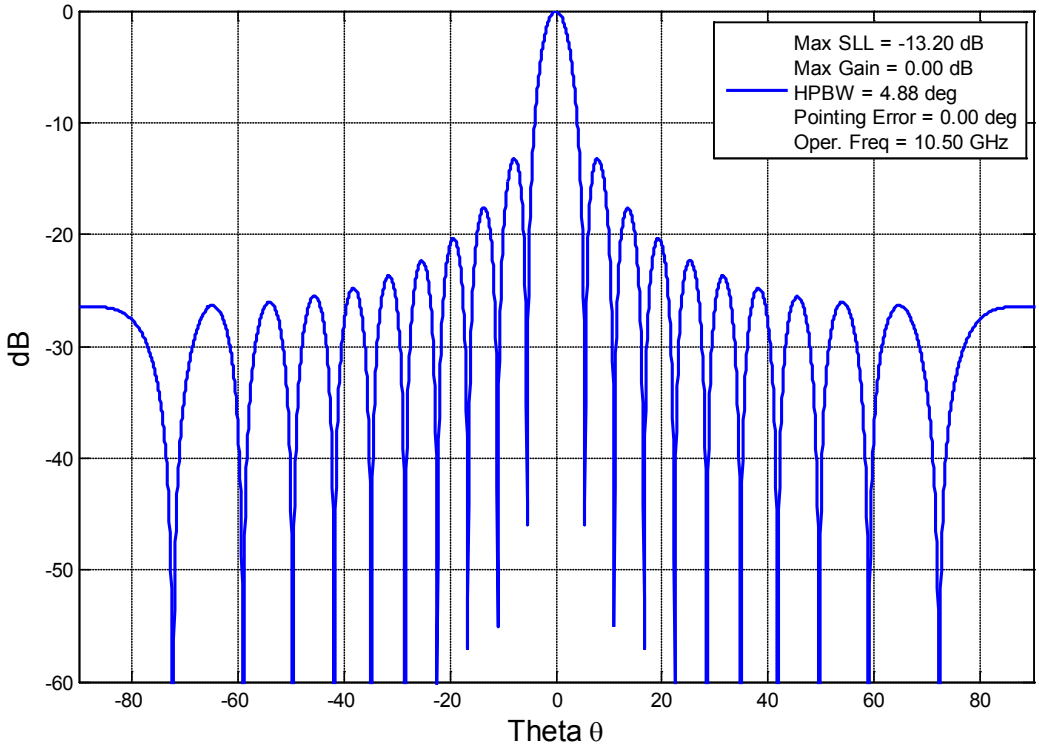

Figure 3.3 Uniformly spaced array with 21 elements. No amplitude taper. (Uniform Illumination)

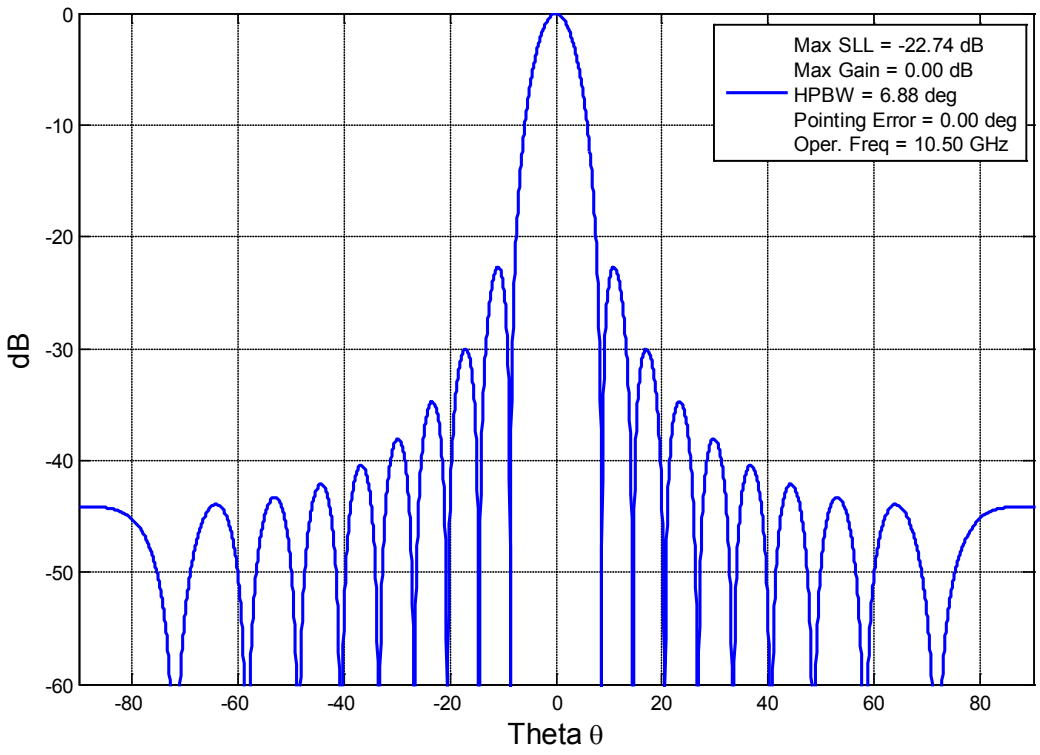

Figure 3.4 Uniformly spaced array with 21 elements. Cosine amplitude taper.

Finally, Figure 3.5 shows the effect of grating lobes on antenna patterns. This figure shows the radiation pattern for a one-wavelength spaced periodic array of 21 isotropic elements. When elements are placed one wavelength apart, radiation from the antennas adds constructively in the +- 90 degree directions. As the array is scanned, the grating lobe shifts into the visible region entirely, as shown in Figure 3.6. Grating lobes are almost always undesirable, especially

in radar applications where a single main beam is needed in order to locate targets. This example shows some of the disadvantages associated with periodically spaced antenna arrays.

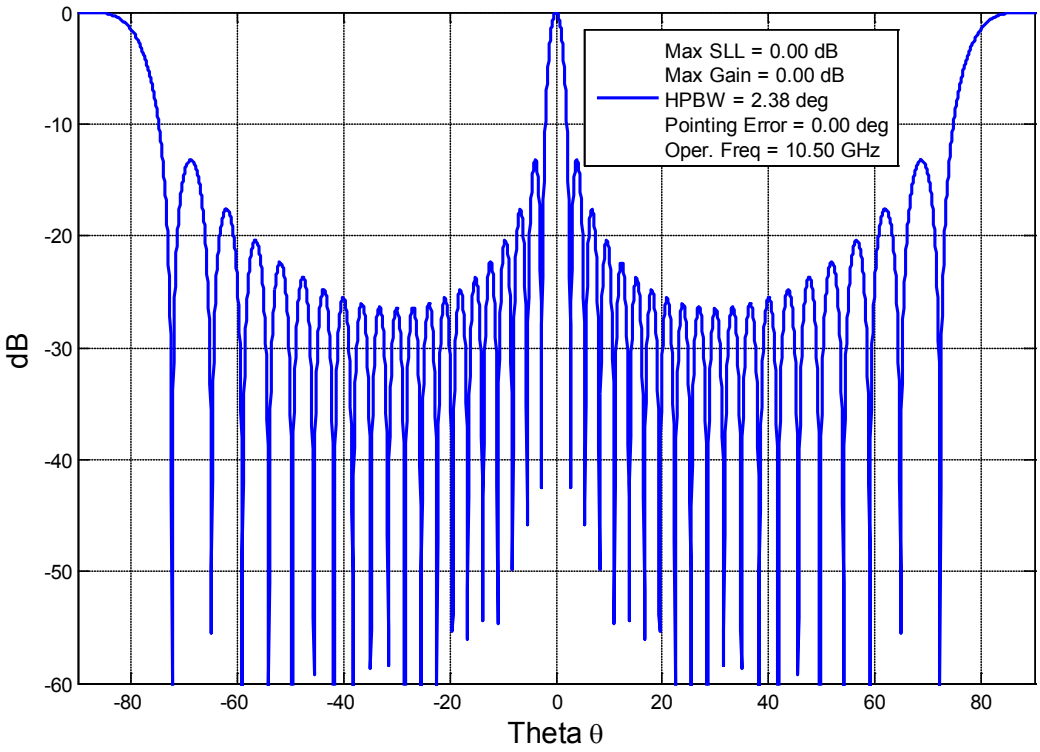

Figure 3.5 One-wavelength spaced uniform array. Grating lobe is entering visible region.

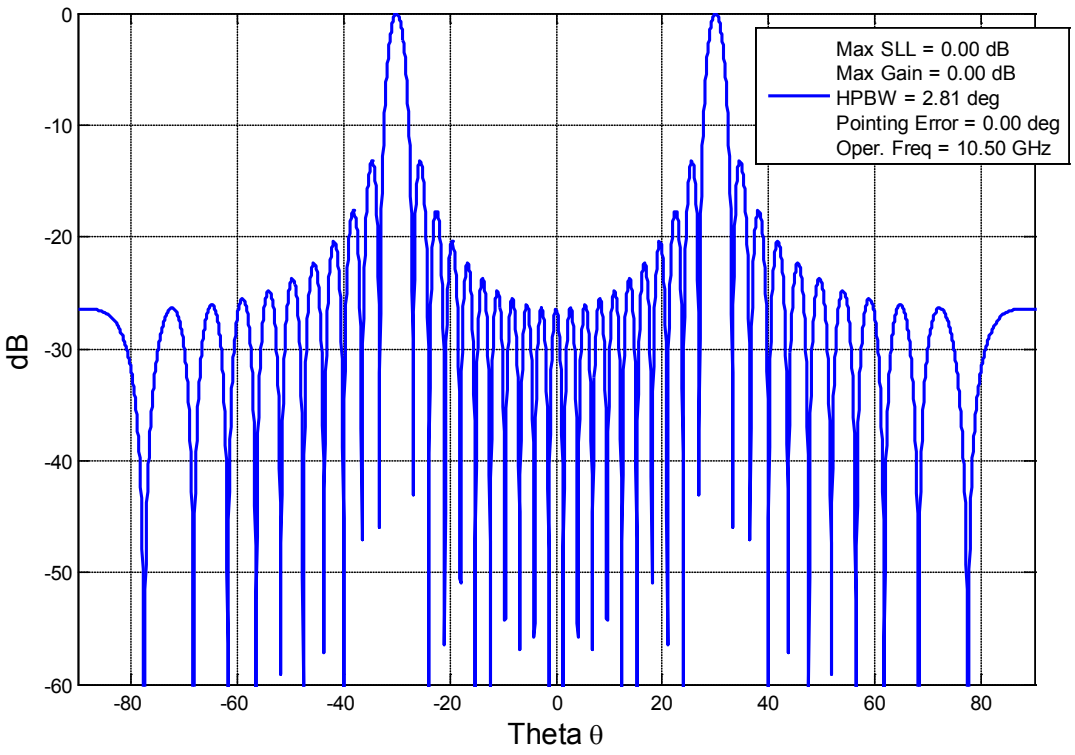

Figure 3.6 One-wavelength spaced uniform array scanned to +30° with grating lobe visible.

Periodic arrays have many advantages that allow them to be the prime choice of today. Low sidelobes, high directivity, ease of construction, and existing feeding networks are all examples of some of the benefits that periodic arrays provide. However, periodic arrays require a large number of antenna elements in electrically large arrays. This causes them to be very expensive to build. Also, there is demand for increased bandwidth of these arrays. Because of

the fixed element spacing and mutual coupling issues, periodic arrays are not well suited to wideband applications. These applications require the array to operate over a wide frequency range with acceptable, sometimes constant, performance. This includes pattern, gain, impedance, polarization, and many other parameters. For these reasons, there has been increased research interest in the area of antenna arrays in an attempt to find a solution to this problem.

3.3 Aperiodic Array Theory

Aperiodic antenna arrays are arrays in which the spacing between elements is irregular across the aperture. This provides many advantages over the periodic counterpart. For example, aperiodic arrays can allow multiple frequency of operation without sacrificing pattern performance. The average spacing between elements can exceed a half-wavelength and simultaneously eliminate the grating lobe that would appear in the periodic array. Because of this larger average inter-element spacing, aperiodic arrays can be designed to require fewer elements than the periodic array. This reduction in antenna elements can reduce the weight and cost of the system in large array applications. Also, the irregular spacing allows the antenna grid spacing to become larger than a half wavelength. This is important in very high frequency applications where the wavelength is very small. Constructing a periodic array with half-wavelength spacing can be mechanically difficult at these ultra high frequencies because of the low tolerance for error.

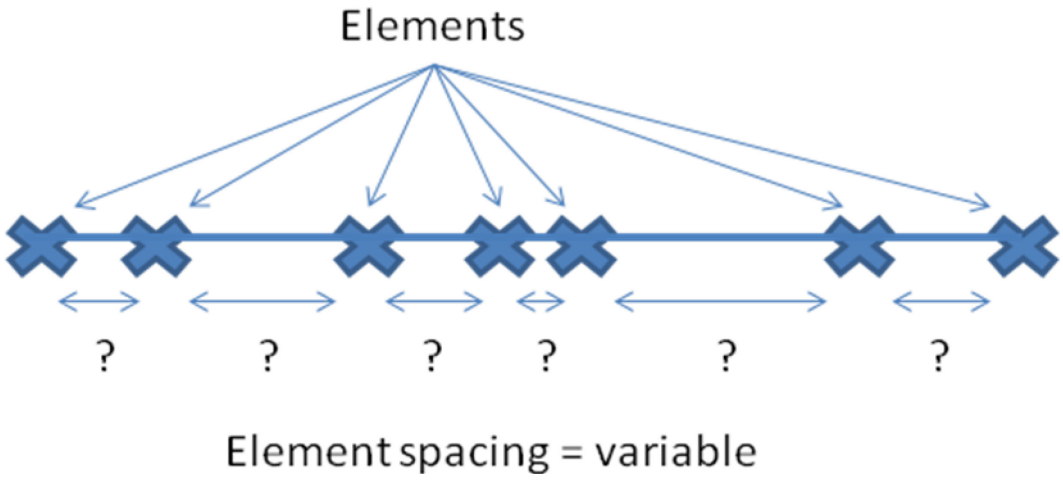

Figure 3.7 Aperiodic antenna array with variable spacing between elements

Aperiodic arrays do have a few drawbacks. First, the irregular spacing makes mechanical design of the array much more difficult. Also, a specially designed feed network with varying cable lengths or phase shifters has to be implemented in order to take into account the variable spacing between elements. Finally, mathematical calculations are more complicated than for periodic arrays. In periodic arrays, there are N degrees of freedom associated with the individual element complex amplitudes across the aperture. Aperiodic arrays allow for 2N degrees of freedom with the additional degree coming from the variable element location. This causes the calculation of the far-field pattern to become a highly non-linear problem. Because of this complexity, traditional mathematical techniques for evaluating the pattern of such arrays are computationally draining. In the last section, Equation 3.8 presented a simplified array factor for periodically spaced antenna arrays. Unfortunately, the additional degree of freedom associated with aperiodic arrays does not allow one to use this simplified formula. The array factor for an

aperiodic array of elements must be calculated as a summation of fields using Equation 3.9 below [12].

$$AF = I_0 + I_1 e^{j\beta d_1 \cos\theta} + I_2 e^{j\beta d_2 \cos\theta} + \cdots \qquad \textbf{Equation 3.9}$$

I_n represents the complex amplitude applied to the n^{th} element, β represents the free-space wave number, d_n represents the distance from the origin to the n^{th} element, and θ is the far-field observation angle.

The variable spacing between elements does not allow for this equation to be simplified as in the periodic case. These arrays are very difficult to evaluate analytically and in very large arrays, designing them can be computationally strenuous. These inconveniences have created an interest in finding alternative techniques to analyze these aperiodic arrays.

3.4 Aperiodic Array Optimization

As discussed earlier, far-field patterns for aperiodic arrays are very difficult to solve analytically. One way to solve this problem is to turn the design into an optimization problem. There are many different optimization algorithms that are well suited for this application. Particle Swarm Optimization, Genetic Algorithm, and Least Means Square Optimization have all been used to approach this particular problem. Each one has shown promise in finding an optimal solution to the aperiodic array problem.

Genetic Algorithm, or GA, is a popular optimization method being applied to many different fields of study, including antenna synthesis. This algorithm uses evolutionary biology and Charles Darwin's "survival of the fittest" as a means of searching the solution space for an

optimal answer that satisfies some pre defined goal. Each solution to the problem is encoded as a chromosome. Each chromosome is assigned a fitness based on a pre-determined fitness function. The more fit chromosomes survive and the less fit chromosomes are eliminated. All of the fit chromosomes are then mated with each other to produce a new generation of chromosomes. This is called selective breeding. Random mutations are introduced in the new generation at a predefined rate in order to add some diversity to the population. Finally, the whole process is repeated for several thousand iterations, or until a pre determined optimal answer is achieved. Figure 3.8 below presents a flow chart diagram of the Genetic Algorithm [10].

Figure 3.8 Genetic Algorithm flow chart

Particle Swarm Optimization is a recently invented algorithm that is proving to be a highly desirable high-performance optimizer in many areas of study. This algorithm is based on the swarming nature of bees. For a problem that requires N variables to be optimized, a swarm of particles is defined, where each particle is assigned a random location and velocity within the N-dimensional solution space. Each particle's location represents a unique solution to the optimization problem. Each particle is evaluated at its current location and assigned a fitness score based on how well it solves the problem, much like in Genetic Algorithm. As shown in Figure 3.9, each particle then swarms through the solution space, moving in the direction of its velocity vector which is defined by both deterministic and random update rules. Each particle knows the location of its highest fitness ever, called the local best. Each particle also knows the location of any particle's highest fitness, called the global best. During each iteration, the new best locations are identified and all of the particles are slowly pulled toward these locations. This combination of self knowledge and group knowledge causes the particles to eventually swarm around an optimal location. After thousands of iterations, this location is determined as the optimal answer and a solution is found [13].

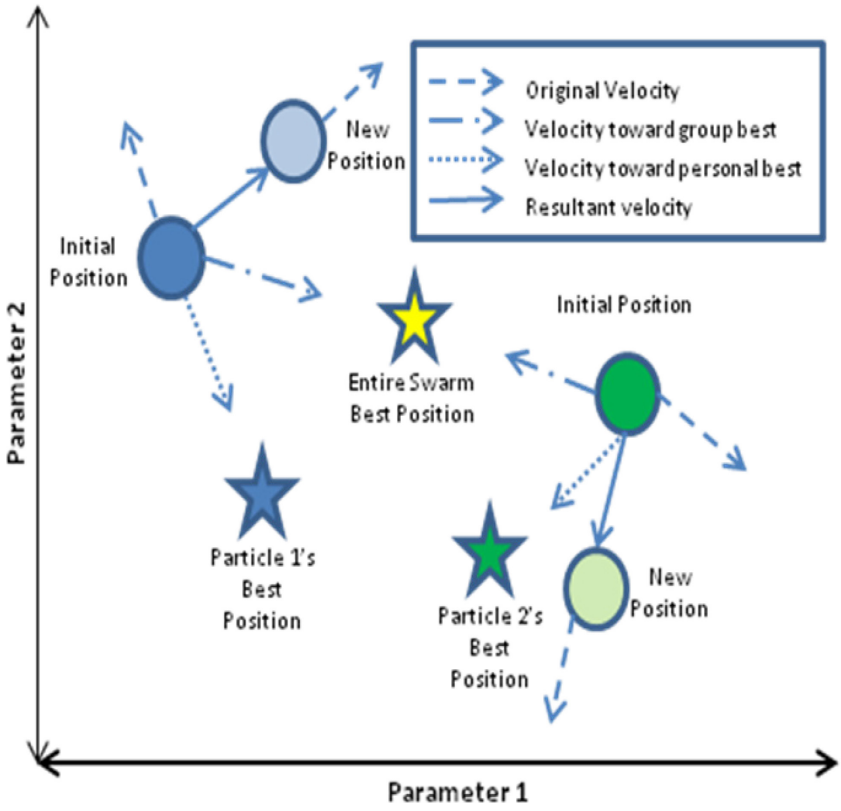

Figure 3.9 Particle Swarm Optimization

In this thesis, Particle Swarm Optimization (PSO) was chosen as the preferred algorithm. Both algorithms have been shown to obtain optimal results [13], however the PSO tends to converge on an optimal answer more quickly than GA. Also, PSO requires fewer lines of code and much less bookkeeping than the GA. Section 4.5 presents a detailed discussion of the particle swarm optimizer used in this research. Future work may consist of a Genetic Algorithm approach to this problem to see how the results compare.

3.5 Aperiodic Array Applications

Aperiodic antenna arrays have the potential to be useful in many different antenna applications. Applications requiring high frequency of operation or wideband operation will benefit tremendously from these arrays. The ability to have inter-element spacing greater than half a wavelength allows the array to operate over a wide frequency range while simultaneously eliminating grating lobes while scanning. The larger spacing will also help to loosen the antenna grid, allowing for a greater mechanical tolerance for error when constructing these ultra high frequency arrays.

One application that could benefit greatly from aperiodic arrays is noise radar. Noise radar is a radar proposed by Dr. Eric K. Walton of Ohio State University. This system claims to be an undetectable radar by transmitting and receiving a wideband noise signal. The transmitted signal reflects off the target and is returned to the receiver, just as in regular radar. This returned signal is then correlated with a time-delayed copy of the transmitted signal. Correlation spikes correspond to target range. This radar design claims to be undetectable because the total power is spread over a wide range of frequencies, and the transmitted signal resembles RF noise. Radar receivers are designed to reject noise from the sun, galaxy, power lines, other RF sources, etc. Therefore, the signal from this noise radar would be picked up by the receivers as regular noise and will be filtered out. Also, because the power is spread over multiple frequencies, traditional detectors which search for high powered signals at a single frequency will only hear more noise. The wide frequency range required by noise radar allows them to benefit greatly from aperiodic antenna arrays [14].

Another application for aperiodic antenna arrays is in chirp radar. In this system, the transmitted signal is chirped, allowing the frequency of the signal to vary with time. This causes

the pulse to be long, allowing more energy to be emitted and ultimately received by the radar. Range is measured by correlating the received signal to the sent signal. This signal is then passed to a dispersive delay line that has the property of varying propagation velocity based on frequency. This causes the pulse to be compressed in time, allowing for a much greater radar range resolution [15].

The radar frequency band is usually the limiting factor in how large of a sweep that can be performed on the signal. Indoor radar cross section (RCS) modeling may have some requirements for such a large sweep. There is also the possibility of lowering the probability of radar detection if the sweep is large enough, allowing the power spectral density to be spread over several different frequencies. The fact that this radar can benefit from a wideband sweep of frequencies makes it a very useful candidate for aperiodic antenna arrays.

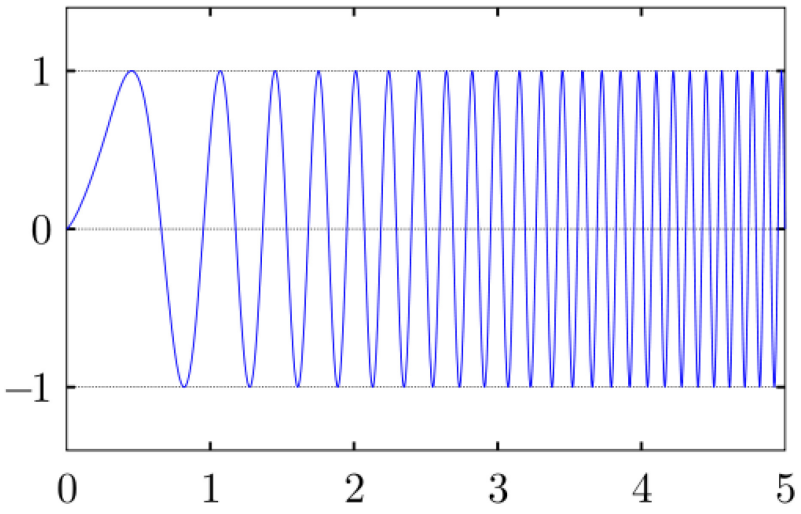

Figure 3.10 A linear chirp signal. As shown, the frequency increases over time.

Chapter 4

Simulations and Design

4.1 Chapter Overview

The goal of this thesis is to design an aperiodically spaced uniformly illuminated antenna array with ± 45 degree scanning ability as well as 2-to-1 operational bandwidth while simultaneously eliminating grating lobes from the visible region. These requirements enforce certain rules that the Particle Swarm optimizer must follow.

Since the antenna array has irregular spacing, the distance between two elements could be less than half-wavelength. If this occurred, mutual coupling between the individual elements would be significant and would have to be accounted for [12]. This thesis does not ignore mutual coupling, but rather claims that the coupling is minimal and can be dismissed when using the helix element described in Section 4.2. By making the minimum spacing between any two elements equal to a half-wavelength, one can claim that the coupling between antenna elements will be negligible. Section 4.3 shows simulated FEKO results that prove that mutual coupling can be ignored if we impose this minimum spacing condition on the helical antenna used in the design of the array.

Bandwidth of the array is also an important requirement for this design. The design objective for this array was operation over a 2-to-1 bandwidth. This bandwidth is defined as a combination of pattern bandwidth and impedance bandwidth. In order for this to happen, there must be a minimum spacing constraint between elements at the upper frequency, f2. As mentioned earlier, the minimum spacing between any two elements is set to a half-wavelength at frequency f1. If the array operates at a frequency f2, which is equal to twice that of f1, then the minimum spacing between any two elements becomes one wavelength at the upper frequency. Therefore, the optimizer is designed to assume a minimum spacing of one wavelength at the upper frequency. This constraint ensures that the array will perform over a 2-to-1 bandwidth. Section 4.4 shows results from a MATLAB function designed to enforce this condition in the optimization process.

Scanning ability is another requirement for this antenna array. The array should be able to scan to ±45 degrees without the introduction of grating lobes within the visible region. This scan angle was arbitrarily chosen for this design. Some arrays have mechanical as well as electronic scanning ability. This scan range is sufficient for many radar applications today. The fitness function of the Particle Swarm optimizer is based on the maximum sidelobe level. The best answer will have the lowest sidelobe level while maintaining a small HPBW. In order to guarantee the lowest sidelobe levels, the array will be optimized while it is scanned to +45 degrees in azimuth. In general, as arrays are scanned the sidelobe levels increase and the beamwidth widens. Optimizing the array at the farthest scan angle ensures a worst case scenario. When the array is phased back to broadside, it should have lower sidelobes and a smaller HPBW.

All of the previous requirements are dependent not only on the array, but the antenna element itself. In order to maintain 2-to-1 bandwidth of the array, the element must be able to achieve 2-to-1 bandwidth. Also, in order to have the array scan to ±45 degrees, the antenna element must have at least a 90 degree HPBW. These special requirements warrant the design of

a unique antenna element. The axial-mode helix was chosen for its high bandwidth characteristics. Chapter 4.2 presents full wave simulation results for the design of this element using the software package FEKO. The optimizer incorporates the element pattern from FEKO and optimizes the total power pattern, not just the array factor. Many previous research attempts in the area of aperiodic arrays assume isotropic radiators and only optimize the array factor [10, 13]. Optimizing the pattern this way does not produce a realistic optimal power pattern. Once an element pattern is brought into the equation, the antenna pattern is changed significantly and may no longer be optimal.

4.2 Axial Mode Helix Design

Bandwidth requirements as well as scanning ability of the array warrant the design of a unique antenna element. The ability to achieve approximately 2-to-1 bandwidth while maintaining a 90 degree HPBW eliminated many different potential element candidates. Consideration was given to several different antenna elements including the log periodic, spiral, and helix. After additional research, the axial-mode helix antenna was chosen as the best candidate element for the array.

4.2.1 Axial Mode Helix Background

The axial-mode helix is a helix antenna where the helix circumference C is approximately one wavelength. This causes the antenna to radiate as an endfire antenna with a single main beam forming along the axis of the antenna. Figures 4.1 and 4.2 below shows the geometry of a typical axial-mode helix. Figure 4.2 shows the relationships between S,C,D,L and α for a single turn helix that has been stretched out flat [12].

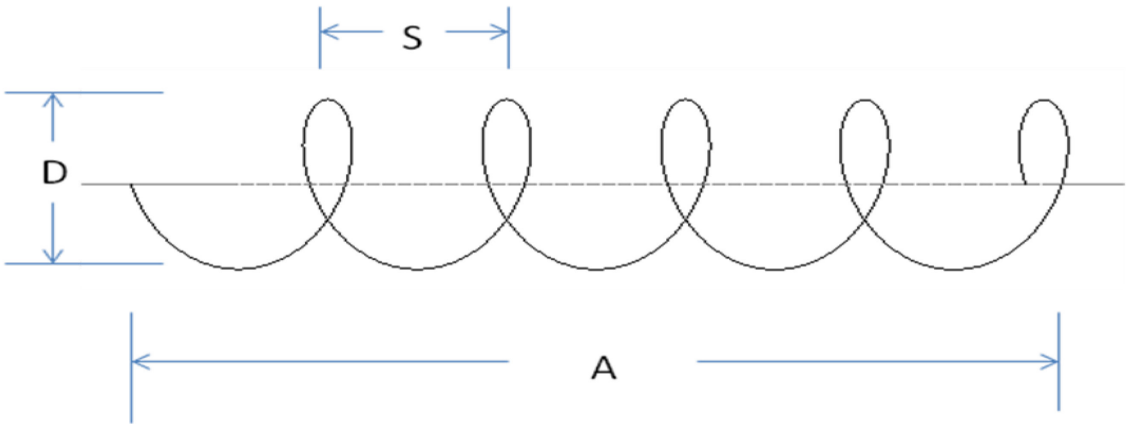

Figure 4.1 Axial mode helix geometry

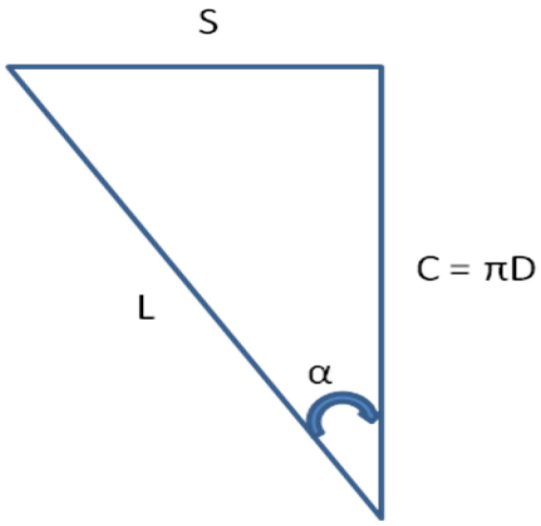

Figure 4.2 The relationships between S, C, D, L and α

If the helix has many turns, circular polarization is transmitted from the antenna. Also, the main beam narrows as more turns are added. This antenna works well over the frequency range corresponding to [12]

$$\frac{3}{4}\lambda \leq C \leq \frac{4}{3}\lambda \qquad \textbf{Equation 4.1}$$

This range corresponds to a bandwidth ratio of 1.78:1

Kraus [16] studied the axial-mode helix in depth and came up with many different approximations for helices with three turns or more and pitch angles between twelve and fifteen degrees.

The half-power beamwidth in degrees is given by [12]

$$HP = \frac{65^{\circ}}{\frac{C}{\lambda}\sqrt{N\frac{S}{\lambda}}} \qquad \textbf{Equation 4.2}$$

where C is the circumference of one turn, N is the number of turns, and S is the spacing between turns.

The gain of the axial-mode helix is calculated from the empirical formula (not in dB) [12]

$$G = \frac{26{,}000}{HP^2} = 6.2\left(\frac{C}{\lambda}\right)^2 N\frac{S}{\lambda} \qquad \textbf{Equation 4.3}$$

The axial-ratio of the antenna is [12]

$$|AR| = \frac{2N+1}{2N} \qquad \textbf{Equation 4.4}$$

Finally, the input resistance is given by [12]

$$R_A = 140\frac{C}{\lambda}\Omega \qquad \textbf{Equation 4.5}$$

The input impedance of a properly designed axial-mode helix is resistive due to the traveling wave behavior of the helix.

The desired helix element has a 90 degree HPBW while maintaining approximately 2-to-1 operational bandwidth. The circumference, C, is fixed at one wavelength in order to produce the desired endfire beam. Also, the pitch angle of the antenna, α, is confined between the angles of 12 to 15 degrees in order to achieve optimal performance according to Kraus [16]. Therefore, the only parameter that can be changed in Equation 4.2 in order to get the desired 90 degree beamwidth is N, the number of turns in the helix. This value must be decreased to achieve the HPBW required. However, once N is decreased below three, all of the above approximation equations may no longer apply. A full-wave simulation using software such as FEKO must be used to design the proper antenna element.

4.2.2 FEKO Designed Element

The initial starting point of this design consisted of creating a 10-turn axial-mode helix with the software package FEKO. This antenna was designed at a center frequency of 8 GHz with a helix circumference equal to 0.92λ. The pitch angle was set to 13 degrees. The goal of this design was to compare full-wave simulation results to reference results in order to validate the use of FEKO as a proper design tool for this problem. According to Equation 4.1 through Equation 4.5 above, this 10-turn helix antenna should have the following properties.

3-dB Beamwidth	48°
Maximum Gain	10.5 dB
Axial Ratio	1.05
Input Resistance	128.8 Ω

Table 4.1 Helix element design parameters

This antenna element was simulated in FEKO, and is shown in Figure 4.3 below. Far-field patterns as well as S-parameters were calculated to show the results of the full-wave simulation. The FEKO results are very close to the textbook calculations, validating the use of FEKO as a proper tool for this antenna design. The gain, beamwidth, and axial ratio are almost exactly the same as the textbook values. The impedance from FEKO differs by 17%, but this could be because an infinite ground plane approach was used in FEKO. Figure 4.4 and Table 4.2 show the simulated results reported by FEKO.

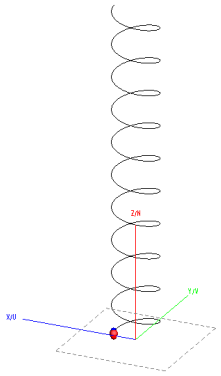

Figure 4.3 10-turn axial mode helix designed at 8 GHz

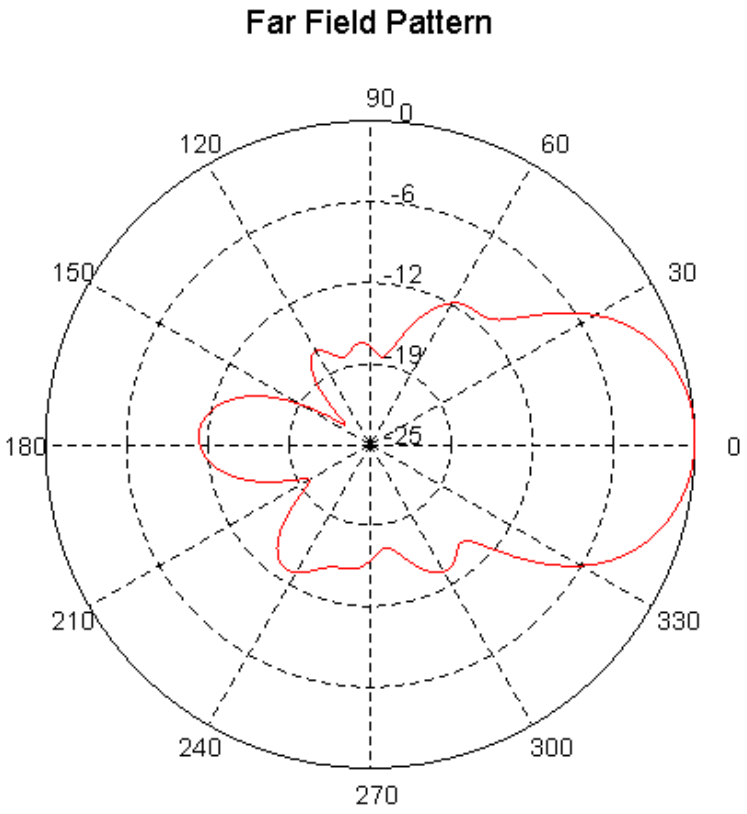

Figure 4.4 Far-field pattern of 10-turn helix at 8 GHz

3-dB Beamwidth	46°
Maximum Gain	11.0 dB
Axial Ratio	0.94
Input Resistance	153 Ω

Table 4.2 10-turn helix parameters at 8 GHz

To increase the HPBW to the desired 90 degrees, the 10-turn element was decreased to a 1-turn element. Also, the helix circumference was set to equal one wavelength. All other parameters remained the same. FEKO results are shown.

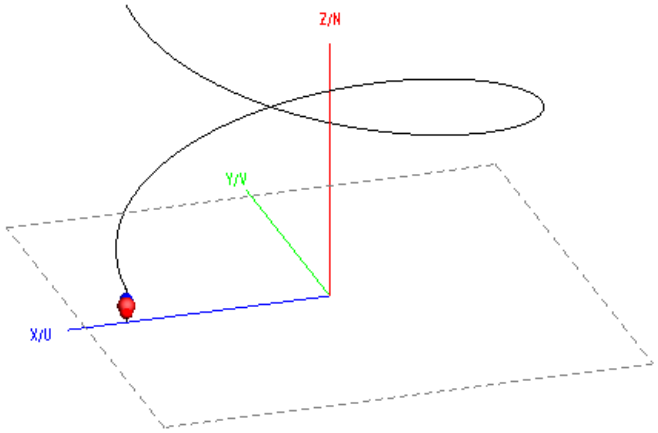

Figure 4.5 1-turn axial mode helix

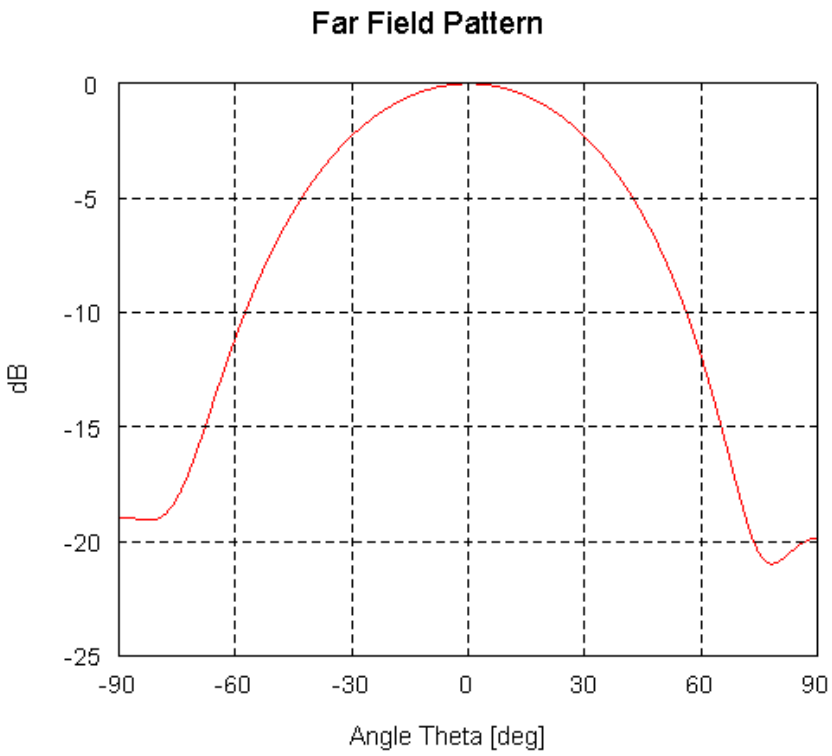

Figure 4.6 1-turn helix far-field pattern

The HPBW has increased to 68° but at the expense of input impedance. Because the element is so short, the element is not acting in its usual traveling wave manner. There is a large capacitive component in the input impedance which is very undesirable. However, this may be overcome with a suitable matching network. Also, this element is not very stable over the 2-to-1 bandwidth. Polarization is highly variable over the half-space with near linear polarization forming in the axial direction.

3-dB Beamwidth	68°
Maximum Gain	8.4 dB
Axial Ratio	0.16
Input Resistance	297.8 - j284.1 Ω

Table 4.3 FEKO obtained parameters for 1-turn helix

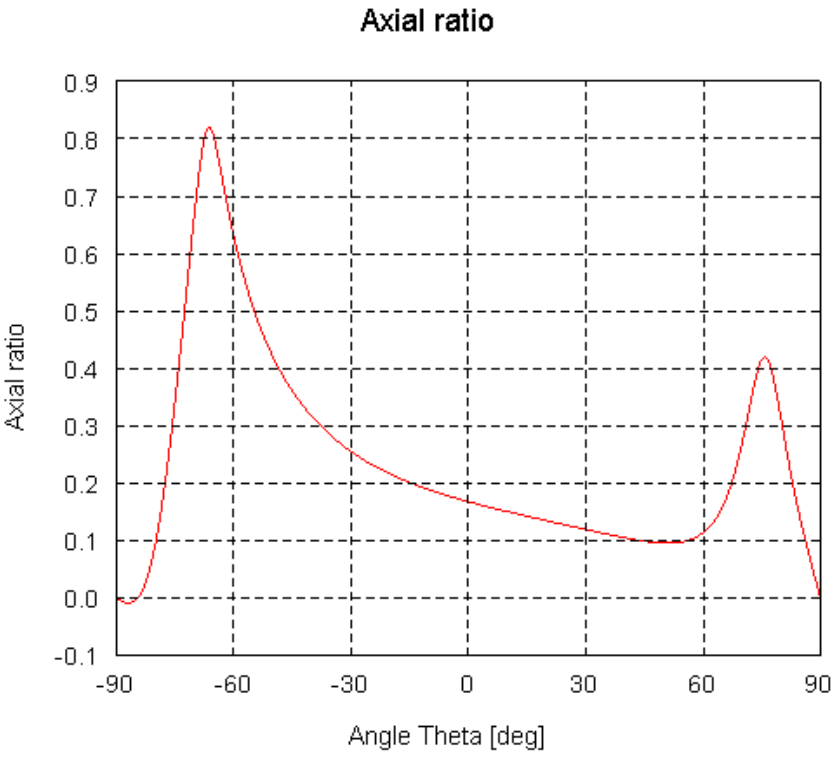

Figure 4.7 Axial ratio of 1-turn helix versus angle in space

As shown above, there is a tradeoff between impedance performance and beamwidth. Wider beamwidth requires a shorter antenna, which in turn produces poorer input impedance. This is a standard antenna trade-off problem. Because of these competing issues, an ideal 2-to-1 bandwidth helix antenna with 90 degree HPBW could not be achieved. Tradeoffs had to be made in order to create a realistic antenna element.

The final design consisted of a 2-turn axial mode helix, designed at a center frequency of 8 GHz. This antenna had a pitch angle of 13 degrees and a helix circumference equal to one wavelength. FEKO results for this design are shown below in Figure 4.8 through Figure 4.12

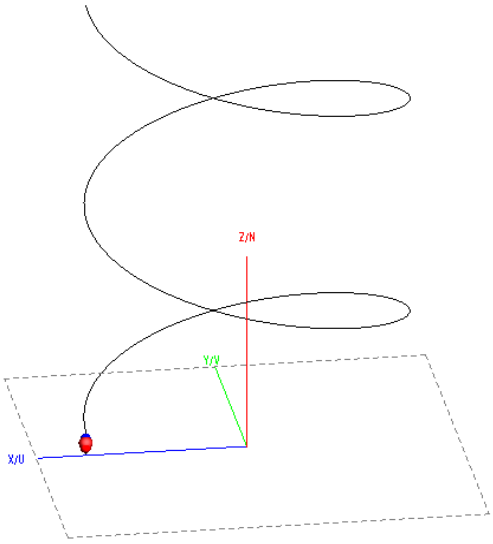

Figure 4.8 2-turn axial mode helix designed at 8 GHz

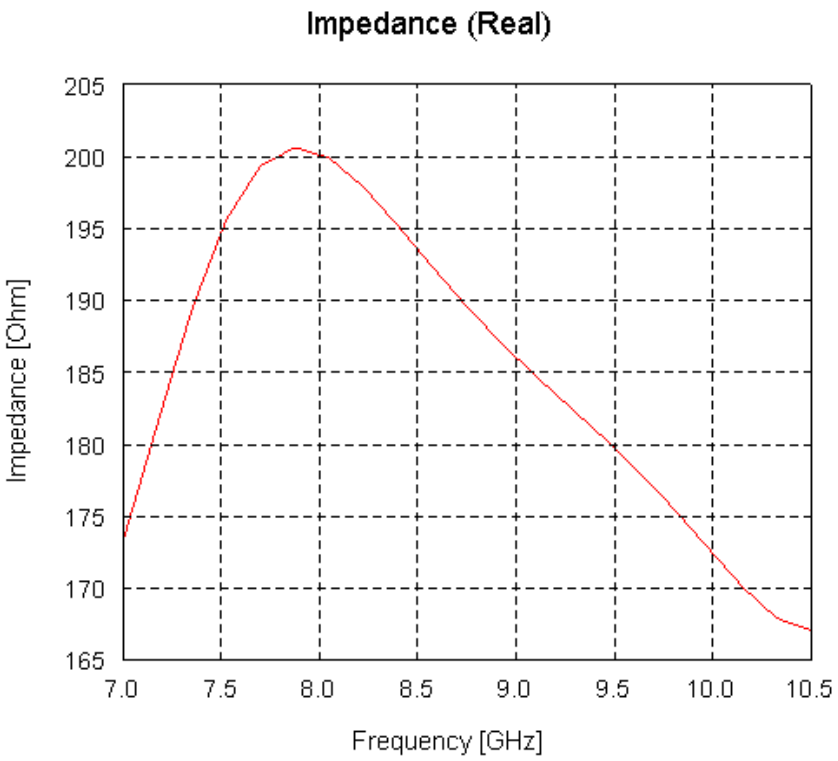

Figure 4.9 Resistive impedance of 2-turn helix vs. frequency

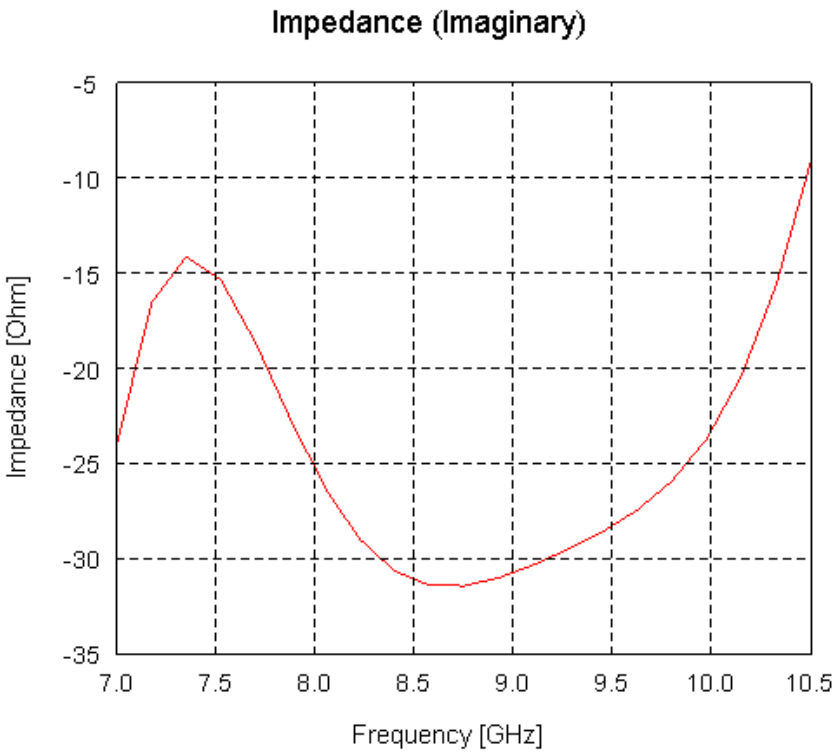

Figure 4.10 Reactive impedance of 2-turn helix vs. frequency

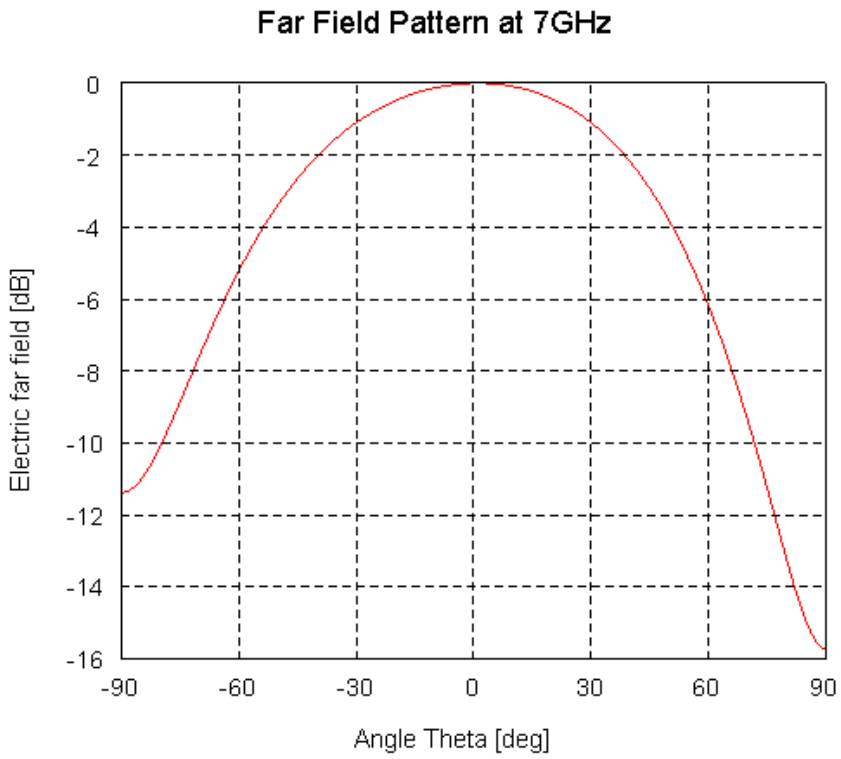

Figure 4.11 Far-field pattern of 2-turn helix at 7 GHz

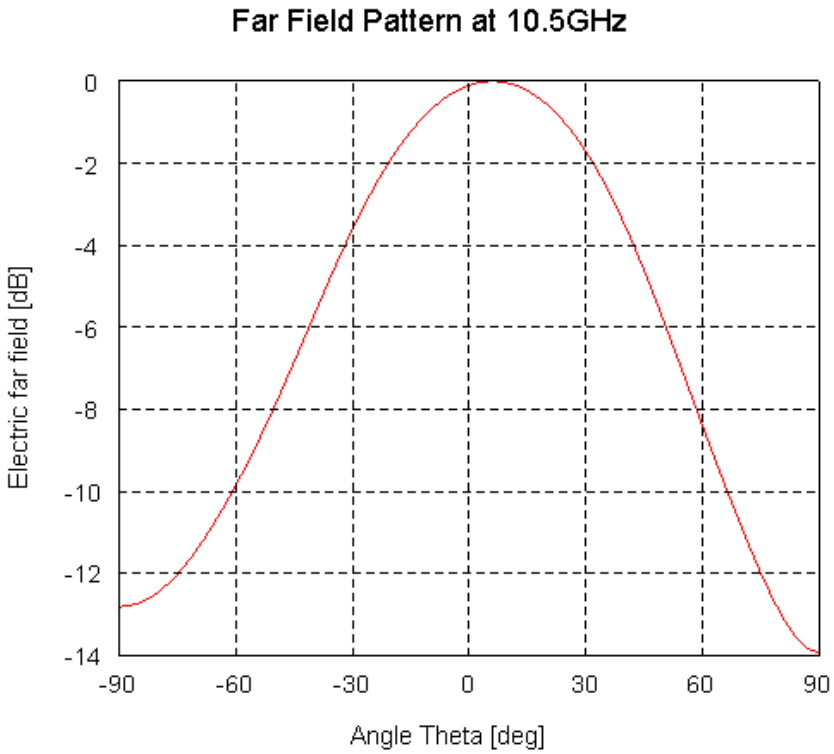

Figure 4.12 Far-field pattern of 2-turn helix at 10.5 GHz

As the figures show, this helix maintains greater than 60 degree HPBW with a fairly constant input impedance over a 1.5-to-1 bandwidth. The far-field pattern also stays relatively constant over this range. This antenna was chosen as the final design antenna to consider in the aperiodic array. Table 4.4 below summarizes the properties of the final antenna design.

Frequency Range, f_L - f_U	7.0 GHz - 10.5 GHz
Bandwidth Ratio, BW	1.5-to-1
Scanning Ability, θ	±30°
Design Frequency, f_C	8 GHz
Helix Circumference, C	One wavelength (λ) at 8 GHz
Pitch Angle, α	13°

Table 4.4 Final 2-turn axial mode helix design values

4.3 Mutual Coupling Analysis

4.3.1 Mutual Coupling Theory

Mutual coupling is defined as the electromagnetic interaction between individual elements of an array. Up to this point, we have assumed an ideal array, one in which pattern multiplication is valid and where the individual elements are isolated and do not interact with each other. In a realistic array, elements interact with each other and alter the currents and impedances that would otherwise exist if the elements were isolated. This interaction changes the current magnitude, phase, and distribution on each individual element, changing the far-field pattern completely from the ideal case [12]. Depending on the type of element used and the spacing between elements, mutual coupling can range from significant to negligible. Typically, if the spacing between elements is half a wavelength or greater, mutual coupling isn't an important issue for most antenna elements. To properly account for mutual coupling in a large area is a very complex problem, requiring very large impedance matrices to account for the coupling between each individual element. The impedance matrix is set up using traditional circuit analysis [12].

$$V_1 = Z_{11}I_1 + Z_{12}I_2 + \cdots + Z_{1N}I_N$$
$$V_2 = Z_{12}I_1 + Z_{22}I_2 + \cdots + Z_{2N}I_N \qquad \textbf{Equation 4.6}$$
$$V_N = Z_{1N}I_1 + Z_{2N}I_2 + \cdots + Z_{NN}I_N$$

where V_N and I_N are impressed voltage and current on the n^{th} element. Z_{nn} is the self-impedance of the n^{th} element when all of the other elements are open-circuited. Z_{mn} is the mutual impedance between the two terminals of element m and n. It is defined as [12]

$$Z_{mn} = \frac{V_m}{I_n} \qquad \textbf{Equation 4.7}$$

which assumes all terminals of the other elements are open-circuited.

Mutual impedance between elements in a large array is very difficult to calculate. Numerical techniques such as Moment of Methods can be used to calculate mutual impedance, but the process is long and computationally complex. Therefore, this thesis assumes a minimum spacing between any two elements of half a wavelength at the lower frequency of operation and a helix element that exhibits low mutual coupling. This allows us to claim that mutual coupling is negligible, and thus the complex computations can be avoided. A full-wave simulation using the software package FEKO is used to justify this claim.

4.3.2 FEKO Mutual Coupling Analysis

The software package FEKO was used to prove that mutual coupling at half-wavelength spacing is negligible for the particular antenna element used in this study. The helix element from Section 4.2 was used as the antenna element to be considered in this study.

Frequency Range, f_L - f_U	7.0 GHz - 10.5 GHz
Bandwidth Ratio, BW	1.5-to-1
Scanning Ability, θ	±30°
Design Frequency, f_C	8 GHz
Helix Circumference, C	One wavelength (λ) at 8 GHz
Pitch Angle, α	13°

Table 4.5 Final 2-turn axial mode helix design values

The input impedance of the antenna was measured at the lower operating frequency of 7 GHz. The measure was taken at 7 GHz because this is the frequency where the spacing of the array will be half a wavelength. The input impedance was calculated to be 173.2 - j23.96 at 7 GHz. In order to prove that mutual coupling is not a major issue at this frequency and spacing, the input impedance must not change dramatically when placed in an array of identical elements spaced half a wavelength apart. In addition, the impedance must not change drastically as the antenna array is scanned from broadside. The more the input impedance changes, the more coupling that is occurring between the elements. An array of 5 helix elements was designed and analyzed using FEKO to investigate the effects of mutual coupling between helix elements. Figure 4.13 below shows the physical arrangement of the array.

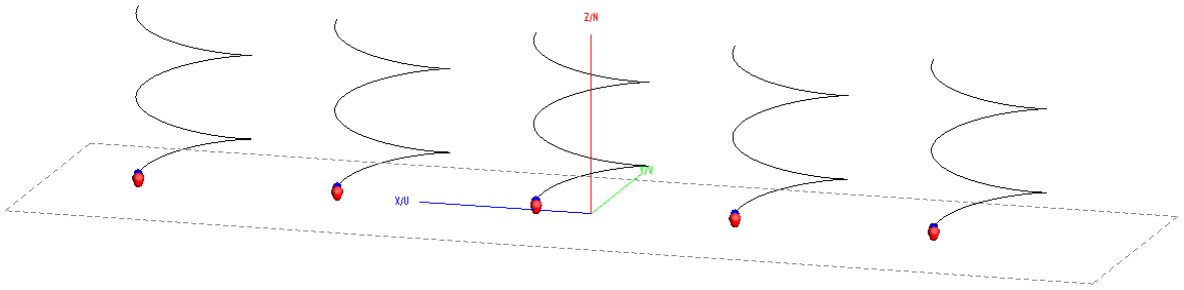

Figure 4.13 5 element periodic array used to test mutual coupling

Each element in this array is spaced periodically half a wavelength from its neighbor. A full-wave simulation was performed on this array at broadside to calculate the input impedance of each individual element in the array. Table 4.6 summarizes the findings. The elements are numbered one to five starting from left of Figure 4.13.

$Z_{in}1$	184.1 - j55.8 Ω
$Z_{in}2$	143.5 - j100.1 Ω
$Z_{in}3$	185.8 - j76.2 Ω
$Z_{in}4$	144.1 - j102.1 Ω
$Z_{in}5$	179.5 - j51.7 Ω

Table 4.6 Input impedance of individual elements in array at broadside

As the data shows, the center element's input impedance has changed from 173.2 - j23.96 Ω to 185.8 - j76.2 Ω with the addition of the four other elements. This shows that the additional

elements are coupling to the center element; however, the input impedance has changed only slightly. This helps justify that coupling is not a major factor with these elements at half-wavelength spacing.

To further justify this claim, the five element array was electronically scanned to determine the effect on input impedance. Significant coupling should cause the input impedance of each individual element to change significantly during antenna scanning. A full-wave simulation in FEKO was performed where each individual element was fed a 45° progressive phase shift in relation to its neighbor, with a resulting scan angle of 15 degrees in azimuth. Table 4.7 summarizes the results.

$Z_{in}1$	158.2 - j49.1 Ω
$Z_{in}2$	185.6 - j100.7 Ω
$Z_{in}3$	157.5 - j86.8 Ω
$Z_{in}4$	159.7 - j71.4 Ω
$Z_{in}5$	200.5 - j61.6 Ω

Table 4.7 Input impedance of individual elements in array during scanning

Table 4.8 below shows the difference in impedance between the broadside and scanned case. The magnitude of the impedances was calculated for both cases and the percentage difference between them is shown.

$Z_{in}1$	-13.9 %
$Z_{in}2$	+20.0 %
$Z_{in}3$	-10.5 %
$Z_{in}4$	-1.0 %
$Z_{in}5$	+12.3 %

Table 4.8 Input impedance magnitude change from broadside to scanned array

This data shows that the input impedance is not largely affected by the phase shift across the antenna array as the beam is scanned. The imaginary part of the impedances remained capacitive and did not change greatly. Therefore, it can be claimed that mutual coupling is not a major factor at a minimum spacing of half-wavelength between elements. This data serves as a first check to justify the claim that mutual coupling is not a major issue. Section 5.4 shows a full-wave simulation of the optimized array and compares it to the theoretical MATLAB prediction. This full-wave antenna pattern takes into account mutual coupling between all of the elements, further justifying this claim.

4.4 Minimum Spacing Constraint

As mentioned in Section 4.3, mutual coupling can be ignored in this analysis if the minimum spacing between elements is set to half a wavelength at the lowest frequency of operation. In a periodic array, this would create an array factor with low sidelobes, high gain, and scanning ability up to ±90° with no introduction of grating lobes into the visible region. However, such arrays can only operate over a very small bandwidth. If the operating frequency is increased, the electrical spacing between elements will become greater than half a wavelength, and grating

lobes will appear. If the frequency is decreased, the electrical distance between elements will decrease, and mutual coupling will become a major factor. Because of these reasons, periodic arrays are not well suited for high bandwidth applications [12].

In this thesis, the goal was to design a 2-to-1 bandwidth array with scanning ability of ± 45°. Section 4.2 showed the design of the individual helix element. It was shown that the element could achieve only 1.5-to-1 bandwidth and a scanning ability of ± 30° in azimuth. This requirement is still considered high bandwidth, and a periodic array would not be able to perform adequately because the large inter-element spacing would introduce a grating lobe into the visible region. Therefore, there must be a minimum spacing requirement enforced on the array to allow for high bandwidth applications. To achieve 1.5-to-1 bandwidth and maintain a minimum spacing of half a wavelength at the lower frequency, a minimum spacing of 0.75 wavelengths at the highest operating frequency must be enforced. This requirement allows the minimum spacing to be a half-wavelength at the lower operating frequency.

MATLAB software was used to develop an algorithm for maintaining this minimum spacing between elements. Elements are originally placed at random across the array aperture. The function iteratively checks each set of spacings to determine if each satisfies the minimum spacing requirement. If not, the elements are moved accordingly and the remaining elements are shifted. This process continues, pushing elements back and forth until all distances satisfy the minimum spacing requirement. It is worth noting that during this process, the overall dimension of the array does not change. The first and last element of the array remain at fixed locations, locking in the total size of the array. If too many elements exist and cannot fit within the given dimensions, a flag is thrown and the software decreases the number of elements being used. Figure 4.14 shows an example of a random distribution of elements. This array is then processed with a minimum distance between elements of a half-wavelength. Figure 4.15 shows the algorithm operating, pushing elements in order to satisfy the minimum spacing requirement.

Figure 4.16 shows another iteration of the function as more elements are separated. Finally, Figure 4.17 shows the final result; the same sized array but with the minimum spacing requirement satisfied. In this specific example, the array becomes a periodic array with half wavelength spacing between elements. This is because the total dimension of the array is fixed and the number of elements used, combined with the minimum spacing constraint, causes it to become periodic.

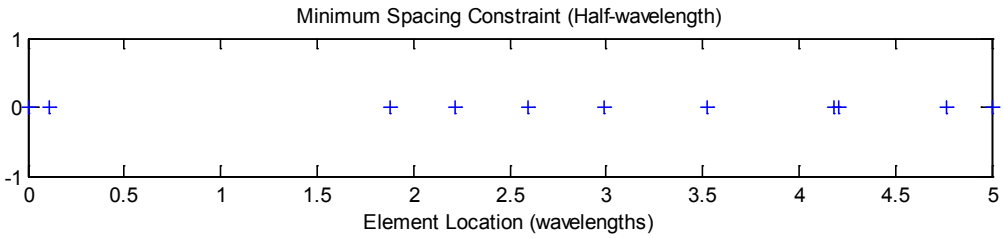

Figure 4.14 Elements randomly distributed across array aperture

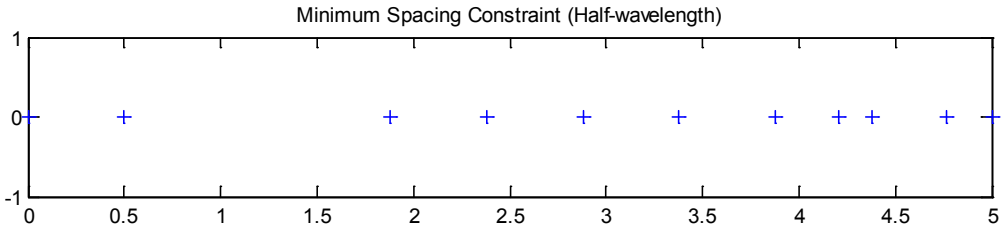

Figure 4.15 Algorithm working to enforce minimum distance constraint

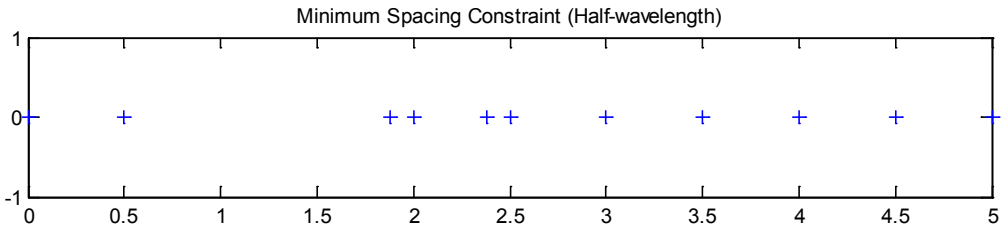

Figure 4.16 Elements pushed and pulled to maintain minimum distance constraint

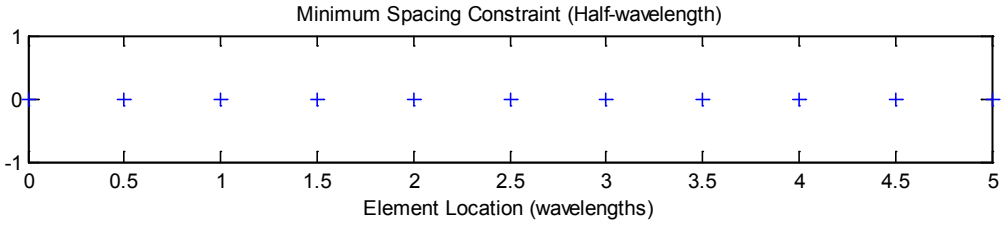

Figure 4.17 Final array satisfying minimum distance constraint

4.5 Design of Particle Swarm Optimizer

4.5.1 Particle Swarm Algorithm

As mentioned in Chapter 3, Particle Swarm Optimization, or PSO, is a semi-heuristic method of searching the solution space for an optimal answer to a given problem. In this thesis, the location of the individual elements in the array is what is being optimized. All elements are assumed to be axial-mode helices from Section 4.2. Each element is fed with equal amplitude so

that no complex amplitude tapering is required. Each element must maintain a minimum distance of 0.75 wavelengths from its neighbors while the maximum dimension of the array remains constant. All of these special requirements warrant the unique design of a particle swarm optimizer. This section describes all assumptions and techniques used to design the PSO.

In this study, the maximum dimension of the array is set to 60 wavelengths. With a minimum distance between elements set to 0.75 λ at 10.5 GHz, a total of 81 elements can fit within the dimensions of this array. If 81 elements are used, elements are spaced equally 0.75 λ apart and the array is considered periodic. The optimizer initially thins the array by one element, allowing 80 element locations to be optimized. The PSO initializes 70 particles with random locations and velocity vectors in this 80-dimensional hyperspace. The particle locations are constrained between zero and one in each dimension. The particle velocities are constrained between -1 and 1 in each dimension. Each particle's 80 element position vector is mapped to 80 antenna element locations on the array. Therefore, each of the 70 particles represent a unique antenna array, with variable antenna element locations. Each particle, or array, is scored based on how well it solves the problem. The fitness function, as it is called, is proportional to the absolute value of the maximum sidelobe value. This was chosen as the fitness criterion because of the desire to eliminate the grating lobe that would occur in the periodic array with equal bandwidth. The lower the sidelobe level, the higher the score. Each particle in the optimizer is scored and the best performer is identified as the initial global best [13].

Now the particles are flown through the solution space for 1000 iterations. During each iteration, each particle's velocity is updated separately along each dimension according to velocity update rules. These velocity update rules are shown below in Equation 4.8 [13].

$$V_{new} = \omega * V_{old} + \Phi_1 * rand * (X_{local\_best} - X_{current}) + \Phi_2 * rand * (X_{global\_best} - X_{current}) \quad \textbf{Equation 4.8}$$

There are three components that contribute to the new velocity. The first is called inertia. This is represented by the constant ω and is the tendency of the particle to continue moving in its initial direction. Much research has been done into the value of ω and how to make it optimal. In this thesis, ω is taken to be a constant 0.4 throughout the entire optimization due to Boeringer's suggestion [13]. The second component of the velocity rule in Equation 4.8 is a linear attraction toward the best location ever found by that individual particle. This location is called the local best. Each particle remembers its own personal best location as well as the best location of the entire 70 particle swarm. This linear attraction is represented by the constant Φ_1 multiplied by a random value ranging from zero to one. The third component represents a linear attraction toward the best location found by any particle in the swarm, called the global best. This is also known as group knowledge, since every particle in the swarm knows the location of this best solution. This is represented by Φ_2 multiplied by a random value from zero to one. Much like ω, the optimal values of Φ_1 and Φ_2 have been debated constantly. In this thesis, Φ_1 and Φ_2 are set to a constant of two throughout the entire optimization process. This allows the particles to equally benefit from their own discoveries as well as the discoveries of the entire swarm. It is worth noting that the resulting velocity is clipped if $|V| \geq 1$. If this is the case, the velocity is set to either -1 or +1 along each separate dimension, depending on its initial direction of travel [13].

The next step in the optimization process is to update the new position of the particles. The position equation below is used to update the new location. X_{new} represents the new updated location, X_{old} is the particle's previous location, and $V_{current}$ represents the particle's current velocity vector. A unit time step is assumed.

$$X_{new} = X_{old} + V_{current}*t \qquad \textbf{Equation 4.9}$$

Just like the velocity, if the position does not stay within the boundary of zero to one, the new position is clipped to stay within this range. Each particle's new location is then mapped to antenna element locations on an array and the far-field pattern is calculated and scored. If the particle's fitness is the highest it has ever achieved, then this location is updated as the new local best. Also, if the particle's fitness is the highest ever achieved in the entire swarm, then this particle is also updated as the new global best.

After 1000 iterations, the final global best is taken as the optimal array solution. The optimizer then restarts the entire process, thinning the array by one more element and repeating the entire algorithm. This process continues for a fixed number of iterations set by the user. The end result is a thinned array with aperiodic spacings that has a more desirable far-field pattern than the periodic counterpart [13].

4.5.2 Test Function

Before the optimizer was started, a test function was created in order to test the validity of the PSO. A test function is a function with a known optimal answer. This function is used as a diagnostic tool in order to see if the optimizer is able to find the optimal solution. In this thesis, the test function below was used.

$$sinc(x) * sinc(y) \qquad \textbf{Equation 4.10}$$

A two dimensional test function was chosen so that plots could be shown of the actual particles flying through the 2-dimensional solution space. The goal of this test was to find the maximum of Equation 4.10 above. It is known that this function is maximum at x = 0, y = 0. The PSO was initialized with 15 particles randomly located in the 2-dimensional hyperspace shown in Figure 4.18 below.

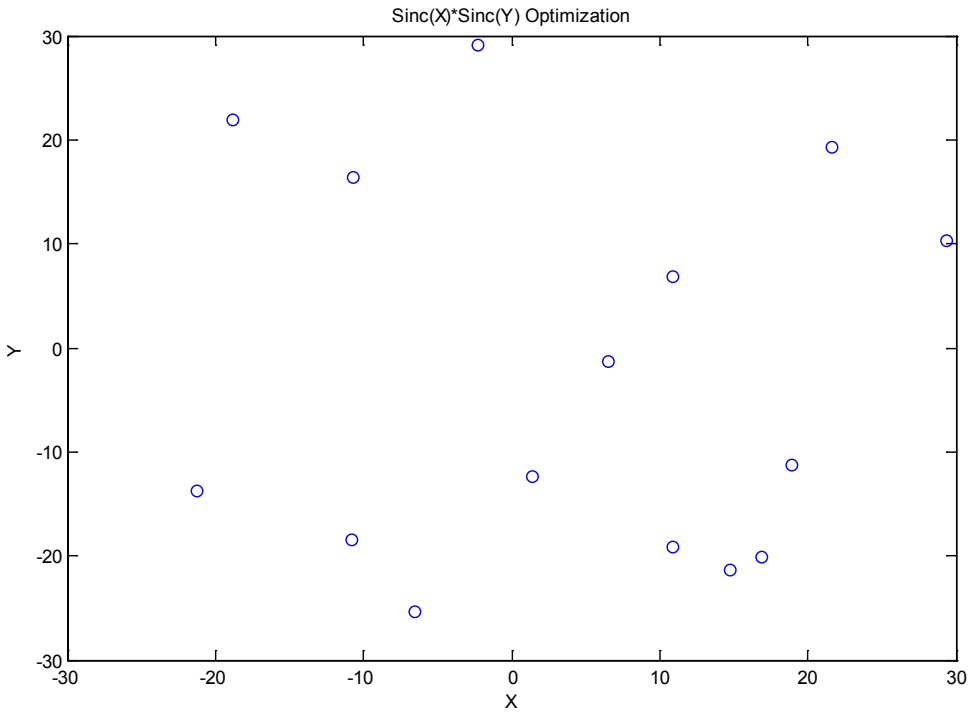

Figure 4.18 Particles placed with initial random locations

The algorithm was initiated and the particles began to fly through the solution space, updating positions based on the rules described above. Figure 4.19 below shows the locations of the particles after only 10 iterations. As can be seen in Figure 4.19, they are starting to move towards the (0,0) location.

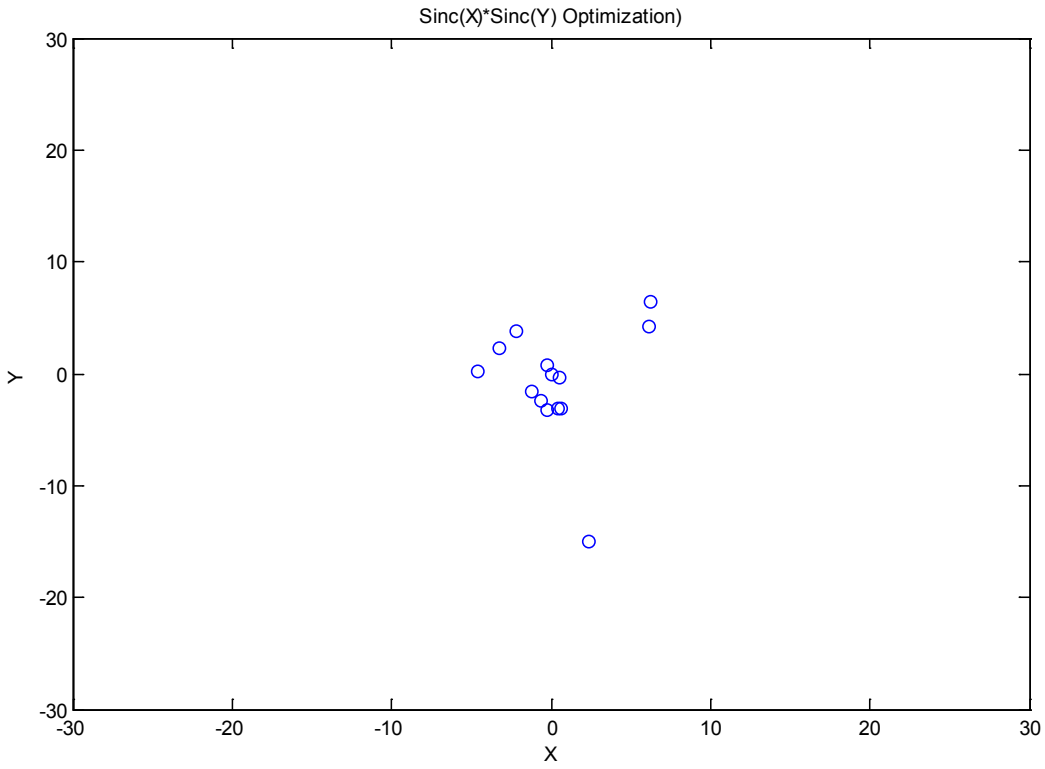

Figure 4.19 Particle's locations after 10 iterations

After 25 iterations, the particles are swarming around this optimal location. They are using their own self knowledge, as well as group knowledge, to be linearly attracted to this location.

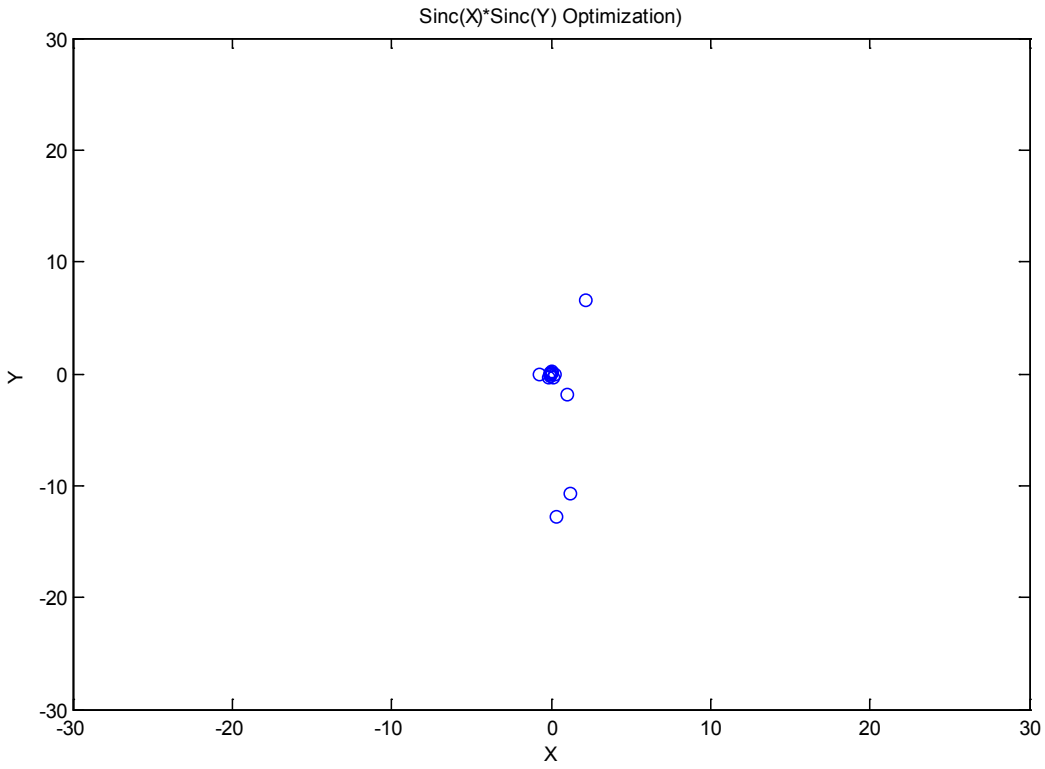

Figure 4.20 Particle's locations after 25 iterations

Finally, after only 50 iterations, the particles have completely converged and found the optimal answer. This test function shows that the algorithm is working properly, and the optimizer is able to find the best solution to any problem that it is given.

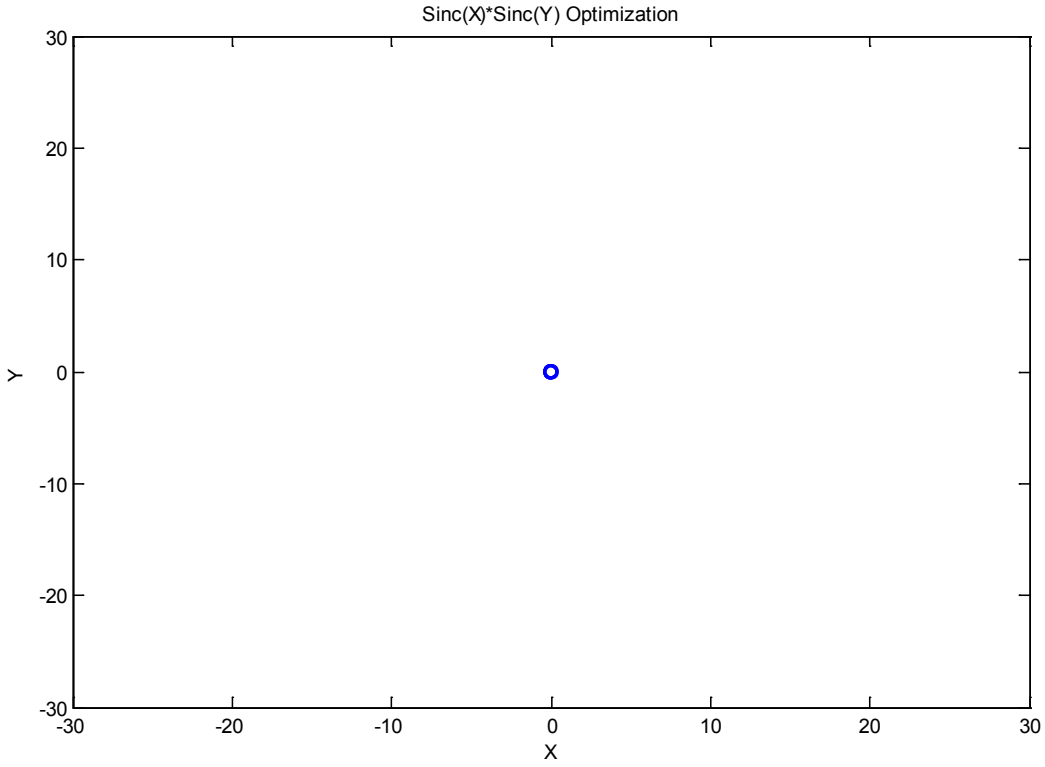

Figure 4.21 Plot showing final convergence of particles to optimal location after 50 iterations

4.6 Fitness Function

4.6.1 Array Factor Method

The fitness function is defined as a function which determines whether the optimizer has found a good or bad solution to the problem. The fitness function in this study is based on sidelobe level. The lower the sidelobes, the higher the solution is scored. In order to calculate sidelobe level and beamwidth, the array factor must be calculated for each individual candidate array. MATLAB code was written which takes any arbitrary array factor and calculates the maximum sidelobe level and half-power beamwidth. The optimizer then takes this data and assigns a fitness to the array. This process continues throughout the entire optimization algorithm, as discussed above in Section 4.5.

To calculate the fitness, the array factor must first be calculated using Equation 4.11 below [12].

$$AF = A_0 \sum_{n=0}^{N-1} e^{jn\psi} \qquad \textbf{Equation 4.11}$$

where A_0 is the uniform amplitude excitation applied across the array and

$$\psi = \beta d \cos\theta + \alpha \qquad \textbf{Equation 4.12}$$

where α represents the progressive phase shift applied across the array.

Once the array factor is calculated, it is normalized and converted to decibels (dB). This pattern is then plotted in a MATLAB graph for viewing before the calculations are completed. Figure 4.22 below shows an example of a 21 element uniformly illuminated periodic array

pattern that is produced from this code. This array assumes isotropic antennas as the radiating element.

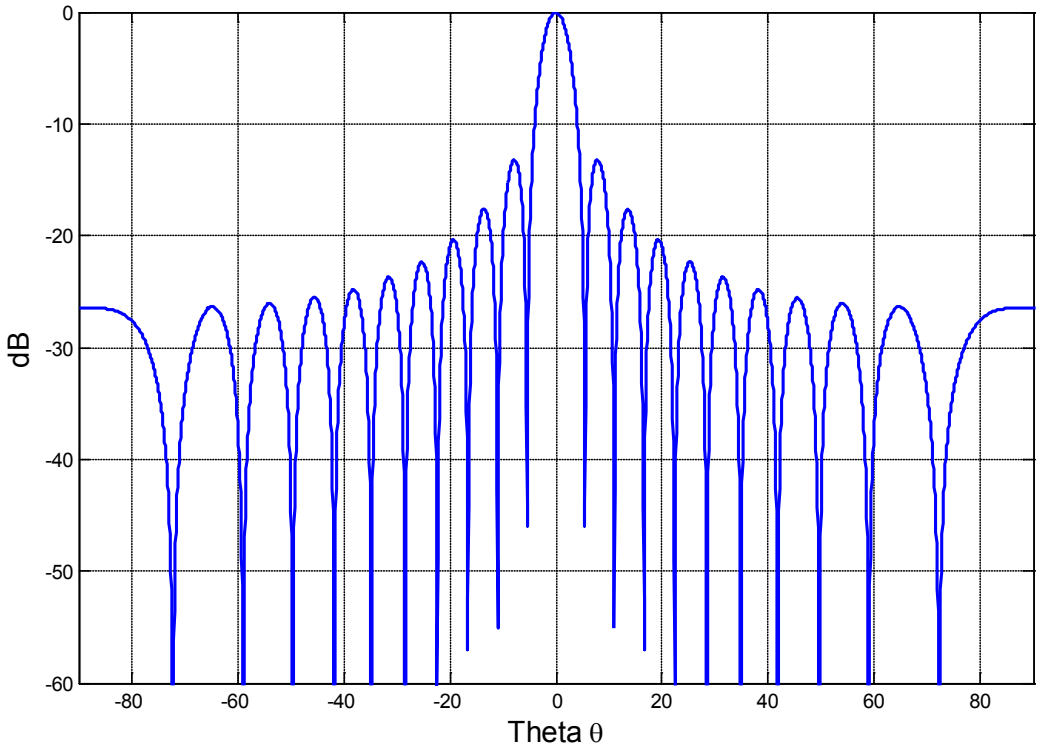

Figure 4.22 Far-field pattern produced by MATLAB code for a uniform array

The next step is to calculate the beamwidth of the pattern. Since the maximum gain is already normalized to 0 dB, this step is very straightforward. The function starts at the

maximum value of the main beam and iteratively moves down until it reaches -3 dB on the right side of the main beam. This same process occurs on the left side of the main beam. Once the -3 dB points are found, a flag is thrown and the algorithm terminates. These two points are then matched to their respective angular positions in azimuth. These angles are then subtracted, resulting in the half-power beamwidth of the array.

Finally, the function must calculate the maximum sidelobe level of the array. Once again, the function starts at the maximum value of the main beam (0 dB) and iteratively moves down until a null is reached on the right side of the main beam. This same process occurs on the left side of the main beam. Once the two nulls are reached, a flag is thrown and the algorithm terminates. This data that the algorithm has searched through is considered to be the main beam. All of the data from the main beam is set to -100 dB, essentially notching out the main beam entirely. After the main beam is notched out, a simple maximum value search on the rest of the data finds the highest sidelobe level in the visible region. This value is considered to be the critical sidelobe level and is used in scoring the solution. Figure 4.23 below shows a notched out pattern. Figure 4.24 shows a final antenna pattern for the 21 element array with sidelobe level displayed. As shown, the sidelobe level is reported at -13.2 dB, which is the well known result for the first sidelobe level of a uniformly illuminated periodic array [12].

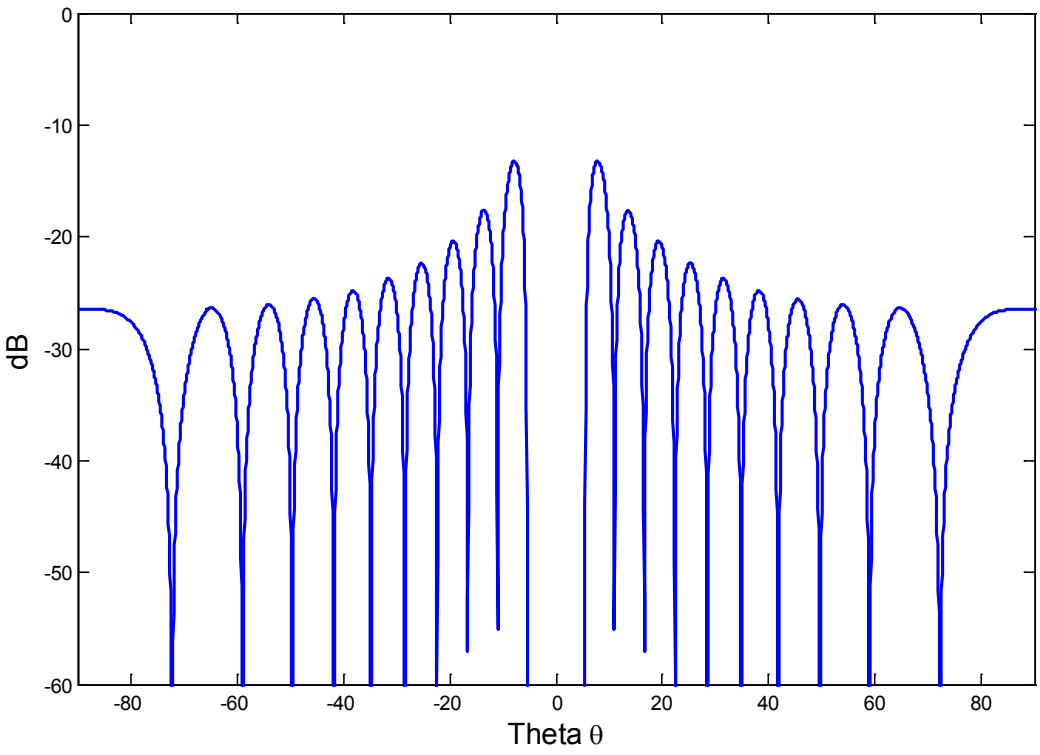

Figure 4.23 Far-field pattern of uniform array with main beam notched out

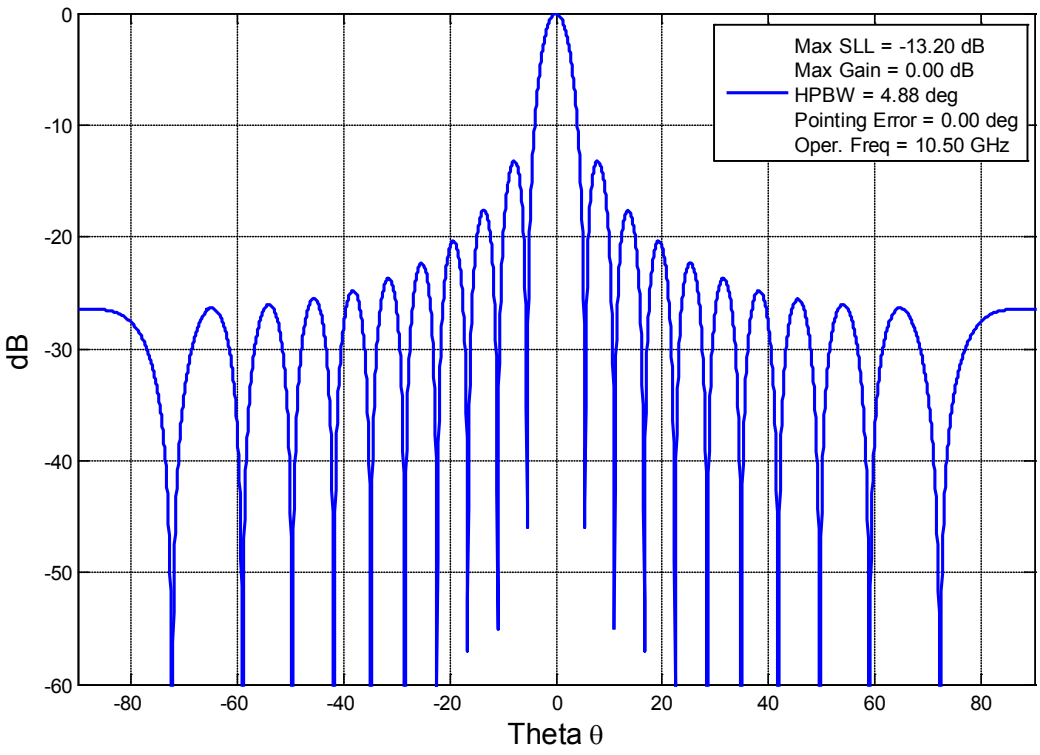

Figure 4.24 Far-field pattern of uniform array with parameters labeled

This array factor method is very accurate and gives good results. The only problem is the long computation time. Each array pattern takes several seconds to compute. Under normal circumstances this would be considered fast. However, the particle swarm optimizer requires 1000 iterations with 50 array patterns to be calculated during each iteration. In addition, the optimization process is carried out multiple times with a different sized array each time. The number of calculations quickly adds up and the entire process ends up taking days to complete.

This was the way the optimizer was originally designed in this study, but it was soon determined that this method was not practical. Each optimization took over 3 hours to complete, so a faster solution was required.

4.6.2 Fast Fourier Transform (FFT) Method

According to basic array theory, the distribution of current across an aperture is related to the far field pattern by the Fourier Transform. One can take the Fourier transform of the current distribution on the array and obtain the far-field pattern, and vice versa. Using this knowledge, the Fast Fourier Transform (FFT) was researched as a possible solution to calculating the far-field pattern of an arbitrary array much more quickly than by the array factor method. The FFT produces the same result as the Discrete Fourier Transform (DFT), only faster. MATLAB has a premade FFT function that makes the calculation of the Fourier transform quick and easy.

To calculate the far-field pattern using the FFT, the array must have periodic spacing between the elements. Figure 4.25 below shows the far-field pattern of the same 21 element uniformly illuminated periodic array as in Section 4.6.1 computed with the FFT compared to the Array Factor Method. The pattern is almost identical to that calculated using the array factor and was calculated in less than half the time.

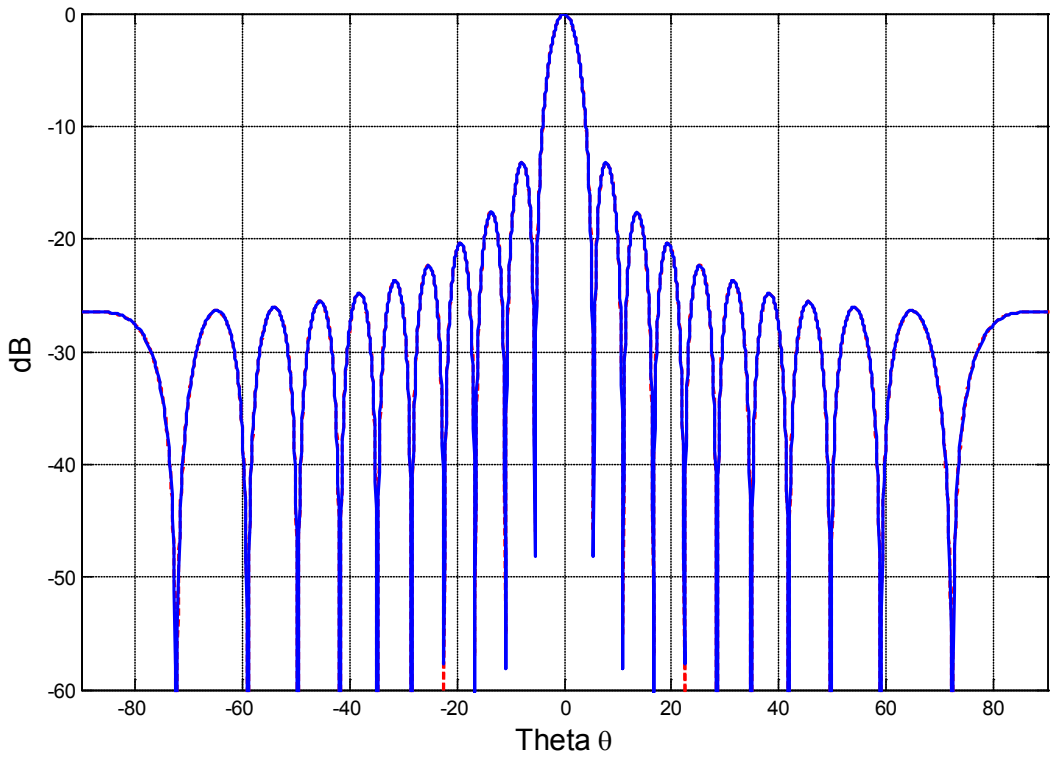

Figure 4.25 Fast Fourier Transform (FFT) far field pattern compared to Array Factor Method. FFT results are in blue (solid line). Array Factor Method results are in red (dashed line).

Tricks must be played in order to calculate the far-field pattern of an aperiodic array because of the FFT requirement for uniformly spaced data points. A fine periodic grid is designed in which antennas can be placed with a grid spacing of 0.125 λ. To make the array aperiodic, specific elements are either turned on or off to create the proper spacing. Having elements turned off allows an FFT input that is uniform and large, but mostly zeros due to the

fake elements. This allows the FFT to calculate the far-field pattern, while simultaneously having aperiodic spacing between the elements.

The result of the FFT approach to this problem is a much faster calculation of the far-field pattern. The results are almost identical to the array factor method, but many times faster. The optimization process went from taking several hours to complete, to several seconds. The results presented in the remainder of this thesis used the FFT to calculate far-field patterns during the optimization process [12].

Chapter 5

Results

5.1 Optimized Array Design

The particle swarm optimizer discussed in Section 4.5 was used to optimize an 81 element periodic reference array. The goal was to thin the array, allowing the array to become aperiodic. This aperiodic array was then optimized to achieve equal or better performance to the equivalent periodic array in terms of sidelobe level, beamwidth, bandwidth, and scanning ability. The final specifications of the array have changed slightly because of restrictions imposed by the antenna element design of Section 4.2. Table 5.1 below discusses the goals of this array design.

Frequency of Operation	7GHz - 10.5 GHz
Array Bandwidth	1.5-to-1
Azimuth Scanning Ability	±30°
Maximum Sidelobe Level	Lower than or equal to periodic array
3-dB Beamwidth	Not drastically different from periodic array
Number of Elements	Fewer than periodic array
Dimension of Array	60 λ @ 10.5 GHz
Antenna Element	2-Turn Axial-Mode Helix

Table 5.1 Design goals for optimized aperiodic antenna array

To optimize an array with the above characteristics, the PSO was set up using the following conditions. The parameter ω represents the inertia effect that is imposed on each particle. The parameters Φ_1 and Φ_2 represent attraction to the global best and the local best solution respectively. They are set equal to encourage global and well as local searching. The dimensions represent the number of things to be optimized. In this research, the dimensions represent the number of elements in the array [13].

Iterations	1000
Number of Particles	50
Ω	0.4
Φ_1	2
Φ_2	2
Dimensions	Variable

Table 5.2 Particle swarm optimization parameter values

5.2 Far-Field Pattern Results

The optimizer started by thinning the 81-element array by two elements, for a total of 79 elements. The array was then optimized and the results were saved. This process was continued until the array was thinned to the point where the performance started degrading. Each optimization included the effect of the two-turn axial mode helix and uniform amplitude tapering in the far-field pattern. The far-field pattern results are shown below.

Shown below in Figure 5.1 is the far-field pattern of the 81-element periodic reference array with 0.75 λ spacing and uniform amplitude tapering. Due to the periodicity, a grating lobe

appears as the array is scanned from broadside, shown in Figure 5.2. The grating lobe is suppressed by the element pattern but is still noticeable. Also, the overall gain of the antenna is reduced by 1.62 dB due to the element pattern as the array is scanned to +30°. The goal of the optimization process is to create an aperiodic array with fewer elements and better pattern performance than this periodic array while maintaining a 1.5-to-1 operational bandwidth.

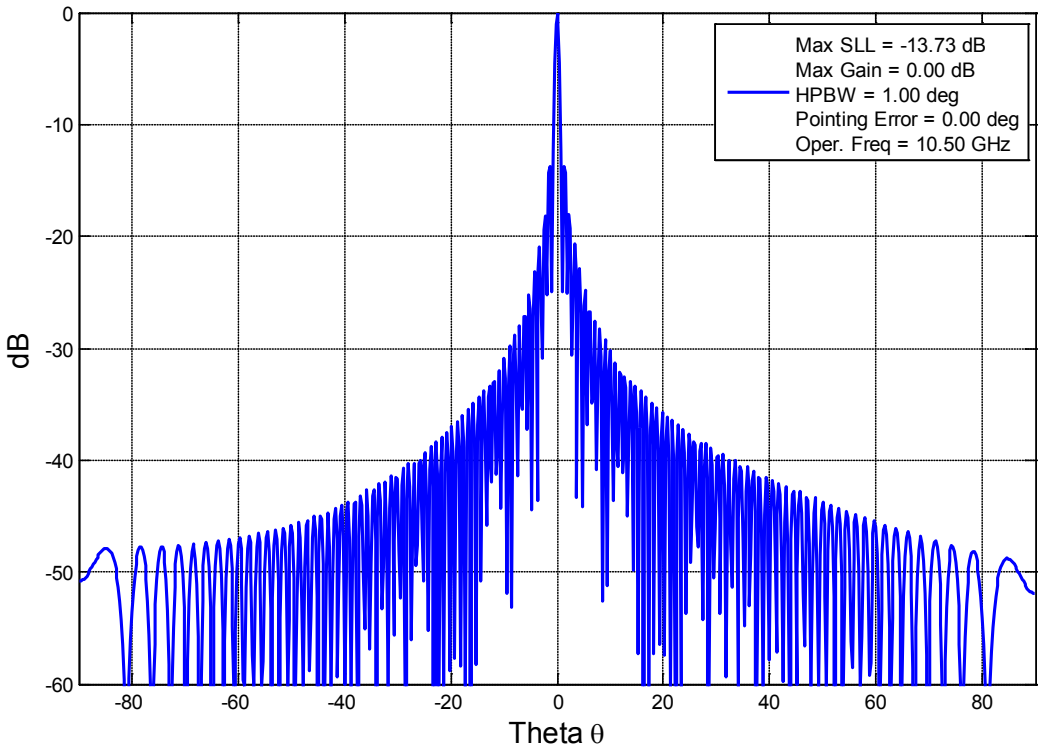

Figure 5.1 Periodic reference array with 81 elements. Element spacing is 0.75 λ.

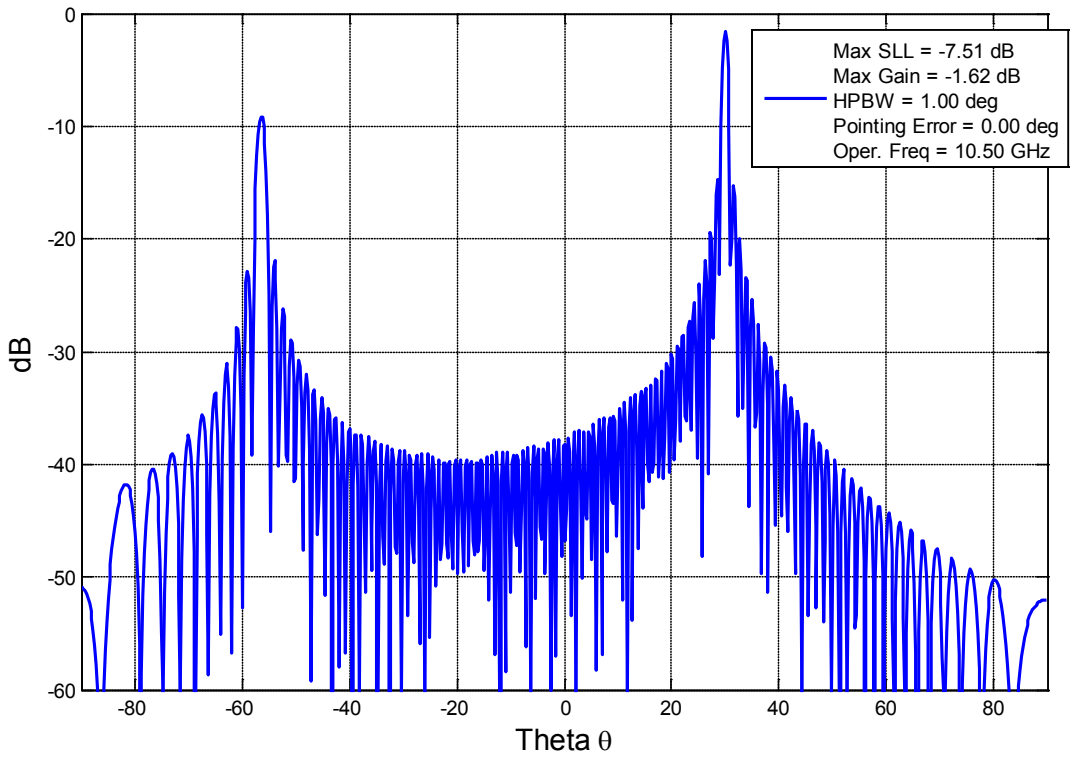

Figure 5.2 Reference periodic array with 0.75 λ spacing scanned to +30°. Grating lobe is entering the visible region

The first optimized aperiodic array pattern is shown in Figure 5.3. This array consists of 79 helical elements for a total aperture dimension of 60 λ. The locations of the elements are shown in Figure 5.5. As can be seen in Figure 5.4, the grating lobe that is introduced during scanning is reduced to -13.3 dB in the aperiodic array as opposed to -7.5 dB for the periodic array. Meanwhile, the half-power beamwidth has remained a constant 1.00 degree at broadside

and 1.13 degrees while scanned to +30°. This result shows that even thinning the array by two elements provides enough degrees of freedom to create a superior array in terms of beamwidth and sidelobe level. The minimum distance between any two elements in this array, as well as all of the other optimized arrays is set to 0.75 λ in order to ensure a 1.5-to-1 bandwidth capability. One thing to note is that the MATLAB code is only accurate to every 0.25° in half-power beamwidth. Therefore, all scanned cases should increase the HPBW proportional to the cosine of the scan angle. This change is not reflected in the MATLAB plots.

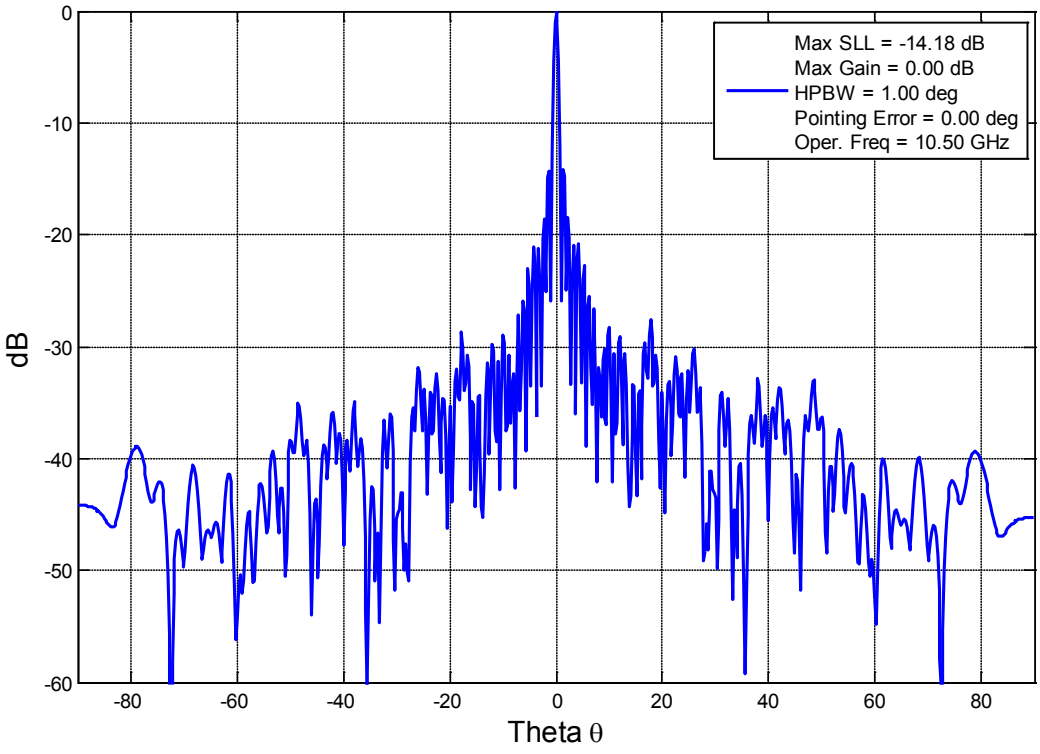

Figure 5.3 79 element aperiodic array at broadside

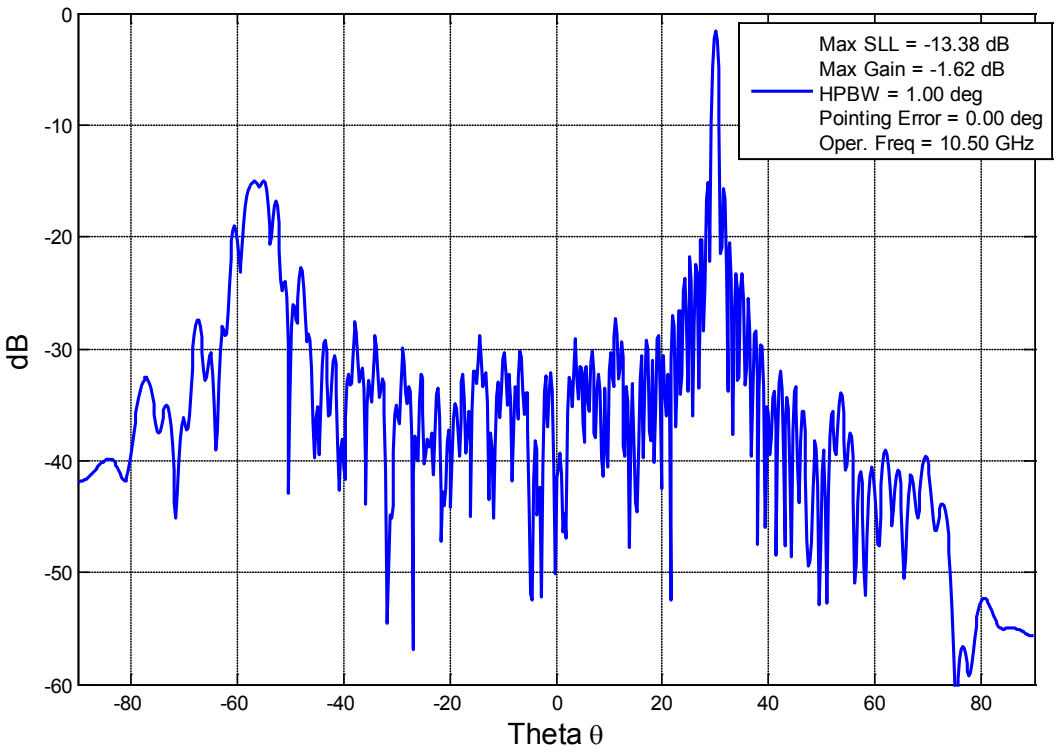

Figure 5.4 79 element aperiodic array scanned to +30°

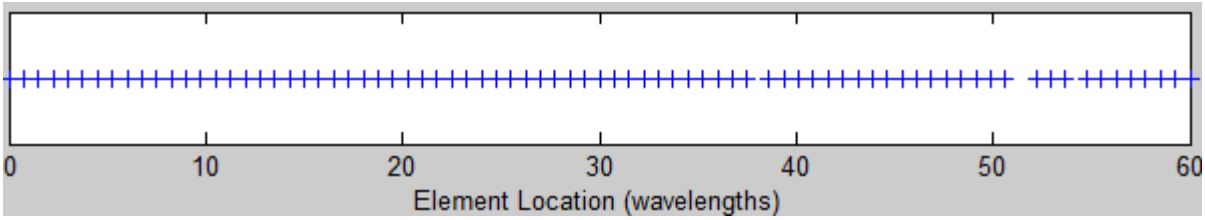

Figure 5.5 Picture showing array set up for 79 element aperiodic array.
X's represent individual element positions.

As the optimization continues, more elements are thinned and the new array is optimized. The process maintains an odd number of elements for array symmetry. Shown below is the optimized far-field pattern for an array consisting of 73 elements with uniform amplitude tapering. Once again, the HPBW has not changed drastically, staying within +0.125° of 1.00° at broadside. Also, the maximum sidelobe level has decreased, creating a new optimal array.

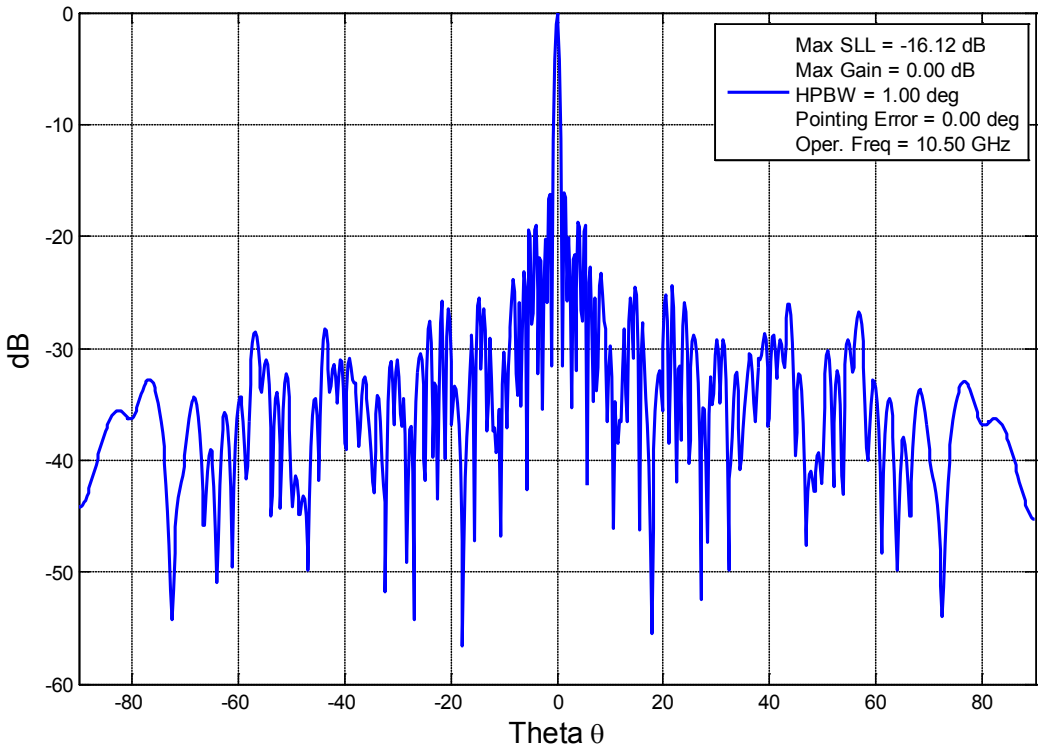

Figure 5.6 73 element aperiodic array scanned to broadside

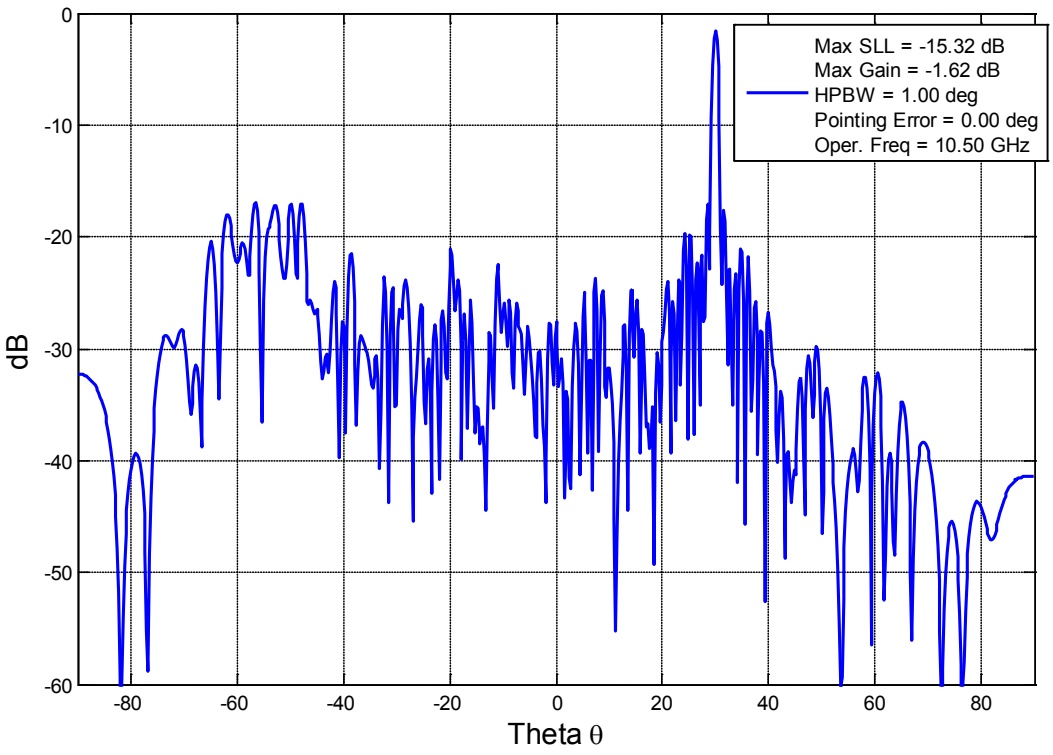

Figure 5.7 73 element aperiodic array scanned to +30°

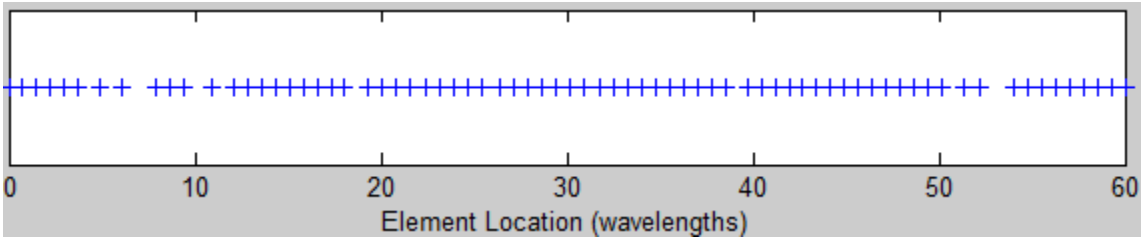

Figure 5.8 Picture showing array set up for 73 element aperiodic array.
X's represent individual element positions.

As the array is continually thinned, it seems that performance improves up to a certain limit. The performance peaks in terms of sidelobe level at an array containing 63 elements. After this array, each successive array tends to decline in sidelobe performance. Finally, when the far-field pattern of an array with 39 elements was computed, the half-power beamwidth increased to 1.5°, decreasing the overall gain of the array. The goal of this thesis is to create an array with optimal sidelobe performance for a given beamwidth which is close to that of the periodic array. Under this definition, the optimal array was achieved with 63 elements. The far-field pattern and element locations of this array are shown below.

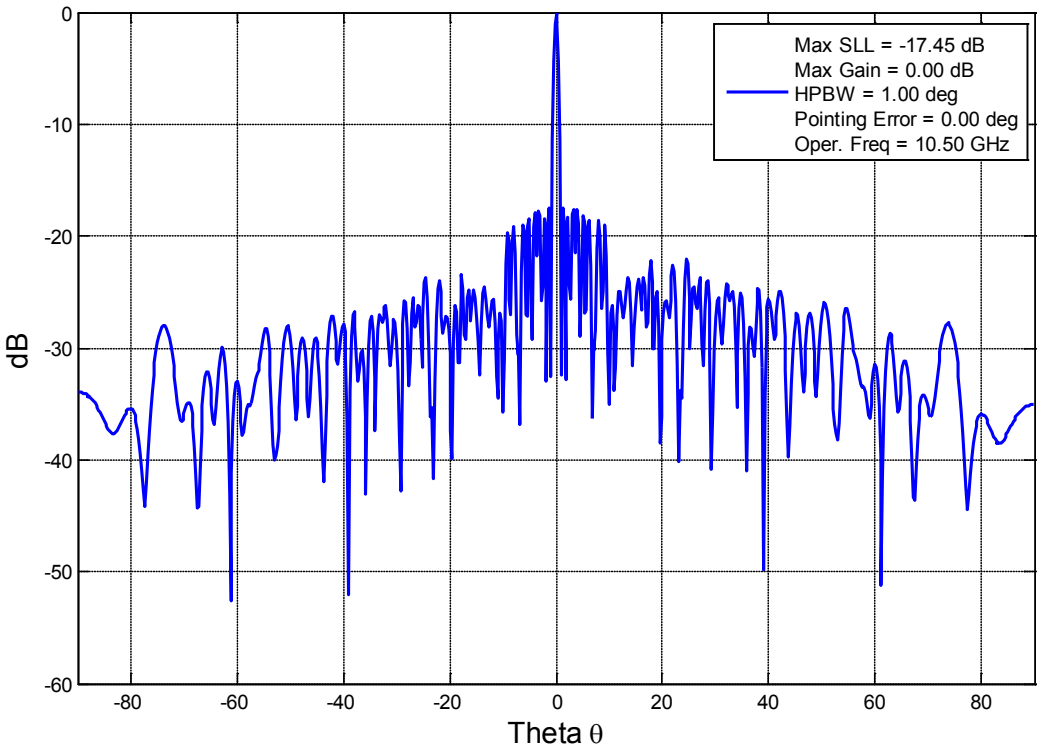

Figure 5.9 63 element aperiodic array at broadside

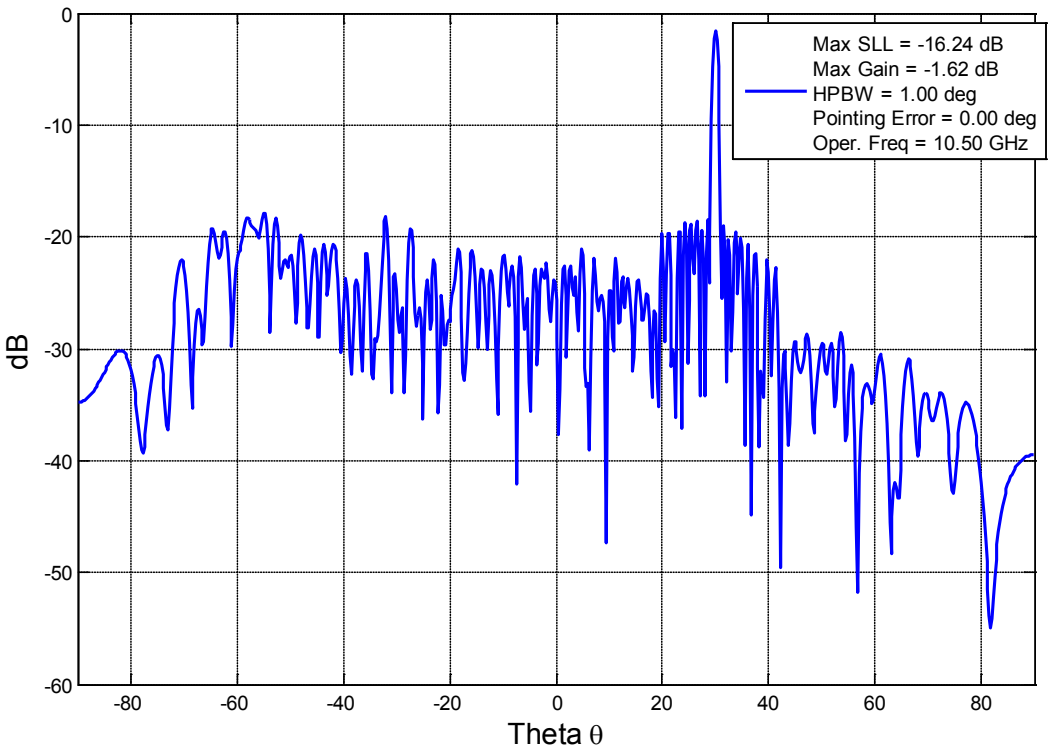

Figure 5.10 63 element aperiodic array scanned to +30°

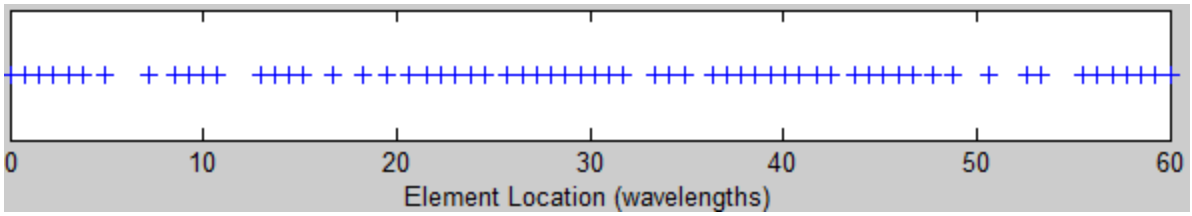

Figure 5.11 Picture showing array set up for 63 element aperiodic array.
X's represent individual element positions.

The 63 element array achieves a maximum sidelobe level of -17.45 dB at broadside and -16.24 dB while scanned to +30 degrees. The beamwidth remains a constant 1.00 degrees at broadside and equals approximately 1.14° at +30°. This array was found to be the best in terms of sidelobe performance for a given beamwidth, and it significantly outperforms the periodic array in terms of maximum sidelobe level. For recap, Figures 5.12 and 5.13 below show the far-field patterns of the periodic array and the optimized aperiodic array while both are scanned to +30 degrees. The periodic array in this figure assumes a spacing between elements of 0.75 λ in order to achieve equal bandwidth performance to the aperiodic array. From this, it is obvious that aperiodic spacings can be used in arrays to improve far-field performance while simultaneously reducing the number of elements needed in the array. Figure 5.14 shows a traditional 121 element periodic array with an inter-element spacing of a half wavelength and a total aperture dimension equal to 60 λ. It can be shown that the maximum sidelobe level of this array is still higher than the aperiodic 63-element optimized array, specifically the close in sidelobes. In addition, this periodic array has no bandwidth properties.

One thing to note is that while the maximum sidelobe level of the aperiodic array is lower than that of the periodic array, the far out sidelobes are much higher for the aperiodic array. This can be a problem in certain radar applications, specifically electronic warfare. The periodic array has low far out sidelobes, which from a jamming point of view may be much preferable to the far higher well removed sidelobes of the aperiodic array. The latter is vulnerable to jamming in a radar application by a stand off jammer putting power into the far out sidelobes. Electronic Counter Measures (ECM) is all about exploiting weaknesses in the opponent's radar. In this case, far out sidelobes susceptible to a stand off jammer are a distinct weakness. However, these problems could be resolved with the use of a combination of space tapering as well as amplitude tapering in the array. With a proper amplitude taper applied, the far out sidelobes of the aperiodic array could be reduced to an accepted level for radar applications. In this case, the

aperiodic array would still require fewer elements than the periodic array, making it much cheaper to build while simultaneously providing adequate far-field performance. There are other applications, such as geostationary satellite arrays, that are less concerned with far out sidelobe level. These applications could benefit tremendously from aperiodic arrays with uniform amplitude tapering.

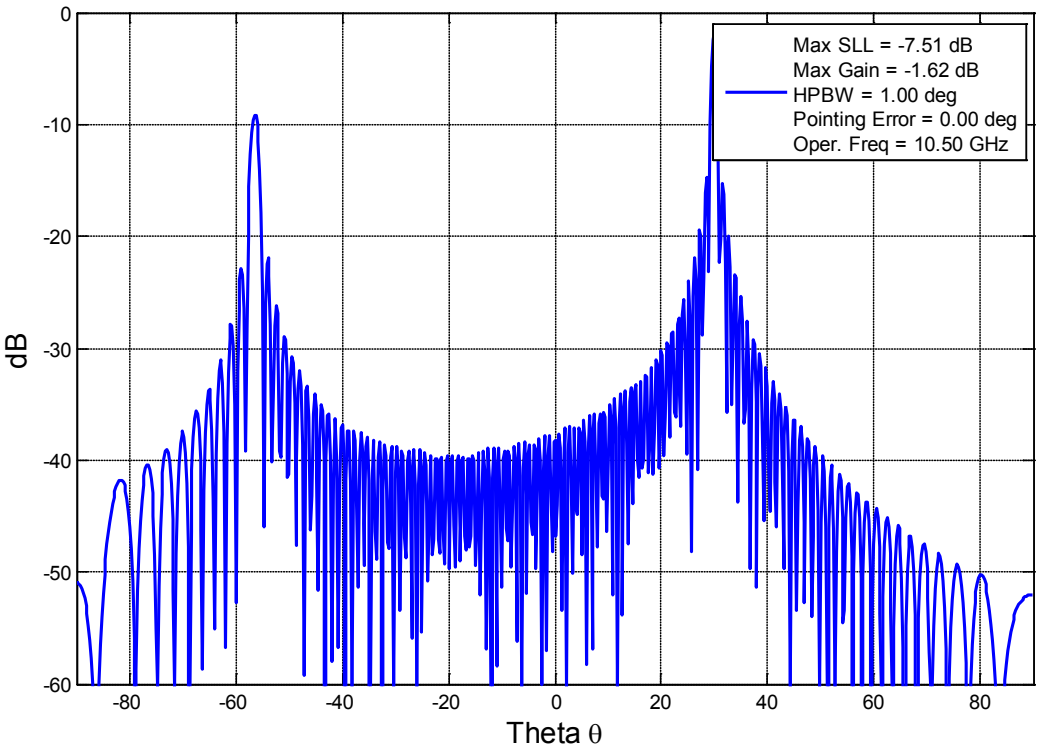

Figure 5.12 Periodic array with 0.75 λ spacing scanned to +30°.
The minimum spacing between elements is 0.75λ in order to achieve 1.5:1 bandwidth

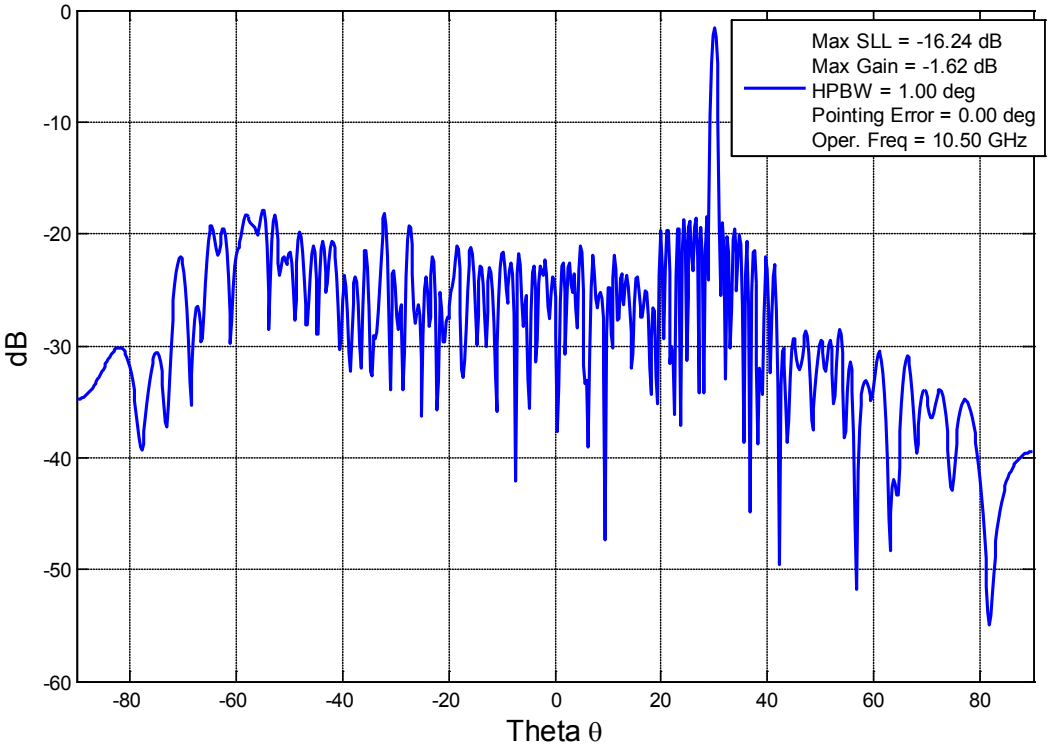

Figure 5.13 63 element aperiodic array scanned to +30° with 1.5:1 bandwidth

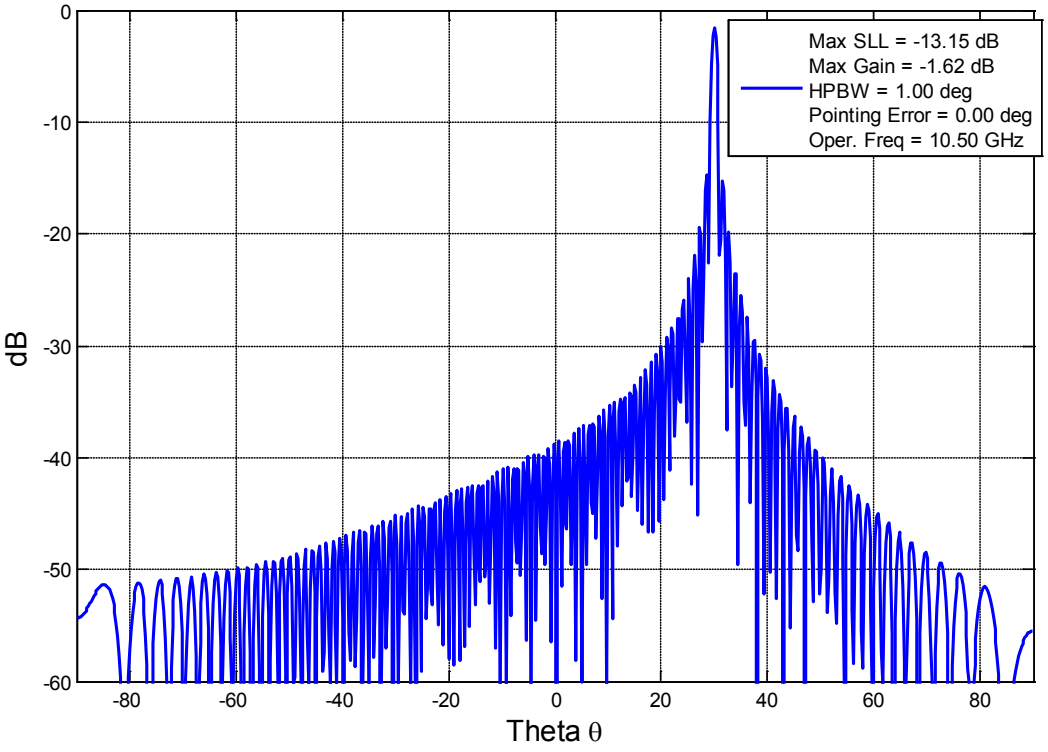

Figure 5.14 Periodic array with 0.50 λ spacing scanned to +30° in azimuth, 121 elements in all. This array can only achieve 1:1 bandwidth and still has sidelobes higher than the 63-element aperiodic array.

If we decrease the number of elements further, we can still achieve performance that is superior to the periodic reference array in terms of maximum sidelobe level. Shown below in Figures 5.15 and 5.16 is an example of a 45 element aperiodic array pattern that maintains less than 1.25 degree HPBW while having a maximum sidelobe level of -13.7 dB during scanning.

In comparison to the -7.5 dB highest sidelobe level of the periodic array, this aperiodic array still outperforms the periodic array while simultaneously having approximately 45% fewer elements.

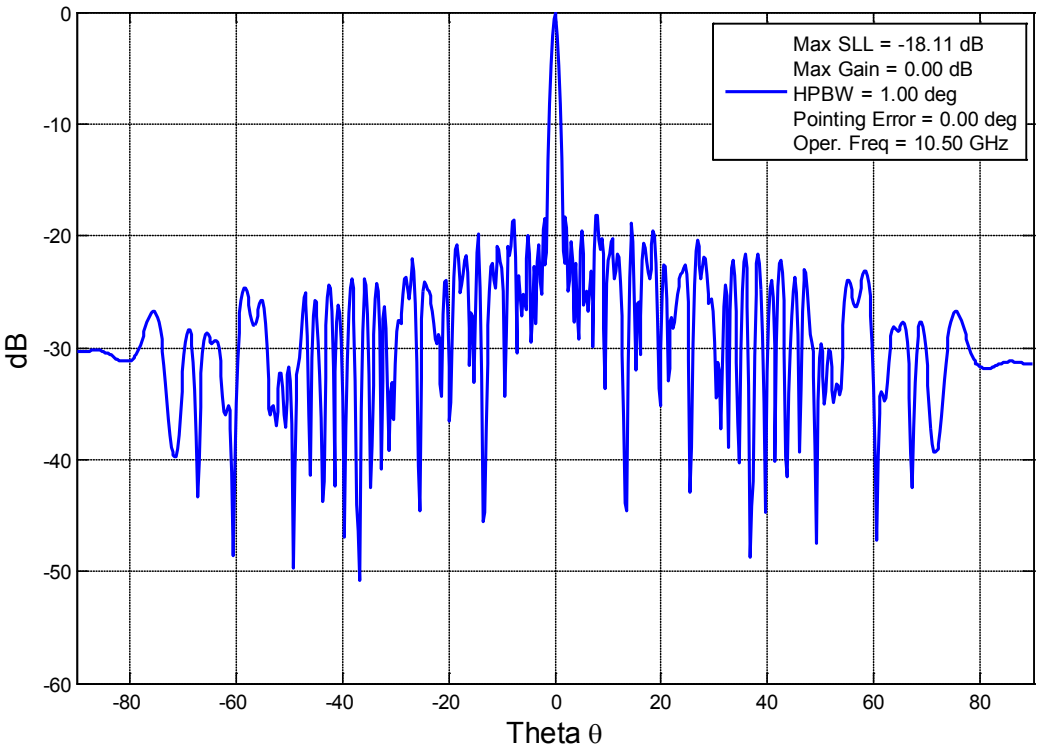

Figure 5.15 45 element aperiodic array pattern at broadside

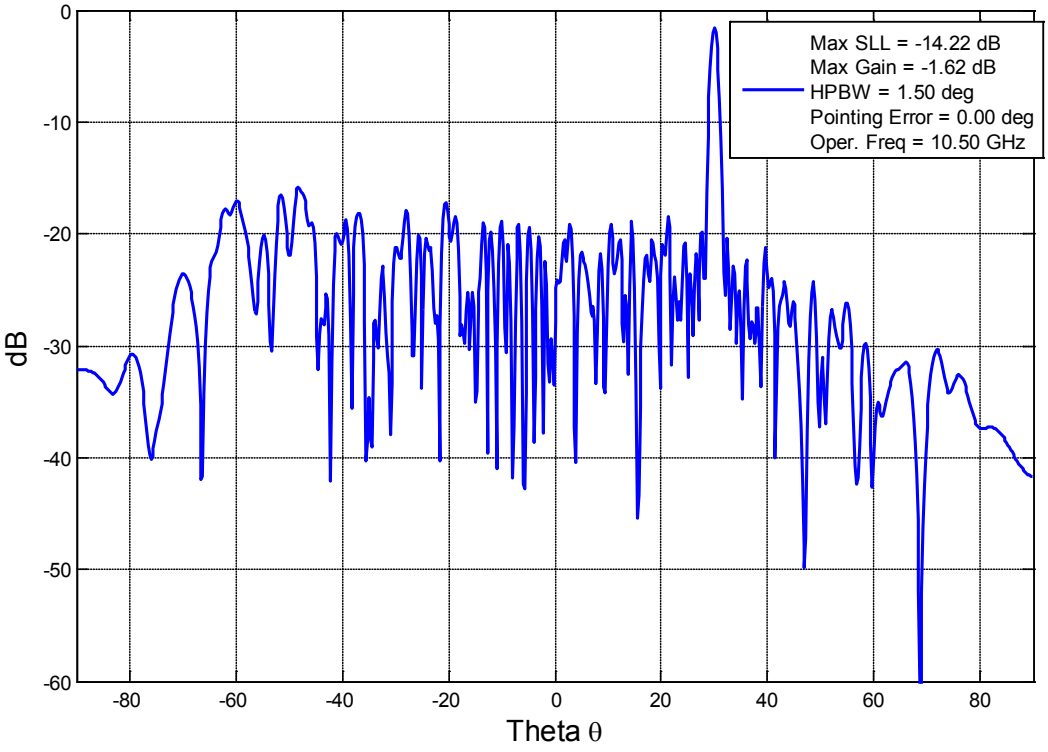

Figure 5.16 45 element aperiodic array pattern while scanned to +30°

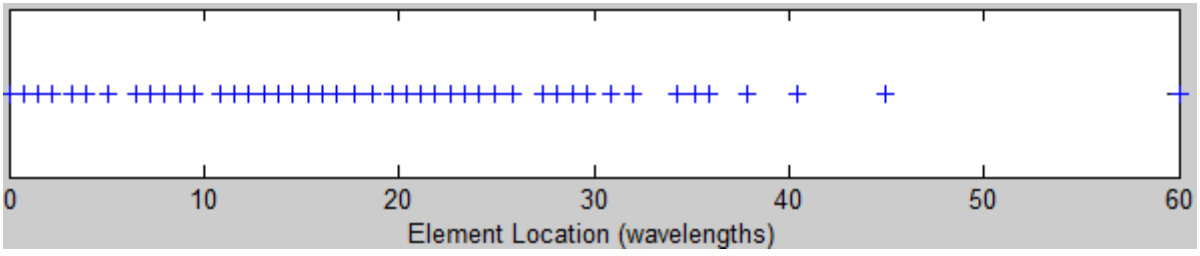

Figure 5.17 Picture showing array set up for 45 element aperiodic array. X's represent individual element positions.

The process of thinning the array can continue down to as few elements as possible; however there is a fundamental limit that is reached. Once the array is thinned past a certain threshold, the half-power beamwidth will increase drastically, reducing directivity of the array. In this example, that limit was 39 elements. From the far-field patterns in Figures 5.18 and 5.19 for the aperiodic array, the maximum sidelobe level is still lower than for the periodic counterpart, specifically the close-in sidelobes. In fact, the maximum sidelobe level of the aperiodic array while scanned to +30 degrees is -14.3 dB compared to -7.5 dB for the periodic array. However, since the array has so few elements, the half-power beamwidth has increased to 1.5 degrees at broadside and approximately 1.7 degrees while scanned to +30°.

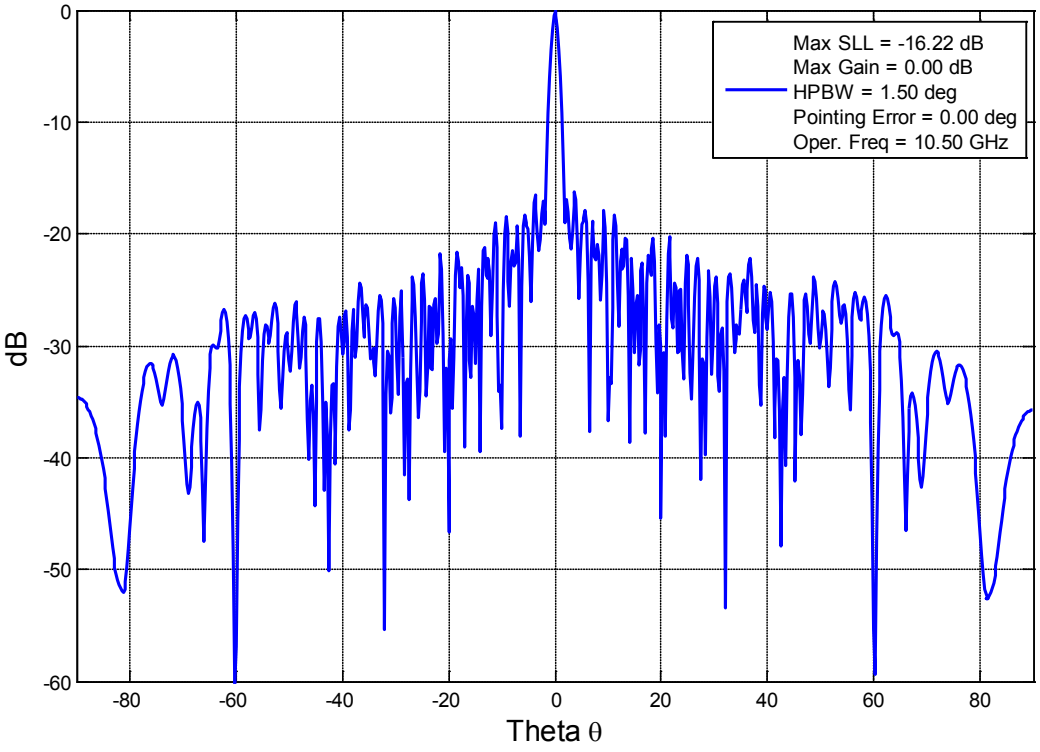

Figure 5.18 39 element aperiodic array pattern at broadside

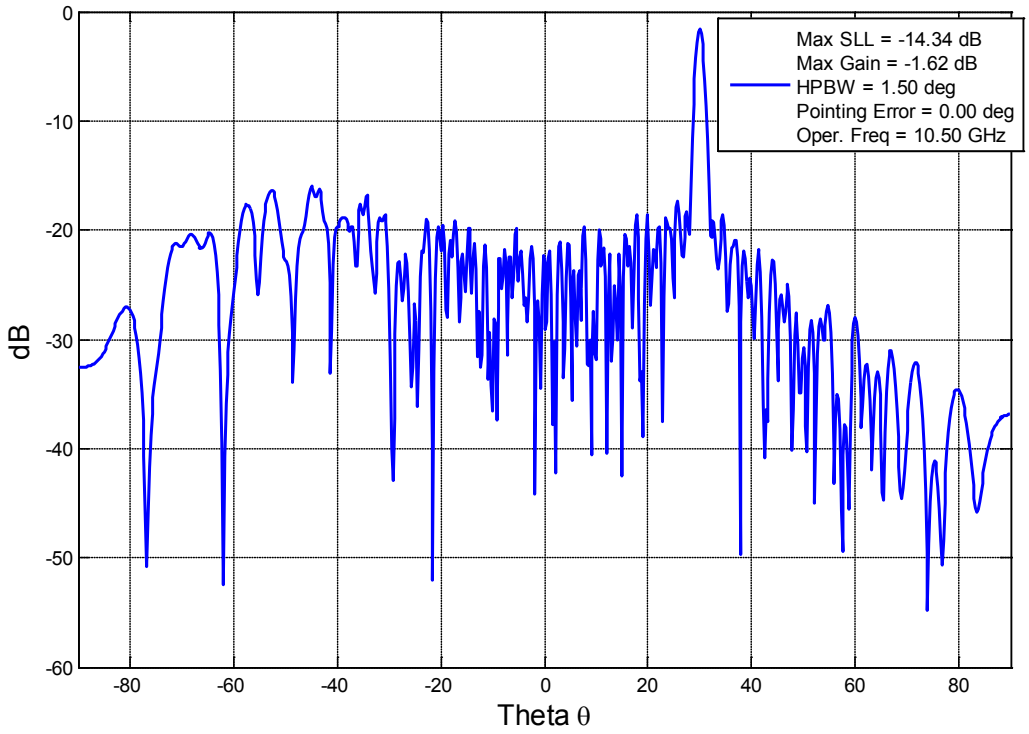

Figure 5.19 39 element aperiodic array pattern scanned to +30°

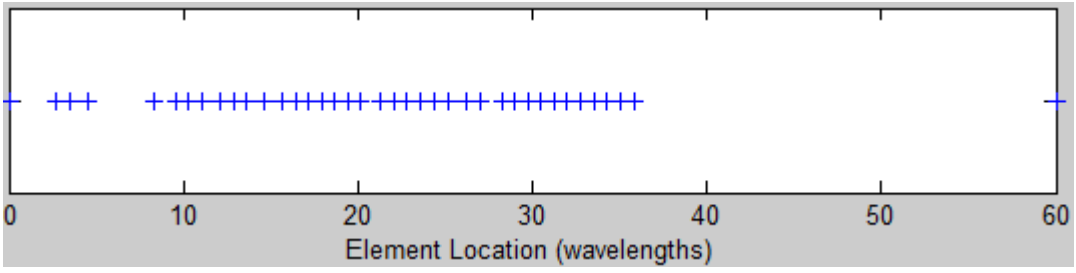

Figure 5.20 Picture showing array set up for 39 element aperiodic array. X's represent individual element positions.

Because of the requirements set forth in this thesis in terms of beamwidth, the optimizer stopped after the 39 element aperiodic array was analyzed. However, if HPBW is not a major concern in other applications, the array could be thinned even more, maintaining low sidelobe levels and decreasing the number of elements even more.

Shown below in Figure 5.21 are graphs of the sidelobe level versus number of elements for the broadside and scanned cases. This figure shows how the optimization peaks in terms of sidelobes at 63 elements and decreases from there. Note that 81 elements is the periodic array case with 0.75 λ spacing and a total aperture dimension of 60 λ.

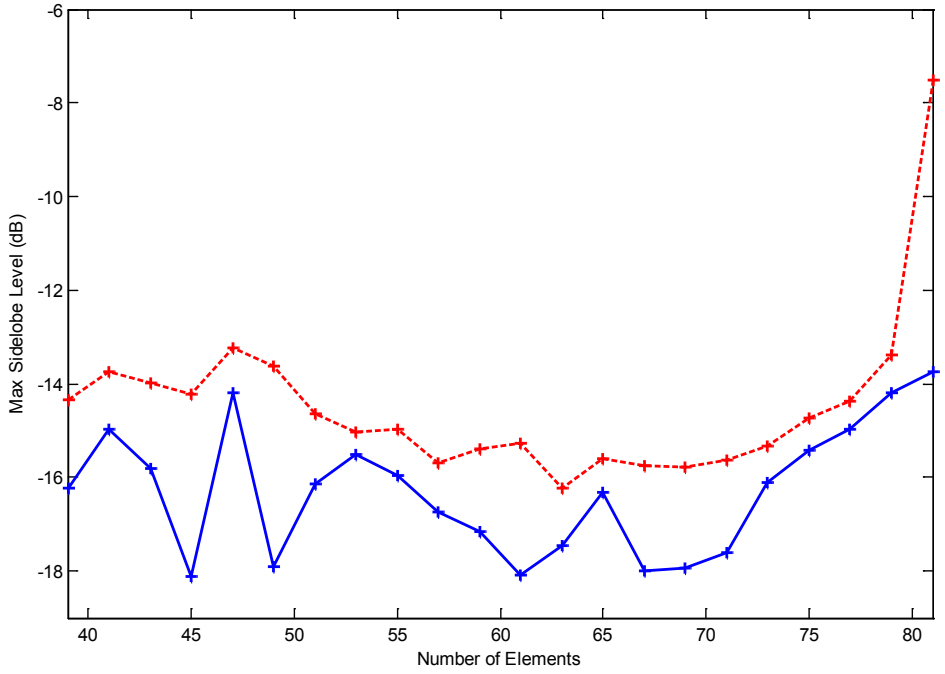

Figure 5.21 Maximum sidelobe level versus the number of elements used in the array. The blue plot (solid line) represents the broadside case. The red plot (dashed line) represents the arrays scanned to +30°. The 81 element case represents the periodic array with 0.75 λ spacing.

5.3 Final Optimized Array

As discussed above in Section 5.2, the final optimal array that was chosen was the 63 element array. This array was chosen because it maintained minimum sidelobe level for a given beamwidth. It outperforms the periodic array in terms of bandwidth and maximum sidelobe level, while maintaining a very similar beamwidth.

In certain applications this array might not be considered optimal. It was chosen as optimal for the specific requirements set forth in this thesis. It is possible to further reduce the number of elements in the array while maintaining lower sidelobes than the periodic case. The final specifications of the 63 element array are shown below in Table 5.3 along with the far-field patterns in Figure 5.22 and Figure 5.23. Also, in order to confirm that the array can operate over a wide band of frequencies, the far-field patterns of the array operated at the lower frequency of 7 GHz are given below. The patterns do not change significantly during the frequency sweep. As expected, the beamwidth widens; however the maximum sidelobe level remains low.

Frequency of Operation	7GHz - 10.5 GHz
Array Bandwidth	1.5-to-1
Azimuth Scanning Ability	±30°
Maximum Sidelobe Level at Broadside	-17.45 dB
Maximum Sidelobe Level at +30°	-16.24 dB
3-dB Beamwidth at Broadside	1.00°
3-dB Beamwidth at +30°	1.14°
Number of Elements	63
Percentage Thinned	77%
Dimension of Array	60 λ @ 10.5 GHz
Antenna Element	2-Turn Axial-Mode Helix

Table 5.3 Final aperiodic array results (MATLAB) while operated at 10.5 GHz

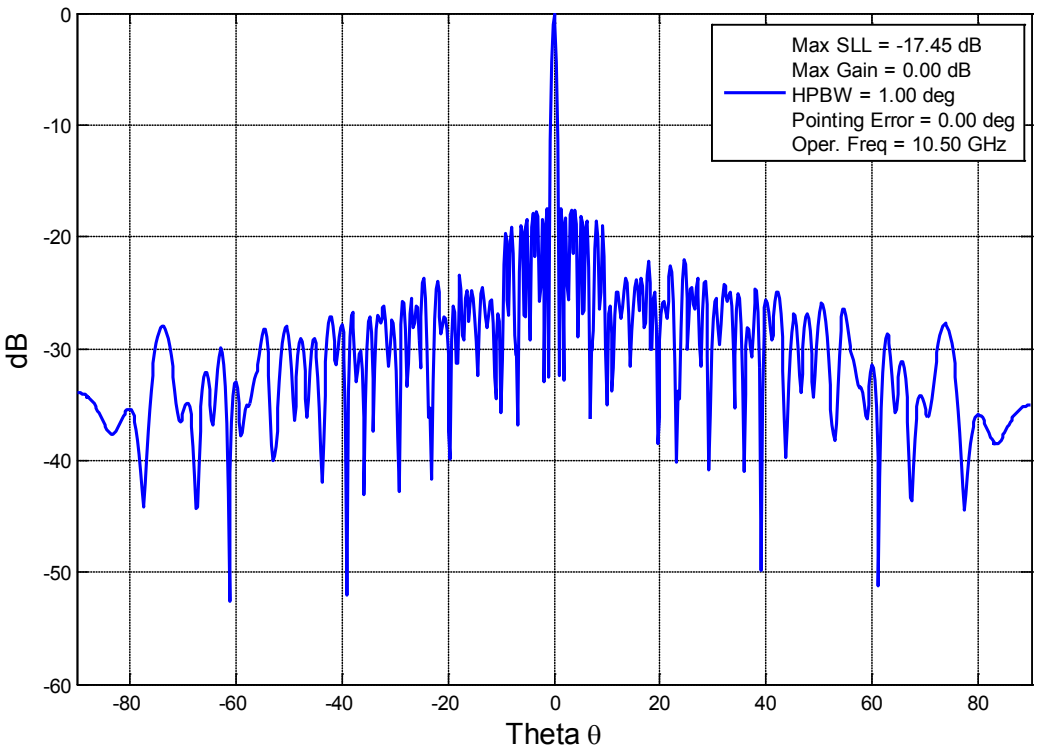

Figure 5.22 63 element aperiodic array at broadside operated at 10.5GHz

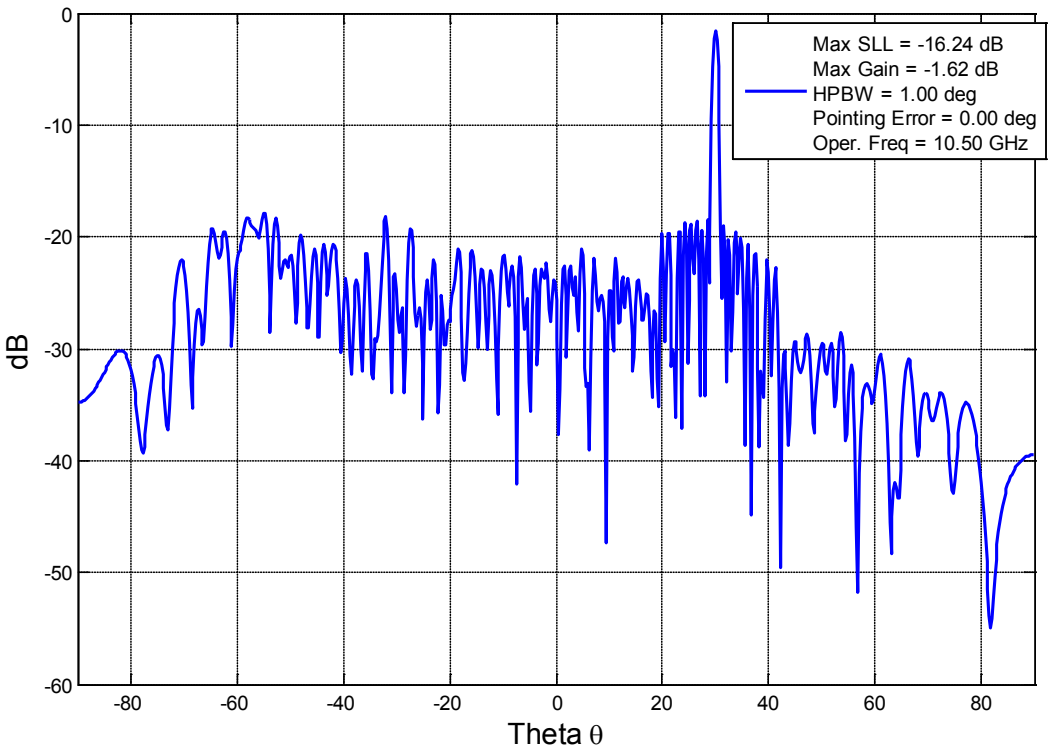

Figure 5.23 63 element aperiodic array scanned to +30° operated at 10.5 GHz

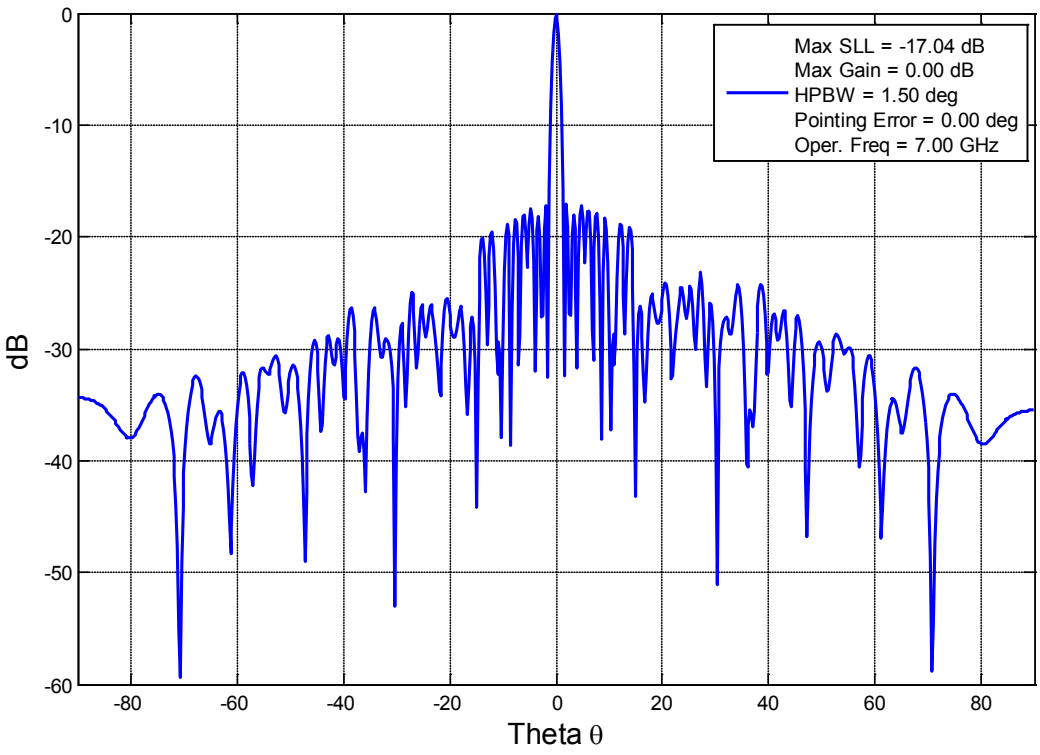

Figure 5.24 63 element aperiodic array operated at 7 GHz at broadside

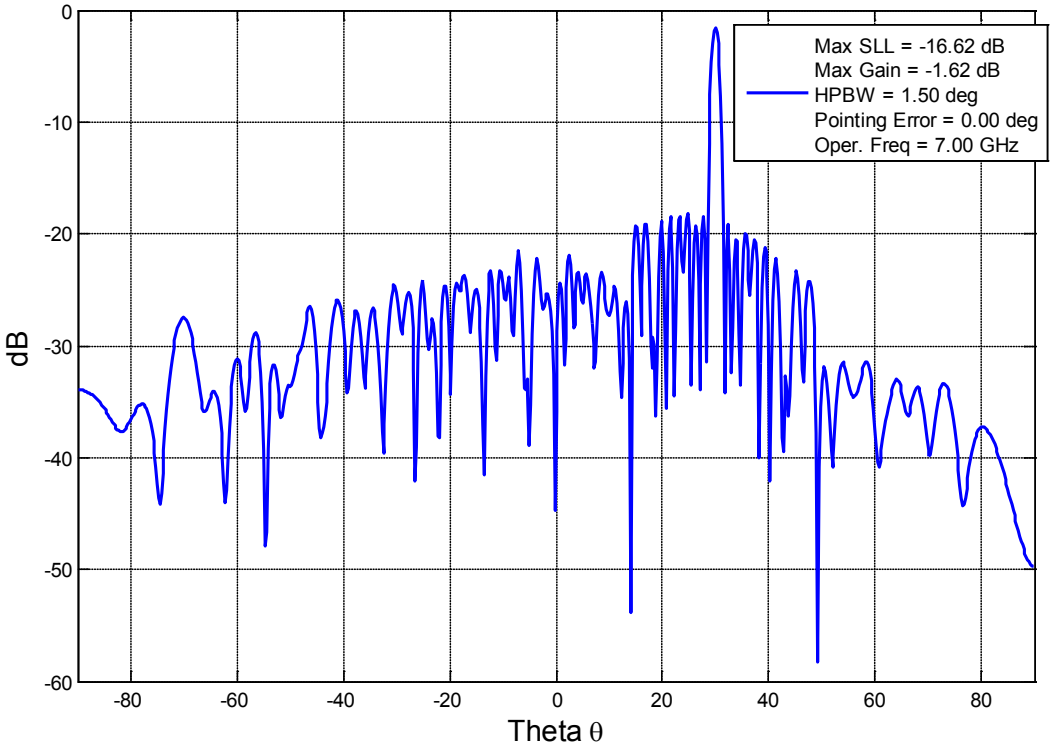

Figure 5.25 63 element aperiodic array operated at 7 GHz scanned to +30°

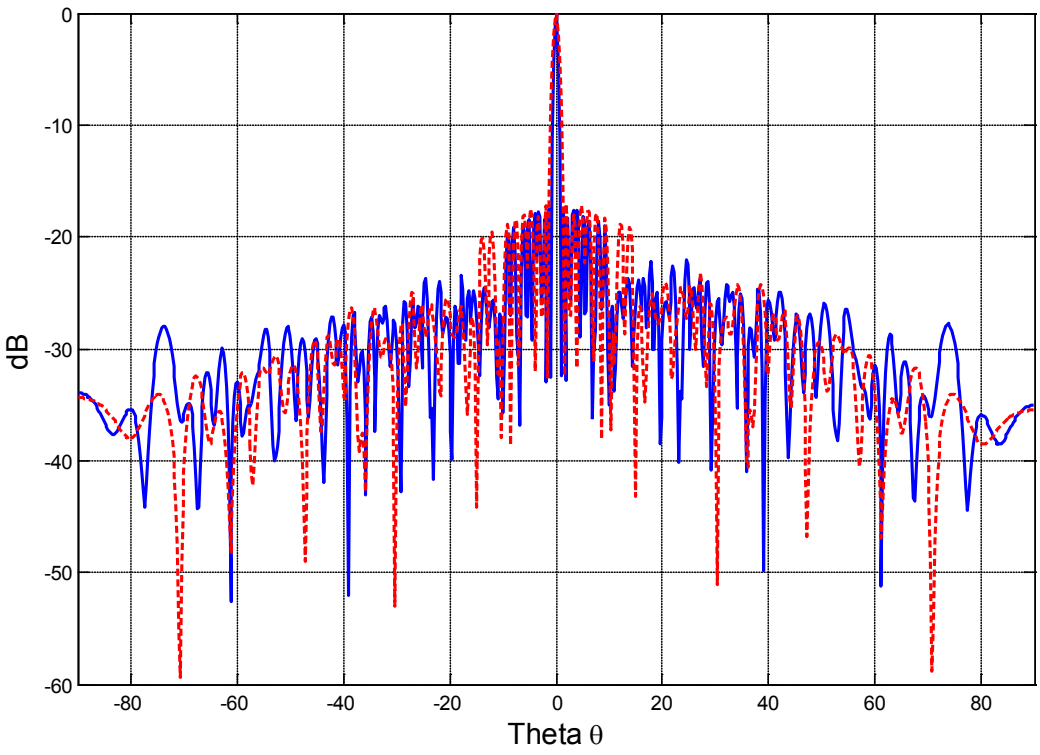

Figure 5.26 63 element aperiodic array operated at 10.5 GHz and 7 GHz overlaid at broadside. 10.5 GHz is blue (solid line). 7 GHz is red (dashed line).

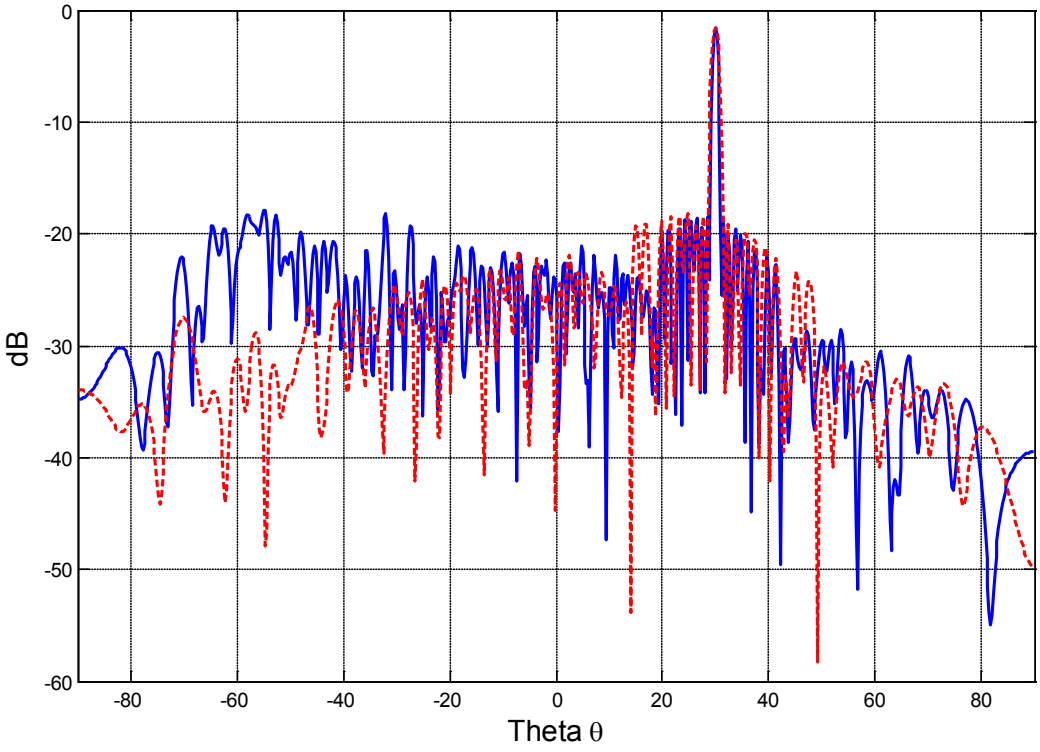

Figure 5.27 63 element aperiodic array operated at 10.5 GHz and 7 GHz overlaid scanned to +30°. 10.5 GHz is blue (solid line). 7 GHz is red (dashed line).

5.4 FEKO Analysis of Final Design

In order to validate the optimized array from Section 5.3, a full-wave electromagnetic analysis was performed using the software package FEKO. This full-wave analysis takes into account mutual coupling and other real-life interactions that were previously avoided in this project. From Section 4.3, it was shown that mutual coupling at half-wavelength spacing should not be a major issue. By building the entire 63 element array in FEKO and running a full-wave simulation, we hope to justify this claim. Figure 5.28 below shows the FEKO built array. 63 elements are placed at the precise locations that the particle swarm optimizer suggested.

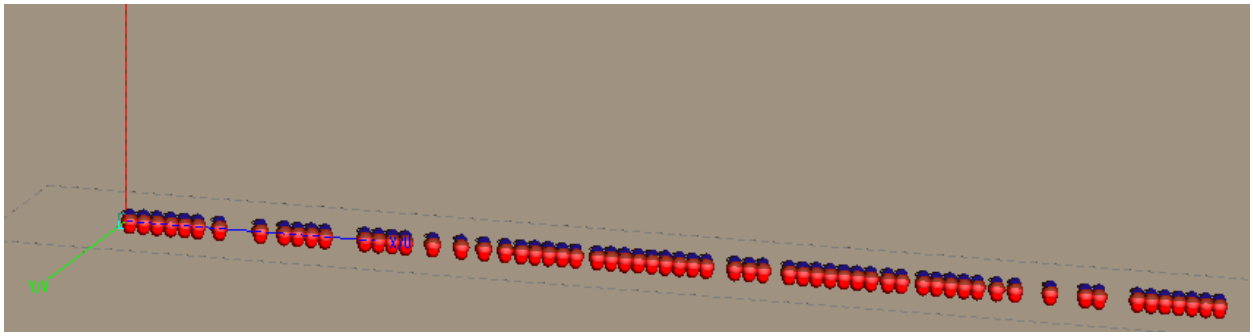

Figure 5.28 Optimized 63 element aperiodic array built in FEKO

The simulation was performed and the far-field pattern was computed. Figure 5.29 below shows the far-field pattern computed with FEKO in comparison to the MATLAB result. The MATLAB calculated far-field pattern and the FEKO calculated pattern are almost identical,

validating the claim that mutual coupling does not play a significant role at this spacing. Table 5.4 gives the final specifications of the array according to FEKO, which are very similar to the values MATLAB provided.

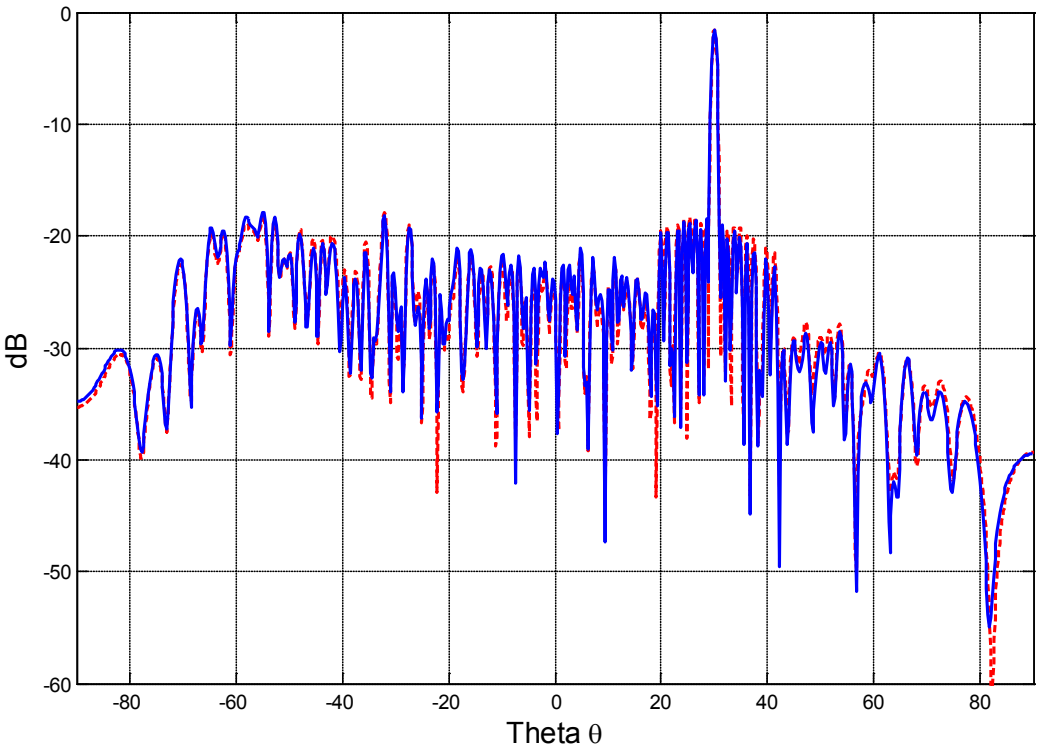

Figure 5.29 63 element aperiodic array operated at 10.5 GHz far field pattern in MATLAB and FEKO. Array is scanned to +30°. MATLAB results are in blue (solid line). FEKO results are in red (dashed line).

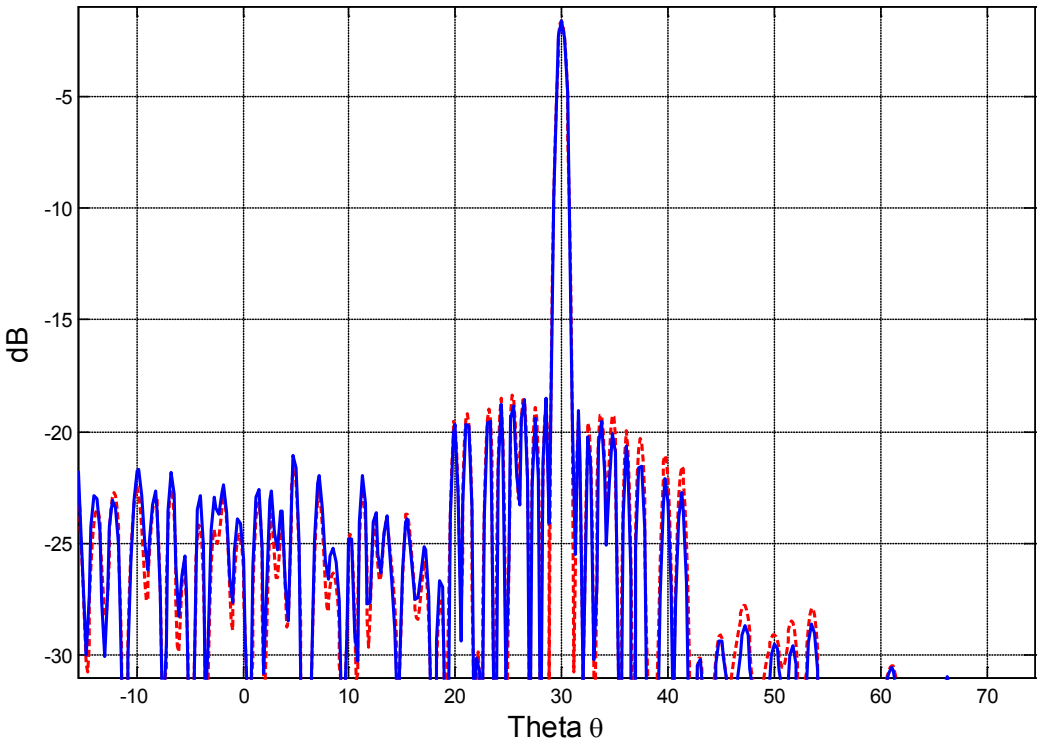

Figure 5.30 63 element aperiodic array operated at 10.5 GHz far field pattern in MATLAB and FEKO. MATLAB results are in blue (solid line). FEKO results are in red (dashed line). Zoomed in view.

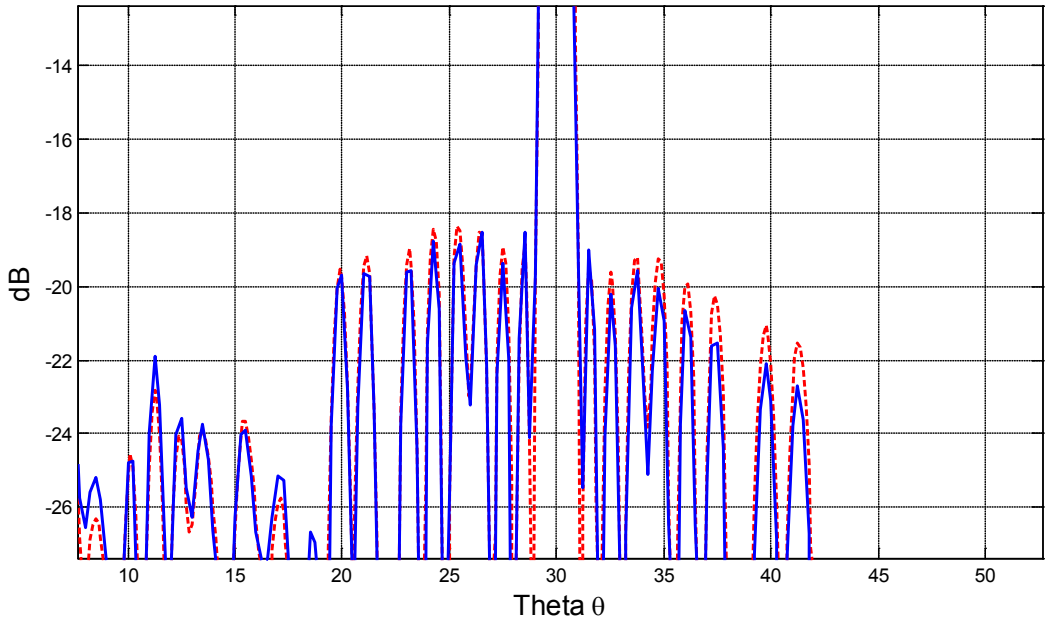

Figure 5.31 MATLAB and FEKO far-field patterns of aperiodic array at +30° operated at 10.5 GHz. MATLAB results are in blue (solid line). FEKO results are in red (dashed line). Zoomed in view showing main beam and first few sidelobes.

The MATLAB results can only achieve a resolution of 0.25 degrees, accounting for the sharper transitions of the far-field pattern. FEKO can achieve a much greater resolution. This provides a much smoother sidelobe transition. This resolution difference explains the slight difference between the MATLAB and FEKO results shown above.

Frequency of Operation	7GHz - 10.5 GHz
Array Bandwidth	1.5-to-1
Azimuth Scanning Ability	±30°
Directivity at Broadside	27.2 dB
Directivity at +30°	25.7 dB
Maximum Sidelobe Level at Broadside	-16.5 dB
Maximum Sidelobe Level at +30°	-16.3 dB
3-dB Beamwidth at Broadside	1.00°
3-dB Beamwidth at +30°	1.14°
Number of Elements	63
Percentage Thinned	77%
Dimension of Array	60 λ @ 10.5 GHz
Antenna Element	2-Turn Axial-Mode Helix

Table 5.4 Final aperiodic array results (FEKO) while operated at 10.5 GHz

Also, the far-field patterns of the array were calculated in FEKO when the array was operated at the lower frequency of 7 GHz. The pattern has not changed drastically over the frequency sweep. The pattern still maintains low sidelobe level and a narrow beamwidth. This confirms that the array is able to perform over a 1.5-to-1 bandwidth.

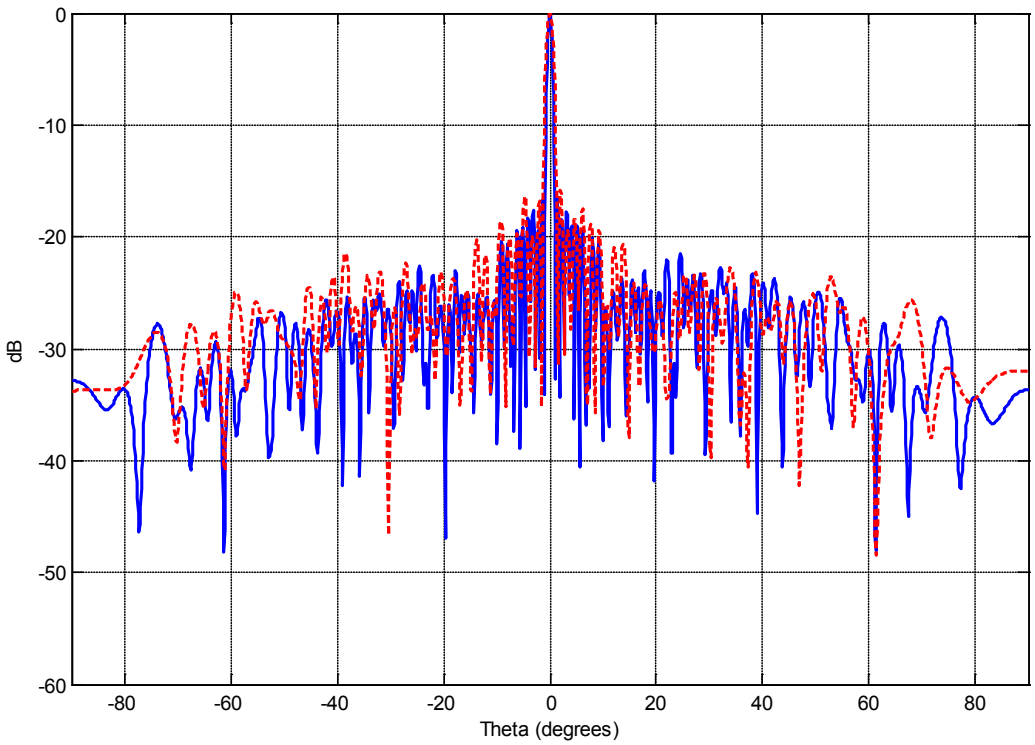

Figure 5.32 FEKO 63 element optimized array operated at 10.5 GHz and 7 GHz at broadside overlaid. 10.5 GHz results are in blue (solid line). 7 GHZ results are in red (dashed line).

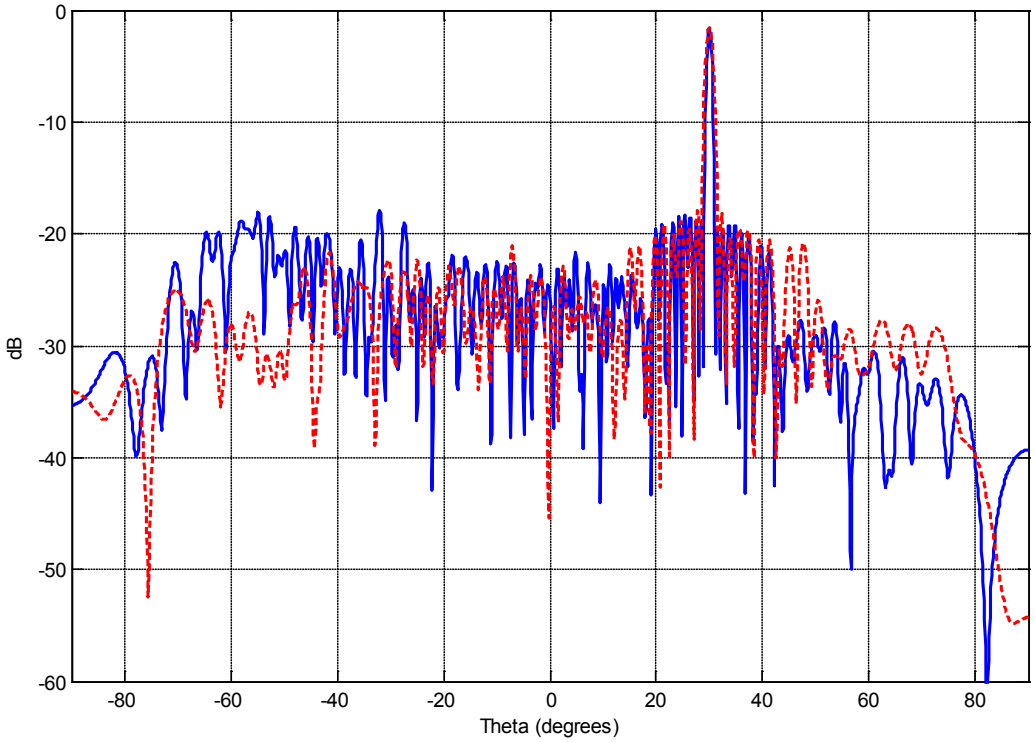

Figure 5.33 FEKO 63 element optimized array operated at 10.5 GHz and 7 GHz scanned to +30 degrees. 10.5 GHz results are in blue (solid line). 7 GHz results are in red (dashed line).

5.5 Analysis of Results

Overall, the optimized array satisfied all of the requirements set forth in this thesis. The aperiodic array is thinned to 77% of the original periodic array. It maintains a maximum sidelobe level well below the periodic reference array. The beamwidth of the aperiodic array is 1.00 degree at broadside, compared to approximately 0.90 degrees for the 0.75 λ spaced periodic reference array. Because of the aperiodicity, the array is able to operate over a wide bandwidth, 1.5-to-1. All of these properties are maintained while the array is scanned to ±30° in azimuth. The minimum spacing requirement set forth in this analysis allowed mutual coupling to have negligible effects on array performance. In real world applications, this array would be lighter, cheaper, and outperform a periodic array in many radar applications. Therefore, it is confirmed that using aperiodic spacing instead of periodic spacing in arrays can provide overall superior performance in many applications. Table 5.5 below compares all of the results of the optimized 63 element aperiodic array versus the reference periodic arrays with 0.5 λ and 0.75 λ spacings.

The only real world issue that was not investigated in this project was the feeding network. It is assumed that a proper feeding and or matching network can be designed to accommodate this array. The design would start with uniform phasing at each element, as is done in a periodic array. An electronically preset phase shifter would have to be added in order to compensate for the unequal spacing. Since the element grid spacing increments every 1/8 of a wavelength, a 3-bit electronically controlled phase shifter would be required in order to provide eight possible increments. This is just one addition to the circuitry associated with each element; however, it does not require active electronic control. The phase shifter can be set by resistors that set the three stages high or low.

	Thinned Aperiodic Array	**Periodic Array with 0.75 λ spacing between elements**	**Periodic Array with 0.5 λ spacing between elements**
Frequency of Operation	7 GHz - 10.5 GHz	7 GHz - 10.5 GHz	10.5 GHz
Array Bandwidth	1.5:1	1.5:1	Narrow
Minimum Element Spacing	0.75 λ	0.75 λ	0.5 λ
Azimuth Scanning Ability	±30°	±19.5°	±90°
Directivity at Broadside	27.2 dB	28.2 dB	28.7 dB
Directivity at +30°	26.0 dB	27.4 dB	28.0 dB
Maximum Sidelobe Level at Broadside	-16.5 dB at +1.25°	-13.2 dB at +1.25°	-13.8 dB at +1.25°
Maximum Sidelobe Level at +30°	-16.3 dB at -55.0°	-7.51 dB at -56.5° (Grating Lobe)	-13.1 dB at +28.5°
3-dB Beamwidth at Broadside	1.00°	0.90°	0.87°
3-dB Beamwidth at +30°	1.14°	0.93°	0.91°
Number of Elements	63	81	121
Percentage Thinned	77%	0%	0%
Dimension of Array	60 λ @ 10.5 GHz	60 λ @ 10.5 GHz	60 λ @ 10.5 GHz
Antenna Element	2-Turn Axial Mode Helix	2-Turn Axial Mode Helix	2-Turn Axial Mode Helix

Table 5.5 Final comparison of arrays operated at 10.5 GHz

Chapter 6

Conclusions

6.1 Non Uniform Array Design

The objective of the research reported in this thesis was to use optimization algorithms to design a uniformly illuminated aperiodically spaced antenna array. The array should achieve superior pattern performance while requiring fewer antenna elements than a periodic array of equal aperture size. A second objective was to maintain these properties over a 2-to-1 operational bandwidth. Chapter 2 provided a literature review of the previous research in the area of aperiodic arrays. It detailed the complexity of the problem and explained why many researchers have turned to optimization as the only realistic method for designing these arrays. Chapter 3 provided the background to the design problem. This chapter explained the details of periodic and aperiodic arrays and how they are solved analytically. It was shown that designing an aperiodic antenna array is a highly non-linear problem and that designing the array analytically is next to impossible. An introduction to optimization algorithms, namely the Particle Swarm Optimization method, is given in this chapter. The optimization is explained in depth and details are given on how this method can be applied to electromagnetics [13].

The development of the array antenna element is discussed in Chapter 4. The final element chosen was a two turn axial-mode helix. This helix element has a 60 degree half-power

beamwidth and 1.5-to-1 operational bandwidth. This chapter also details mutual coupling effects of the helix element. A minimum distance between elements is set and it is shown that mutual coupling effects are negligible at this distance and can be ignored for this helical element. Finally, the particle swarm optimizer is set up specifically for this thesis. All assumptions and methods used for this application are explained in detail. The optimizer is set to enforce a minimum distance between elements. Also, all optimizations are performed while the array is electronically scanned to a maximum angle of 30 degrees in azimuth. This is done to ensure a worst case sidelobe level scenario, since sidelobes tend to increase with scan angle.

The results from this research are original and show the advantages and disadvantages associated with using aperiodic element spacings. Many previous research attempts in the area of aperiodic arrays assume isotropic radiators and only optimize the array factor. Optimizing the pattern this way does not produce a realistic optimal power pattern. Once an element pattern is brought into the equation, the antenna pattern is changed significantly and may no longer be optimal. This thesis assumed an axial mode helix as the antenna element and incorporated its far field pattern into the optimization. The helix antenna element used in this study is an original design. It was designed to have acceptable input impedance as well as scanning ability over a wide bandwidth. Most previous papers have assumed isotropic radiators or simple elements such as dipoles for mathematical convenience. This study is one the few to design a unique antenna element for the specific purpose of aperiodic antenna arrays. Also, many previous papers chose to ignore mutual coupling effects for mathematical convenience. Mutual coupling is a real problem and could significantly affect the results, especially if the spacing between elements is less than a half wavelength. Mutual coupling is investigated in this thesis, and a full-wave simulation of the final antenna array is performed to show the negligible effects it has on the far field antenna pattern in this specific study.

6.2 Final Optimized Aperiodic Array Design

The final design for the aperiodic antenna array presented in Chapter 5 met nearly all of the initial requirements. The array is able to scan to ±30 degrees while maintaining sidelobe levels well below the maximum sidelobe level of the equivalent periodic antenna array. Due to the element constraints, the array is only able to operate over a 1.5-to-1 bandwidth instead of the initial design goal of 2-to-1 bandwidth. The array maintains a similar half-power beamwidth to the periodic array while simultaneously eliminating the grating lobe that would appear in the 0.75 λ spaced periodic array during scanning. The maximum sidelobe level is also shown to be lower than for the periodic array, specifically the close in sidelobes. The far out sidelobes are higher than for the periodic array. This could cause the array to be vulnerable to jamming or other electronic warfare attacks. An amplitude taper could be applied across the array to alleviate this problem. The aperiodic array is also thinned to approximately 78 percent of the original periodic array, while having a directivity reduction of only 1.0 dB at broadside. This reduction in elements allows the array to be built at lower cost. All results for the optimized aperiodic array as well as the periodic reference arrays are summed up in Table 6.1 below.

	Thinned Aperiodic Array	**Periodic Array with 0.75 λ spacing between elements**	**Periodic Array with 0.5 λ spacing between elements**
Frequency of Operation	7 GHz - 10.5 GHz	7 GHz - 10.5 GHz	10.5 GHz
Array Bandwidth	1.5:1	1.5:1	Narrow
Minimum Element Spacing	0.75 λ	0.75 λ	0.5 λ
Azimuth Scanning Ability	±30°	±19.5°	±90°
Directivity at Broadside	27.2 dB	28.2 dB	28.7 dB
Directivity at +30°	26.0 dB	27.4 dB	28.0 dB
Maximum Sidelobe Level at Broadside	-16.5 dB at +1.25°	-13.2 dB at +1.25°	-13.8 dB at +1.25°
Maximum Sidelobe Level at +30°	-16.3 dB at -55.0°	-7.51 dB at -56.5° (Grating Lobe)	-13.1 dB at +28.5°
3-dB Beamwidth at Broadside	1.00°	0.90°	0.87°
3-dB Beamwidth at +30°	1.14°	0.93°	0.91°
Number of Elements	63	81	121
Percentage Thinned	77%	0%	0%
Dimension of Array	60 λ @ 10.5 GHz	60 λ @ 10.5 GHz	60 λ @ 10.5 GHz
Antenna Element	2-Turn Axial Mode Helix	2-Turn Axial Mode Helix	2-Turn Axial Mode Helix

Table 6.1 Final comparison of arrays operated at 10.5 GHz

6.3 Future Work

Possible future work for this project could include the design of a feed network for this aperiodic array. Because of the aperiodicity, the design of a feed network is not as simple as the standard periodic case. The design would start with uniform phasing at each element, as is done in a periodic array. An electronically preset phase shifter would have to be added in order to compensate for the unequal spacing. Since the element grid spacing increments every 1/8 of a wavelength, a 3-bit electronically controlled phase shifter would be required in order to provide eight possible increments. This is just one addition to the circuitry associated with each element; however, it does not require active electronic control. The phase shifter can be set by resistors that set the three stages high or low.

Also, the design of a new antenna element with better scanning ability and bandwidth properties could be an area to investigate. The helix antenna element was a limiting factor in this optimization, reducing the scan angle and bandwidth that the array was able to achieve. Investigating an element with greater bandwidth and scanning ability would improve the results. Conical spirals, cavity backed spirals, biconical, discone, alford loops, log periodic, and rhombic antennas are all examples of antenna elements that can achieve the required beamwidth and bandwidth for this application [12]. Future work could investigate broadband aperiodic arrays using one of these elements.

Finally, the optimization process could be repeated with other optimization algorithms such as Genetic Algorithm [10] or others to compare the performance of the different algorithms at solving this problem. Particle Swarm Optimization was chosen in this research because it is fast and requires virtually no computational bookkeeping. Genetic Algorithm is more complicated and takes much more time to simulate; however, previous research has shown that

Genetic Algorithm can achieve results equal to and sometimes better than Particle Swarm Optimization [13].

References

[1] T. Pratt, "ECE5635 Radar System and Design," Course notes, Virginia Tech, Blacksburg, VA, 2009.

[2] M. G. Andreasen, “Linear arrays with variable interelement spacings,” *IRE Trans. on Antennas and Propagation,* vol. 4P-10, pp. 137-143, March 1962.

[3] H. Unz, “Linear arrays with arbitrarily distributed elements,” *IRE Trans. on Antennas and Propagation,* vol. AP-8, pp. 222-223, March 1960.

[4] D. D. King, R. F. Packard, and R. K. Thomas, "Unequally-spaced, broad-band antenna arrays," *IRE Trans. on Antennas and Propagation,* vol. AP-8, pp. 380-385, July 1960.

[5] Y. T. Lo, "A non-uniform linear array system for the radio telescope at the University of Illinois," 1960 Spring URSI and IRE Joint Meeting, Washington, D.C., subsequently published in the *IRE Trans. on Antennas and Propagation,* vol. AP-9, pp. 9-16, January 1961, under the title, "The University of Illinois radio telescope," by G. W. Swenson and Y. T. Lo.

[6] R. F. Harrington, "Sidelobe reduction by nonuniform element spacing," *IRE Trans. on Antennas and Propagation,* vol. AP-9, pp. 187-192, March 1961.

[7] Willey, R., "Space tapering of linear and planar arrays," *IRE Trans. on Antennas and Propagation*, vol.10, no.4, pp.369-377, July 1962.

[8] Lo, Y. and Lee, S., "A study of space-tapered arrays," *IRE Trans. on Antennas and Propagation*, vol.14, no.1, pp. 22- 30, Jan 1966.

[9] Angeletti, P. and Toso, G., "Aperiodic arrays for space applications: A combined amplitude/density synthesis approach," *Antennas and Propagation, 2009. EuCAP 2009. 3rd European Conference on* , vol., no., pp.2026-2030, 23-27 March 2009.

[10] Haupt, R.L., "Thinned arrays using genetic algorithms," *IRE Trans. on Antennas and Propagation*, vol.42, no.7, pp.993-999, July 1994.

[11] Bray, M.G.; Werner, D.H.; Boeringer, D.W.; Machuga, D.W.; , "Optimization of thinned aperiodic linear phased arrays using genetic algorithms to reduce grating lobes during scanning," *Antennas and Propagation, IEEE Transactions on* , vol.50, no.12, pp. 1732-1742, Dec 2002.

[12] W. L. Stutzman and G. A. Thiele, *Antenna Theory and Design.* New York: John Wiley and Sons, Inc., 1998.

[13] Boeringer, D.W.; Werner, D.H.; , "Particle swarm optimization versus genetic algorithms for phased array synthesis," *Antennas and Propagation, IEEE Transactions on* , vol.52, no.3, pp. 771- 779, March 2004.

[14] "Stealth Radar System," Ohio State University., http://www.researchnews.osu.edu/archive/noiserad.htm; accessed March, 2011.

[15] Yanfen Wang; Ruoshan Chen; Wenjie Zhang; , "Design and Simulation of a Chirp Pulse Compression Ultra-Wideband Communication System," *Electronic Computer Technology, 2009 International Conference on* , vol., no., pp.415-419, 20-22 Feb. 2009.

[16] J. D. Kraus, *Antennas,* 2nd. Ed., McGraw-Hill: New York, 1988.